In presenting the dissertation as a partial fulfillment of the requirements for an advanced degree from the Georgia Institute of Technology, I agree that the Library of the Institute shall make it available for inspection and circulation in accordance with its regulations governing materials of this type. I agree that permission to copy from, or to publish from, this dissertation may be granted by the professor under whose direction it was written, or, in his absence, by the Dean of the Graduate Division when such copying or publication is solely for scholarly purposes and does not involve potential financial gain. It is understood that any copying from, or publication of, this dissertation which involves potential financial gain will not be allowed without written permission.

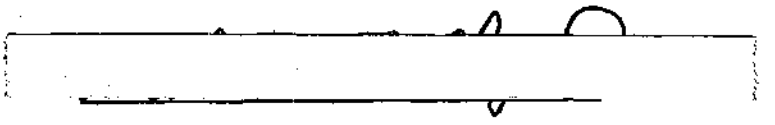

3/17/65
b

THERMODYNAMIC ANALYSIS OF VISCOUS COMPRESSIBLE FLOW IN A NOZZLE CONSIDERING REAL GAS EFFECTS

A THESIS

Presented to

The Faculty of the Graduate Division

by

William S. Shepard

In Partial Fulfillment

of the Requirements for the Degree

Doctor of Philosophy

in the School of Mechanical Engineering

Georgia Institute of Technology

June, 1965

THERMODYNAMIC ANALYSIS OF VISCOUS COMPRESSIBLE FLOW IN A NOZZLE CONSIDERING REAL GAS EFFECTS

Approved:

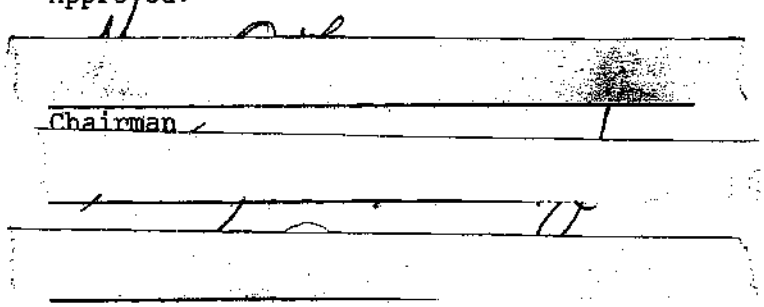

Chairman

Date approved by Chairman: 21 Feb, 1966

ACKNOWLEDGMENTS

I cannot conceive of a better time or place to sincerely and gratefully thank the many people who have contributed to the writing of this dissertation by giving me more than my share of moral and financial support. I especially want to express my gratitude to my wife for her patience, understanding, and the perseverance without which this thesis might never have been completed; my advisor, Dr. W. O. Carlson, whose guidance, encouragement and assistance were fundamental to the writing of this dissertation; my readers, Dr. C. W. Gorton and Dr. H. A. McGee, Jr.; and the Rich Electronic Computer Center for its time and assistance with this work.

Finally and certainly not least, I wish to express my gratitude to the Southern Fellowship Foundation, the Ford Foundation, and the Mechanical Engineering Department at Georgia Tech for their generous financial support.

TABLE OF CONTENTS

LIST OF TABLES

LIST OF ILLUSTRATIONS

SUMMARY

The objective of this research is to investigate analytically the flow through a supersonic nozzle, including the effects of heat transfer, friction, and chemical reaction imposed by the boundary layer region. Although the research was stimulated by interest in plasma jet engines, the results are applicable to any nozzle that is supplied with a high temperature dissociated gas in laminar flow.

A possible application of this research would be for a nozzle on a space vehicle rocket engine with a thrust in the vicinity of one pound. Hydrogen would be used for the propellant, being supplied to the nozzle at a pressure of one atmosphere and a temperature of 9,000°R.

It is assumed that the solution to the nozzle flow is completely divorced from the events that take place within the thrust chamber and that a uniform velocity gas in thermodynamic equilibrium enters the nozzle. There is no ionization present in the gas, it being a binary mixture of monatomic and diatomic species of the same element.

The solution to the flow is divided into two regions, an inviscid core and a boundary layer region. The inviscid core solution is straightforward and is easily handled by conventional one-dimensional compressible flow equations. Consideration is given to the effect of the boundary layer on the inviscous core solution and it is assumed that thermodynamic equilibrium exists up to the nozzle throat with frozen flow continuing to the nozzle exit.

The major effort of this analysis is concentrated on solving the

boundary layer flow through the nozzle. Local similarity is assumed to exist in the boundary layer throughout the nozzle. For the solutions, the Lees-Dorodnitsyn transformations are applied to the axially-symmetric boundary layer equations to transform them into total differential equations. The resulting differential equations are of the two-point boundary value type with four boundary conditions at the wall and three in the free stream.

Variable properties are used in the solution of the boundary layer equations. Since hydrogen is most likely to be used in actual applications, expressions for viscosity, thermal conductivity, diffusion coefficient, Prandtl number, and Schmidt number are developed for hydrogen as a function of the similarity variables and these functions are used in the integration of the viscous flow equations. The expressions for thermal conductivity, thermal diffusion, and Schmidt number evolved indirectly from Enskog's solutions to Boltzmann's equations for the singlet-velocity distribution function. Across the boundary layer the change in the Prandtl number is very small, and therefore it is assumed constant for the calculations.

The boundary layer is considered to be frozen with a fully catalytic wall; therefore, the atom concentration at the wall is determined by the temperature of the wall.

The three boundary layer equations are reduced to seven first order equations so that they can be integrated numerically by the Runge-Kutta method on the Burroughs B5000 electronic computer. For integration, the initial value technique is used with assumed values of the velocity, enthalpy and concentration gradients at the wall. Four

separate integrations are carried out across the boundary layer to an η of 7 with a small change in each of the assumed gradients for the last three integrations. A linear interpolation procedure is then used to evaluate better values of the gradients at the wall, and the integration procedure is repeated until the boundary conditions in the free stream are satisfied. For each integration 140 steps are used to give accuracy without very prolonged use of computer time. In all, 65 solutions are obtained for various values of pressure gradient, dissipation, wall enthalpy and wall concentration functions.

Of the unknown boundary values at the nozzle wall, the enthalpy gradient is the only one insensitive to changes in the imposed flow conditions for high temperature walls. The greatest percentage variation is experienced by the surface velocity gradient with the concentration gradient variation being more than the enthalpy gradient change. However, under the restriction of a highly cooled wall, the surface gradients satisfy the requirements of total similarity.

When the dimensionless pressure gradient parameter is greater than 1 and the dissipation function is near zero an interesting result occurs: the displacement thickness is negative. In the boundary layer, a decreasing temperature causes a density increase while the presence of friction reduces the velocity, but the average density velocity product increases, which results in the mass flow rate per unit area being greater in the boundary layer than in the inviscid core.

An analysis of a particular nozzle, one with 9000°R hydrogen entering it at a pressure of one atmosphere, is presented. The inviscous flow is solved for the pressure gradient and dissipation function param-

eters. The property gradients at the wall along with momentum and displacement thickness are presented for this particular nozzle and the local similarity assumption is shown to be valid.

Heat transfer and friction reduce the specific impulse of this nozzle by 11 per cent when a wall temperature of 4700°F is considered. It is shown that by decreasing the wall temperature the performance of the nozzle is further reduced, which is expected.

For the 4700°R wall the heat transfer rates are as high as 40 Btu/in^2-sec. With a single component mixture, at the same conditions, the heat transfer would be a factor of 4 less, illustrating that the recombination of atoms at the surface contributes greatly to the overall cooling load for a nozzle.

The only refined analysis, previously presented for small nozzles, accounted for heat transfer and friction, but the assumption of a constant pressure gradient parameter restricted its results (27). For the design of conventional rocket nozzles, the method presented in this research is too complex, since excellent results can be obtained by considering one-dimensional, frictionless, isentropic flow; and, if it is necessary to correct the solution for the effects of heat transfer and friction, velocity and thrust coefficients can be utilized.

The most important application will be in the design of nozzles for heat transfer experiments with a high velocity dissociated gas. It is possible to predict the heat transfer rate, in order that adequate cooling can be provided for the selected materials, or a suitable material can be chosen. For a given mass flow rate, proper throat sizes can be calculated, or the mass flow rate can be accurately determined for the particular throat.

NOMENCLATURE

English Letters		Units
B	defined by Equation (4-13)	dimensionless
C	mass friction	dimensionless
C_p	specific heat	Btu/lb-°R
D	defined by Equation (4-17)	dimensionless
D_i	diffusion coefficient of component i into the mixture	ft^2/sec
D_{HH_2}	binary diffusion coefficient for an H-H_2 mixture	ft^2/sec
D_i^T	thermal diffusion coefficient	ft^2/sec
F	thrust	lb
f	defined by Equation (4-4)	dimensionless
g	defined by Equation (4-4a)	dimensionless
g_I	defined by Equation (4-23)	dimensionless
h	enthalpy	Btu/lb
h_A^o	enthalpy of formation of atoms	Btu/lb
I	stagnation enthalpy	Btu/lb
I_{sp}	specific impulse	sec
J	defined by Equation (4-29)	dimensionless
K	thermal conductivity	Btu/ft-sec-°R
k	Boltzmann's constant	erg/molecule-°K
L	Lewis number, $\frac{Pr}{S}$	dimensionless
M	molecular weight	lb/lb mol

English Letters		Units
$\bar{M}$	Mach number	dimensionless
$\dot{m}$	mass flow rate	lb/sec
P	pressure	lb/ft^2
Pr	Prandtl number, $\frac{\mu C_p}{K}$	dimensionless
Q	dummy variable	none
$\dot{q}$	heat transfer rate	Btu/in^2-sec
R	nozzle radius	ft
$\bar{R}$	universal gas constant	Btu/lb mol-°R
S	Schmidt number, $\frac{\mu}{\rho D_{12}}$	dimensionless
T	absolute temperature	°R
u	x component of velocity	ft/sec
v	y component of velocity	ft/sec
V	ideal nozzle exit velocity	ft/sec
w	mass rate of formation per unit volume	lb/ft^3-sec
x	coordinate	ft
$\bar{x}$	transformed x coordinate	lb^2/sec^2
y	coordinate normal to x	ft
Y	defined by Equation (5-57)	ft
Z	defined by Equation (4-4b)	dimensionless

Greek Letters		
α	mass fraction of atoms	dimensionless
γ	specific heat ratio	dimensionless
δ	thickness of momentum boundary layer	ft

Greek Letters		Units
δ^*	displacement thickness	ft
η	coordinate across boundary layer	dimensionless
μ	absolute viscosity	lb/ft-sec
θ	momentum thickness	ft
ρ	density	lb/ft^3
ψ	stream function	lb/sec

Subscripts

A	refers to monatomic molecules
A_2	refers to diatomic molecule
e	refers to edge of boundary layer
et	refers to edge of boundary layer at the throat
f	refers to perfect gas portion of enthalpy
H	refers to monatomic hydrogen
H_2	refers to diatomic hydrogen
i	refers to ith species
w	refers to the wall

Superscripts

-	denotes a dimensionless property
'	denotes differentiation with respect to the variable η

CHAPTER I

INTRODUCTION

For some time in the future, chemical rockets will be the device used by the space industry to launch equipment into orbit from the earth's surface. This is due to the large thrusts developed by chemical rockets, their present advanced stage of development, and their adaptability to very large vehicles. The nuclear powered rocket is the only other propulsion device under current investigation that has a high enough thrust-to-weight ratio to overcome the earth's gravitational attraction.

Specific impulse is one of the most important performance parameters used for evaluating rocket engines, and it is defined as the ratio of the thrust developed to the rate of propellant consumption. Consider a rocket engine with an optimum expansion ratio, i.e., the nozzle exit pressure is equal to the surrounding atmospheric pressure. It can be shown (2) that the specific impulse, I_{sp}, is given by

$$I_{sp} = \left[\frac{2 \gamma \bar{R} T_c}{(\gamma-1) g M} \eta_p \right]^{1/2} \qquad (1\text{-}1)$$

where

$$\eta_p = 1 - \left(\frac{P_{ex}}{P} \right)^{\frac{\gamma-1}{\gamma}} \qquad (1\text{-}2)$$

Thus the specific impulse is a function of the variables η_p, γ, T_c, and M. For space applications, the surrounding atmospheric pressure is near zero; therefore the restrictions on η_p will be independent of the particular propellant, gas generator, or combustion chamber, since any nozzle pressure ratio can be obtained. The specific heat ratio for gases in rocket exhausts will vary between 1.2 and 1.67 (42), and with a fixed combustion chamber temperature and gas molecular weight the specific impulse can be increased 55 per cent by reducing k from 1.67 to 1.2; however, in actual practice this cannot readily be accomplished. Therefore, in order to obtain the highest specific impulse of a rocket propellant, the combustion chamber temperature should be increased to material limits and the molecular weight reduced as much as possible.

For a rocket engine which depends upon combustion to provide the energy, the highest specific impulse is obtained with hydrogen and fluorine as the fuel and oxidizer. A propellant mixture with a fluorine-to-hydrogen mass ratio of 7.6 to 1 will supply 1000 psia gas at 7000°R (2). The propellant molecular weight will be 11.8 and its specific heat ratio is 1.33, and under ideal conditions with expansion to space, this will provide a specific impulse of 480 seconds. However, there are still many development problems to be solved before this system can be used successfully.

If it were feasible to use a heated gas, such as hydrogen, then it would be possible to reduce the molecular weight to 1 (atomic hydrogen). With a combustion chamber temperature of 7000°R the specific impulse of the atomic hydrogen would be 1300 seconds.

For space trips the increase in specific impulse realized from

heated hydrogen would result in a considerable reduction in the amount of propellant required, which in turn could lead to much smaller vehicles. Since most vehicles used for interplanetary travel will be launched from earth orbit, it is not necessary to use engines which provide thrust-to-weight ratios greater than one.

Plasma Jet

One type of propulsion device being considered to give very high specific impulses is the plasma or arc jet. The thrust-producing mechanism of the plasma jet is in principle the same as that of chemical rockets; i.e., the thermodynamic expansion of a high temperature propellant through supersonic nozzles to produce thrust. However, the mechanism of providing the high temperature propelling gas is different, since the heating of the gas takes place directly in the gas by an electric arc. Figure 1 illustrates a configuration for a possible plasma jet engine.

The plasma jet is not limited to conventional combustion temperatures and high molecular weight propellants since the energy is supplied by an external electric generator. However, there is an upper limit on temperatures imposed by material requirements and the necessity of providing adequate cooling to the engine. Both of these have to be important criteria in the selection of a desirable propellant.

In Table 1, a comparison of various propellants is given. The specific impulses are based on one half of the available energy being lost due to friction, heat transfer, and incomplete expansion. It is also assumed that there is no ionization in the gas. For a given temperature, hydrogen has the lowest molecular weight and thus the highest

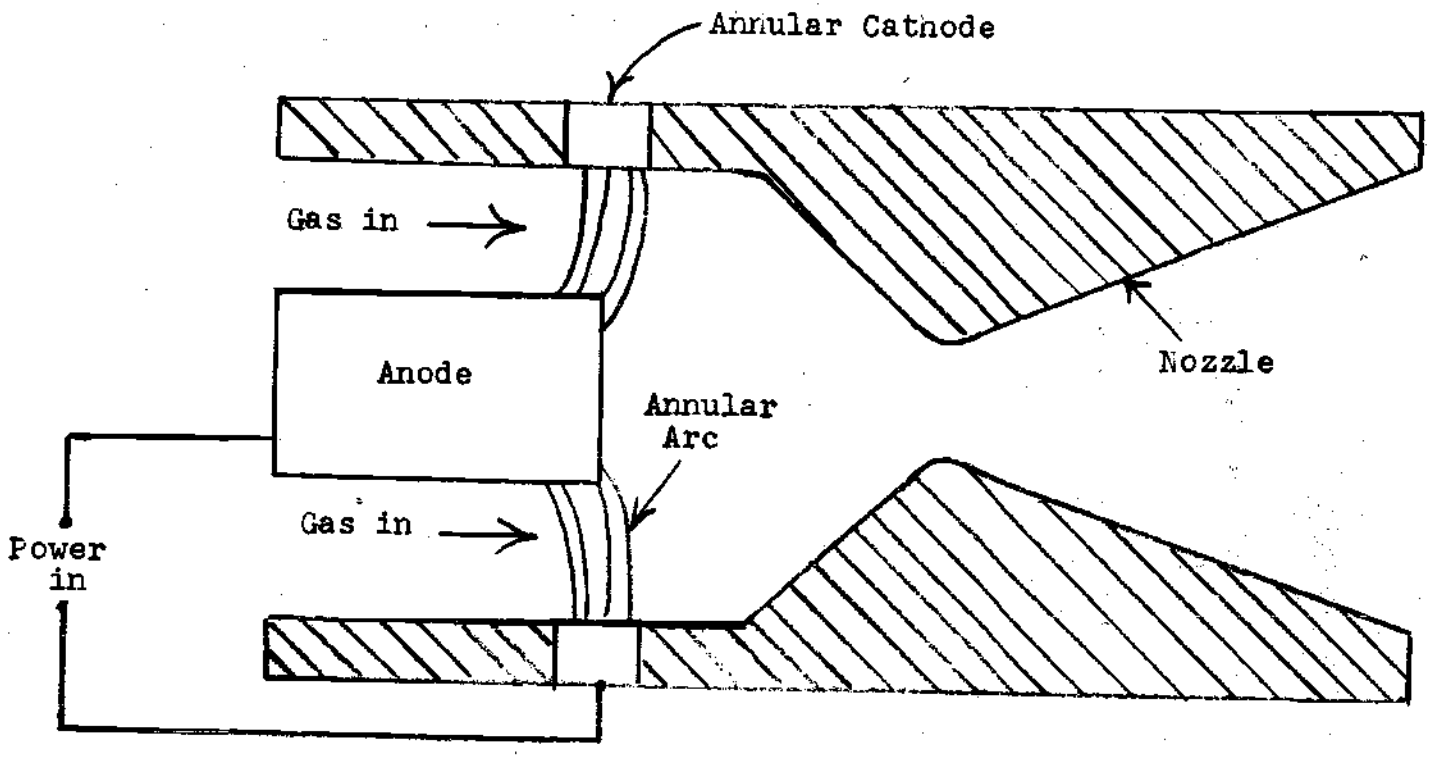

Figure 1. Plasma Jet Schematic

specific impulse, and it is the only gas with a low enough chamber temperature to permit use of refractory materials like carbon, tungsten and tungsten carbide. Use of any of the other propellants would require strong cooling of the chamber and nozzle walls.

If the appropriate design problems are solved, the plasma jet engines can produce specific impulses in the range of 1000 to 2000 seconds. This level of performance will require about 50 kilowatts of electricity per pound of thrust, and the complete propulsion unit including the electrical generator will weigh approximately 500 pounds for one pound of thrust (1).

Table 1. Propellant Performance with 50 Per Cent Conversion Efficiency, Expansion to Zero Pressure and Ionization and Dissociation Neglected.

Gas	Molecular Weight	Specific Impulse in Seconds for Chamber Temperatures of		
		5000°R	10,000°R	15,000°R
H	1	775	1100	1340
H_2	2	730	1035	1280
He	4	388	550	670
L_i	7	290	410	500
N	14	206	295	360
N_2	28	195	275	340

The high weight-to-thrust ratio completely eliminates the possibility of this engine being used to launch equipment from the earth's surface. Some of its possible applications will be orbit corrections for space stations and rotation of these stations about their axes. When it

is necessary to provide an electric generator for normal operation of the space craft, the plasma jet has even greater appeal since it will not be necessary to provide an additional generator for propulsion.

A characteristic comparison of a plasma jet with modern chemical rockets is given in Table 2. In Table 3 the specifications of a one-pound thrust engine is compared with the widely-used H-1 liquid propellant engine. From Table 3 it can be seen that for the arc jet the temperatures are higher, the pressures lower, and the engine is several orders of magnitude smaller than the H-1 rocket engine.

The large thrust rocket engines have very high energy release per unit volume and as a result their heat transfer losses are quite low. Due to the surface area per unit thrust being low, a very small percentage of the kinetic energy of the exhaust gas is dissipated by friction. The combined effects of friction and heat transfer in large rocket engines result in performance losses from 2 to 8 per cent of the total available energy supplied, while the reduction in thrust due to their effects is less. The flow in large nozzles is usually turbulent due to the high densities and large diameters associated with their design. When heat transfer and friction are considered, the analysis is usually simplified by the use of modified empirical methods taken from fully developed flow in constant area pipes.

Arc jet engines tested to date have not met their expected performance specifications, since the thrust produced is much less than anticipated. This reduced performance is partially due to the increased percentage of heat transfer and friction losses associated with the small sizes of the plasma jet engines. It is to be expected that associated

Table 2. Typical Performance Parameters for Rocket Engines[2]

Engine Type	Specific Impulse (sec)	Maximum Temperatures °F	Thrust-to-Weight Ratio	Duration	Specific Power (hp/lb)	Typical Working Fluid
Chemical	200- 480	4,500-7,800	10^{-2}-100	Seconds to a Few Hours	0.1-1000	H_2 & O_2, etc.
Nuclear Fission	500- 1,100	5,000	10^{-2}-30	Same	0.1-1000	H_2
Isotope Decay	400- 700	3,000	10^{-5}-10^{-3}	Days	0.0001-0.01	H_2
Arc Heating	400- 2,000	10,000	10^{-4}-10^{-2}	Days	0.001-1	H_2
Magneto-Plasma	4,000-15,000	...	10^{-5}-10^{-3}	Weeks	0.001-1	H_2
Ion	5,000-25,000	...	10^{-5}-10^{-3}	Months	0.001-1	Cs
Solar Heating	400- 700	2,500	10^{-3}-10^{-2}	Days	0.01-1	H_2

Table 3. Specifications for a 30 KW Plasma Jet and an H-1 Liquid Propellant Engine

Engine	Units	Plasma	H-1
Thrust in Space	Pounds	1	188,000
Chamber Diameter	Inches	1	21
Nozzle Throat	Inches	0.4	16.2
Nozzle Exit	Inches	0.75	45.8
Nozzle Area Ratio		3.7	8.1
Length	Inches	4	86
Propellant		H_2	O_2 & RP-1
I_s in Space	Seconds	1000	288
Thrust	Pounds	1	188,000
Propellant Flow Rate	Pounds/Second	10^{-3}	650
Weight Engine Only	Pounds	4	1500
Power Required	KW	30	---
Thrust Duration		Months	Minutes

with arc jet miniaturization, their lower pressures, higher temperatures and lower mass flow rates, the boundary layer will fill a larger percentage of the total flow area, and this will result in larger performance losses due to the presence of irreversible phenomena.

Arc jet engines will always operate at low pressures in order to take advantage of essentially complete dissociation at lower temperatures and to facilitate satisfactory arc stabilization. The low densities that result, the small diameters of the associated nozzle, and the high viscosity of the high temperature gases will insure that low Reynolds numbers will exist throughout the nozzle. Thus the flow in the plasma jet will still be laminar at the nozzle exit.

In the past it was undesirable to undertake a complete investiga-

tion of the flow through a nozzle considering friction, heat transfer, and chemical recombination due to the complexity of the solution and their relatively small effects on performance. Also, the existing conditions were such as to insure turbulent flow, which makes the solution more difficult. The inadequacies of the available methods to predict the performance of plasma jet nozzles deem it necessary to undertake a more refined investigation. This will not only aid in a more accurate prediction of nozzle performance, but it will help to optimize the system for any given application.

Heat Transfer Experiments

Although the research was stimulated by interest in plasma jet engines, the results will be applicable to any nozzle that is supplied with a high temperature dissociated gas in laminar flow. A source of a high temperature, high velocity, dissociated gas is necessary for many heat transfer experiments, and a nozzle of the type examined here will be required.

In designing nozzles for these experiments, it is necessary to know the heat transfer rates so that proper cooling can be supplied to a suitable material. To give the desired mass flow rate and velocity, the dimensions of the throat and the diverging section have to be correctly chosen. This analysis can be applied directly to such an application.

Objectives

The objectives of this investigation are:

1. To determine analytically the flow solution through a super-

sonic nozzle including the effects of heat transfer, friction, and chemical reaction imposed by the boundary layer region.

2. To apply the results of the analytically determined flow to a particular nozzle.

3. To compare the refined method of analysis to the present method being used.

The first objective requires the solution of the laminar compressible boundary layer equations with chemical reaction. The results of the solution will be presented for various values of local similarity constants and will be applicable to any laminar flow in a nozzle. The various parameters determined will be tabulated in convenient form.

The second and third objectives will be restrictive in the sense that they will apply to only one particular nozzle; however, the procedure to apply them to any nozzle will be clearly described.

CHAPTER II

RELATED RESEARCH

Introductory Remarks

A brief review of related investigations in the fields of laminar boundary layers, rocket nozzles, and plasma jet performance is presented below. The papers mentioned are intended to illustrate the evolution of methods and ideas which lead finally to the subject of nozzle performance as well as the reason for the present analysis.

During the past decade there have been voluminous analytical and experimental investigations into the solution of compressible boundary layer flows, both with and without chemical reaction. However, no one has undertaken a complete investigation considering simultaneously the effects of friction, heat transfer, and chemical recombination on the performance of small throat diameter rocket nozzles, even though many of these investigations have been applied to chemical rocket nozzles and in one case to the flow of ionized gases through a relatively small nozzle.

Boundary Layer

Since its inception by Prandtl in 1904, the theory of thin viscous layers next to solid boundaries, or boundary layer theory, has become a highly developed branch of fluid mechanics. According to Prandtl, the fluid velocity relative to the surface of the body increases from zero at the surface to its maximum value away from the surface in a thin region or boundary layer. This well established fundamental postulate of

fluid mechanics has been directly confirmed by careful measurements of the velocity distribution through the boundary layer region.

Compressible Boundary Layer

There is no general method for solving the fundamental equations of viscous compressible fluids because of the nonlinearity of the equations. Only for a small number of special cases can exact solutions of the Navier-Stokes equations be found, and in these cases assumptions have to be made considering only the simple configurations of the flow pattern.

The compressible boundary layer analysis is further complicated by the presence of a non-vanishing Mach number and therefore the flow may contain appreciable viscous dissipation. In addition, the velocity and thermal boundary layers are interdependent, requiring the simultaneous solution of the momentum and energy equations. In a rocket nozzle high temperatures are encountered which lead to dissociation of the gases present. Additional equations, species continuity, have to be simultaneously satisfied, thus further complicating the solution.

A treatise of the laminar boundary layer in compressible flow has been provided by Cope and Hartree (3), in which the boundary layer equations are derived, reduced to non-dimensional form, and their relation to incompressible flow discussed. Solutions for a few simple cases are presented and methods of solution of more complex problems are outlined. No consideration was given for the case where more than one species was present.

Kármán-Pohlhausen Method

The mathematical difficulty of solving the equations are consider-

able, particularly when there is a pressure gradient along the surface. The Kármán-Pohlhausen method gives an approximate solution to the boundary layer equations with a streamwise pressure gradient, and many of the earlier investigations made use of this method. The solution requires the assumption of velocity and temperature profiles through the boundary layer, and this is its greatest limitation, since in many cases the profiles for sufficient accuracy are so complex that it is very difficult to obtain a solution. All of the papers discussed in this section make use of the Chapman-Rubesin linear viscosity law for the variation of viscosity with temperature through the boundary layer. Only one of the papers dealt with a dissociating gas.

Fourth, sixth, and eighth-order polynomials for the velocity profiles and sixth-order temperature profiles were used by Morris and Smith (4). Arbitrary, but constant Prandtl number, and laminar flow with arbitrary surface temperature and pressure gradients were assumed. Comparisons were presented with exact solutions. Beckwith (5) used a fifth-degree polynomial stagnation enthalpy profile for the case of equal thickness for the thermal and velocity boundary layers. However, the calculations were extended to determine the heat transfer under conditions of equilibrium dissociation in the boundary layer.

Libby and Morduchow (6) used sixth degree velocity profiles and seventh degree stagnation enthalpy profiles for calculating the boundary layer characteristics with an axial pressure gradient and heat transfer. For accuracy, the solution was limited to a Prandtl number of one, and to a uniform wall temperature for flow with a pressure gradient.

Yang (7) presented an improved integral procedure, in which more

accurate profiles are obtained by applying a correction to the assumed profiles to make them more closely agree to the original partial differential equations. Comparisons with some exact solutions for flow with favorable and adverse pressure gradients were given.

Similar Solutions

Similar solutions are presented to the boundary layer equations by Cohen and Reshotko (8), in which they solved Stewartson's equations with pressure gradients varying from that causing separation to an infinitely favorable gradient and wall temperatures from absolute zero to twice the free stream stagnation temperature. It was shown that the velocity within a portion of the boundary layer must exceed the local external velocity for the case of favorable pressure gradients with heated walls. Thwaites' correlation concept was used for an approximate method to extend their work (9) with heat transfer and arbitrary pressure gradient. The advantage of the latter method is that knowledge of the velocity and temperature profiles is not required. The linear Chapman-Rubesin viscosity law was used in the analysis.

A study of compressible viscous flows in slender channels was provided by Williams (10); however, this work applied to very low Reynolds numbers. Similar solutions were presented for many particular applications.

Baron (11) performed an elegant and thorough investigation for a binary mixture boundary layer associated with mass transfer cooling at high speeds. Even though Baron concentrated on exact similar solutions, an integral method was developed. In his work the mass diffusion equa-

tions are solved for cases where carbon dioxide or helium is injected into the boundary layer to cool the surface exposed to aerodynamic heating in air.

Chemical Reactions

The necessity to safely land objects from orbit required the solution of the problems associated with reentry into the earth's atmosphere from space. Thus many investigations of the laminar boundary layer with chemical reactions were initiated. One of the first published was by Fay and Riddell (12), in which two methods of numerical solutions for the stagnation point equations were presented; one for the equilibrium case, the other for the non-equilibrium case. In the non-equilibrium case both catalytic (to atom recombination) and non-catalytic wall surfaces were considered. A solution was presented that showed the transition from the frozen boundary layer to the equilibrium boundary layer.

Lees (13) gave an account of progress and problems in convective heat transfer with chemical reactions, including reactions involving vaporizing or sublimating surface material. This paper was an excellent treatise of the state of the art at the time of its publication, and it with the previous paper (12) were very useful in the development and solution of this research.

Attention was given to the problem of determining the transport properties of partially ionized air by Fay (14). Comparisons were made of the transport properties which had been estimated by various authors, and the heat transfer determined from the solution of the laminar boundary layer equations for stagnation point flow. The heat transfer was

compared with a few experimental measurements.

An integral method for the calculation of heat transfer distributions on yawed cylinders and bodies of revolution in high speed flow was developed by Beckwith and Cohen (15). Comparisons were made, for a Prandtl number of one and a constant density-viscosity product, with other local similarity methods, with experimental heat transfer data on a circular cylinder, and a body of revolution designed for large axial pressure gradients.

The problem of nonequilibrium boundary layers when chemical reaction occurs along the inviscid flow streamlines at the outer edge was examined by Inger (16). Except in the case of a highly cooled body immersed in a slow, hot, dissociating gas stream, it was shown that the inviscid reaction rate can be neglected in analyzing nonequilibrium boundary layer flows encountered in practice. This does not imply that the chemical state of the inviscid flow does not affect the boundary layer, but if the reaction rate at the outer edge of the boundary layer is not properly matched to the inviscid flow rate, only a small error is experienced in solving the boundary layer equations.

A finite difference method was used by Blottner (17) for numerical calculation of the nonequilibrium ionized air boundary layer on a cone-shaped reentry vehicle at several flight conditions. A method of solution of the laminar boundary layer equations for dissociating and ionizing air in chemical nonequilibrium was formulated for arbitrary pressure gradients and body geometry by Pallone, et al. (18), in which a non-similar, multistrip integral technique was employed.

Smith and Jaffe (19) present a general method for solving the non-

equilibrium boundary layer equations of a dissociating gas for two-dimensional or axisymmetric flow. This was a solution to the complete equations and it did not assume local similarity. The predictor-corrector method was used and the equations were solved simultaneously at a given station in the flow direction with an iteration procedure used between equations until convergence was obtained.

Nozzles

Simple analyses have been sufficiently accurate for calculation of the heat transfer in large nozzles. Regenerative and film cooling have been more than adequate to allow continuous operation of liquid propellant rocket engines. However, long thrust duration, solid propellant engines have required extensive development programs and they have helped stimulate interest in the area of heat transfer in nozzles.

In large nozzles the flow is turbulent and the earlier analyses reflect this. Bartz (20) considered boundary layer flow with the one-seventh power law velocity distribution, and Mayer (21) presented a similar analysis for the estimation of convective heat transfer to the cooled walls of spike nozzles, expansion deflection and other external expansion nozzles. Clem, et al. (22), modified the fully developed pipe flow equations to apply to solid propellant rocket nozzles.

Heat transfer coefficients determined by experiment were provided by Massier, et al. (23), and Witte and Harper (24) for liquid propellant rocket engine nozzles. The heat flux distribution in a rocket nozzle was determined experimentally by Rose (25).

The analysis of the heat transfer to a small nozzle with laminar

flow was performed by Massier, et al. (26), and the analysis utilized Cohen and Reshotko's (8) solution to the laminar boundary layer equations. Two analyses were undertaken for the flow of an ionized gas through the nozzle; one with the density-viscosity product constant throughout the nozzle and one with this product allowed to vary along the nozzle, but the product was not allowed to vary across the boundary layer. In both solutions the Prandtl number was one and the solution was compared with experimental results, and good correlation existed. Further experimental results were presented on this by Massier (27).

Plasma Jet Performance

A survey of the plasma (arc) jet propulsion system was given by Heller and Jones (28). The types of devices generally associated with plasma propulsion were discussed including the closely related resistojet. The survey covered some of the problem areas, such as performance parameters, heat transfer problems, and energy balance.

A later survey was presented by Page (29), in which discussions of the development interests of plasma jets were given, and some of the areas of interest were arc mechanism, production methods, propellant choice, heat transfer, materials and the space power source. It pointed out that the present state of the art is a result of primarily empirical and experimental work.

Jack (30) demonstrated the advantages of hydrogen as a propellant. Hydrogen was shown to have the highest frozen flow efficiency and the lowest temperatures of any propellant in the thousand seconds impulse range. For optimum performance in this range a chamber pressure of the

order of magnitude of one atmosphere is desirable. Hydrogen was the only propellant that can provide reasonable specific impulses with conventional materials in the resistojet.

Bennett, et al. (31), gave experimental results on a fast heatup resistojet, and their engine had a thrust of 0.0003 pounds with a power input of 20 watts, and used ammonia at the rate of 0.5×10^{-6} pounds per second. The nozzle throat diameter was 0.012 inches and the specific impulse was limited to approximately 200 seconds.

Summary of Related Research

Solutions presented in the laminar boundary layer investigations usually pertained to flow over a body of revolution, and are restricted in many cases to the stagnation point region. Only a few of them pertained to flow through a nozzle and when they did they were severely restricted.

The large nozzle analyses are primarily concerned with the turbulent boundary layer, which is not applicable to the small nozzles of plasma jet engines where laminar flow exists. In many of the laminar flow solutions the flow is external to a body, thus the flow is not confined. In a nozzle the inviscid core is confined externally by the boundary layer and wall.

With the introduction of the low mass flow rates and high temperatures of the plasma jet nozzle there is a great need for a thermodynamic analysis of the viscous flow in a nozzle considering real gas effects.

This research will satisfy the following five requirements:

1. A changing favorable pressure gradient in the inviscid flow

through the core of the nozzle.

2. The consideration of the effect of chemical recombination of the dissociated gases on the boundary layer along the nozzle.

3. The consideration of the effects of variable thermodynamic and transport properties in the boundary layer analysis.

4. Determination of the boundary layer characteristics within the nozzle.

5. An evaluation of the effects of friction and heat transfer on the performance of a typical plasma jet engine.

CHAPTER III

DEVELOPMENT OF THE PROBLEM

Very little error is obtained when viscous boundary layer effects are neglected in large nozzles, but this is not true with small nozzles. In designing small nozzles for heat transfer experiments or in evaluating the performance of any small rocket engine, it is desirable that the boundary layer be analyzed along with the inviscid core, since both solutions are necessary for an accurate prediction of the flow properties.

Plasma Jet Operation

The determination of the performance of an arc jet engine mathematically is made very complex by restrictions on the flow imposed by the small nozzle dimensions. This was briefly discussed in the previous chapters. A typical configuration for an engine is given in Figure 1. In an actual engine the possibility of obtaining an annular arc is very limited since the arc will always occur along the path of least resistance between the anode and cathode, and it usually has a very small cross sectional area. Thus, when the gas is fed axially into the thrust chamber it will be very difficult to obtain a uniform gas temperature at the nozzle entrance, since there will be little time for mixing to occur between the arc and nozzle and due to the small arc. A small percentage of the total gas will be heated to a very high temperature and the rest must depend upon the heat transfer from the anode, cathode, and slight mixing from the hot gas for its energy.

Researchers at General Electric proposed the development of a three phase alternating current arc with three cathodes placed around the circumference of the chamber. This would set up a rotating arc which would aid in supplying a homogeneous mixture to the nozzle. The advocates of the direct current arc have suggested, and indeed it has been attempted, putting the cathode downstream of the nozzle throat so that the arc passes through the throat, which would allow it to fill a large percentage of the total flow area.

Mixing can be aided by introducing the gas tangentially to the nozzle axis and providing it with a large radial velocity component. The swirling action will aid the mixing action in the chamber and will provide a more homogeneous mixture into the nozzle. However, the uniform mixture is gained at the expense of increased irreversibilities in the flow and much greater heat transfer to the system's walls, and providing an additional cooling problem.

A large amount of development work must be done in the future on arc stabilization between the anode and cathode for optimum performance of plasma jet engines. In addition, excellent nozzle design and life will be required. It is also very important that a uniform mixture be supplied to the nozzle with as few irreversibilities present as possible in order for the engine to efficiently utilize the electrical energy supplied.

This work will be restricted to an analysis only of the flow through the nozzle. It will be assumed that the arc is far enough removed from the nozzle such that the flow through it will be independent of the arc operation. This solution would also apply to cases where the

gas is heated by means other than an arc.

Assumptions and Restrictions

The assumptions made and the restrictions placed on the analysis are discussed below for the flow at the nozzle entrance, for the inviscid core, and for the viscous boundary layer near the nozzle wall.

Nozzle Entrance Conditions

The most promising propellant for an external energy source rocket engine is hydrogen (2,30). Thus, for all considered applications a diatomic gas is used for the propellant. Materials used in construction of the engine and the long operation time will place a limitation on the temperature in the thrust chamber. Pressures of the order of magnitude of one atmosphere are optimum for the most efficient engines.

Temperatures and pressures will be such that considerable dissociation will be present in the gas, and ionization will be neglected. For hydrogen, only 0.003 of the atoms are ionized at a temperature of 14,400°R and a pressure of 14.7 psia (42). In many cases, the equilibrium condition will consist only of monatomic gas. When the gas passes through the arc there will be some ionization present; however, it is assumed that there is sufficient time in the thrust chamber prior to the nozzle for recombination of all ionized products of the arc, and complete thermodynamic equilibrium will be established in the system prior to the time the flow enters the nozzle. The flow entering the nozzle will be one-dimensional and will have a uniform axial velocity.

Inviscid Nozzle Flow

A uniform velocity gas in thermodynamic equilibrium will enter the

nozzle, and at the point of entrance there will be two distinct regions of flow. The boundary layer will start its development here (32) and it, along with the inviscid core, will fill the nozzle.

In the inviscid region there will be very small axial velocity gradients normal to the flow direction and the average radial velocity will be zero, thus the effects of viscosity can be neglected, and the flow can be considered one dimensional.

The temperature and pressure will decrease as the gas expands through the nozzle and to maintain thermodynamic equilibrium there must be some recombination of the atoms. The average velocity is so high that the residence time in the nozzle will be of the order of ten micro-seconds, thus it will be impossible for thermodynamic equilibrium to exist throughout the nozzle. Bray (34) suggests that the shift from equilibrium flow to frozen flow will occur downstream of the nozzle throat, and Lezberg and Lancashire (35) have some experimental evidence to substantiate this with a hydrogen air combustion process.

For a practical compromise it will be assumed that the flow is in equilibrium up to the nozzle throat, and that frozen flow will predominate in the supersonic section. A decreasing temperature will tend to shift equilibrium conditions from the atomic to the molecular state, but this is offset by a decreasing pressure which causes a shift in the other direction. Also, the energy released by the atoms reassociating will offset the normal temperature drop of expansion so there is only a small temperature drop in accelerating the flow to Mach one. Therefore, only a small change in composition will be experienced in the subsonic section.

To solve for the inviscid core properties in the subsonic region a pseudo-frozen flow will be assumed. A suitable average value will be taken for the composition and stagnation properties, and allowances will be made for the recombination energy, which actually aids the engine performance, by using a modified specific heat ratio.

The flow area is restricted by the boundary layer development, and allowances have to be made for this. Other than this necessary precaution, there is no difficulty in solving the inviscid core region of the nozzle flow. The solution methods are given by Shapiro (33).

Viscous Nozzle Flow

The flow is completely nonviscous prior to the time it enters the nozzle, and the growth of the boundary layer will start along the nozzle wall at the point of entrance where it is of zero thickness (32). There is no chance of separation occurring anywhere in the nozzle due to a favorable pressure gradient.

Due to the high temperature and the low pressure for the propelling gas, the viscosity is high and the density is low. In addition, the nozzle dimensions are small; thus, even with high velocities, the Reynolds number will be small enough to give only laminar flow. For example, a typical engine with hydrogen gas might have a nozzle area ratio of 4, chamber pressure of 1 atmosphere, chamber temperature of 9000°R and nozzle length of 1.3 inches. This should produce a thrust of 1 lb., and the Reynolds number based upon length will be less than 5000. Therefore, the pressure and the size could be increased by an order of magnitude before the flow will become turbulent in the nozzle.

It is not feasible at this time to undertake a solution of the

applicable Navier Stokes energy and continuity equations. The boundary layer equations, a set of four nonlinear partial differential equations, must be solved simultaneously to obtain the desired solution. Except for a few simple cases, it is impracticable even to obtain an exact solution to the boundary layer equations.

In Appendix A the boundary layer equations are developed by use of an order of magnitude analysis on the complete equations. The applicable boundary layer equations, (A-17), (A-18), (A-19), and (A-20), are given below with the coordinate system illustrated in Figure 2.

1. Global Continuity

$$\frac{\partial(\rho u R)}{\partial x} + \frac{\partial(\rho v R)}{\partial y} = 0 \qquad (3\text{-}1)$$

2. Momentum

$$\rho u \frac{\partial u}{\partial x} + \rho v \frac{\partial u}{\partial y} = \frac{-dP}{dx} + \frac{\partial}{\partial y}\left[\mu \frac{\partial u}{\partial y}\right] \qquad (3\text{-}2)$$

3. Energy

$$\rho u \frac{\partial I}{\partial x} + \rho v \frac{\partial I}{\partial y} = \frac{\partial}{\partial y}\left[\frac{\mu}{Pr} \frac{\partial I}{\partial y}\right] + \frac{\partial}{\partial y}\left[\mu\left(1 - \frac{1}{Pr}\right) \frac{\partial \frac{u^2}{2}}{\partial y}\right] \qquad (3\text{-}3)$$

$$+ \frac{\partial}{\partial y}\left[\sum_i \rho D_i h_i \left(1 - \frac{1}{L_i}\right) \partial \frac{C_i}{\partial y}\right]$$

4. Species Continuity

$$\rho u \frac{\partial C_i}{\partial x} + \rho v \frac{\partial C_i}{\partial y} = \frac{\partial}{\partial y}\left[\rho D_i \frac{\partial C_i}{\partial y}\right] + w_i \qquad (3\text{-}4)$$

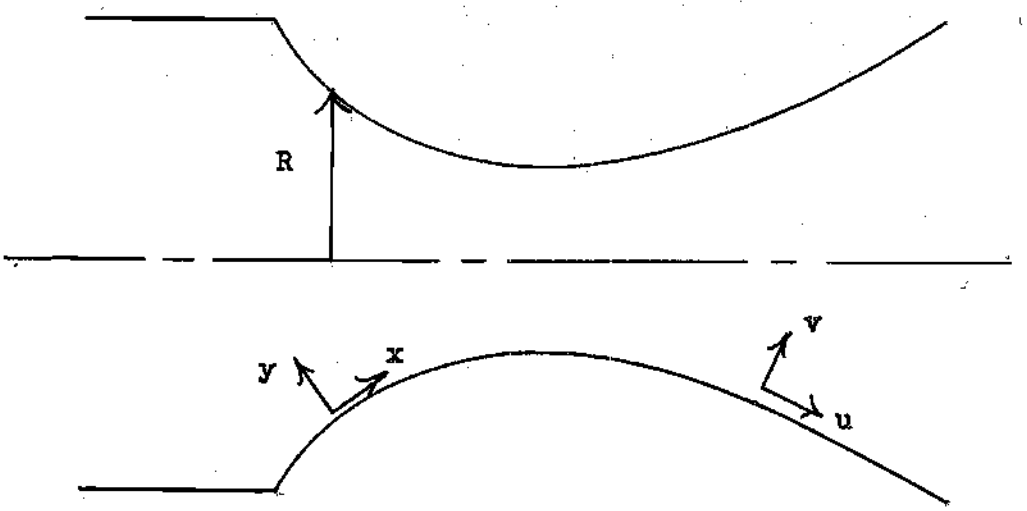

Figure 2. Coordinate System for Boundary Layer Equations.

The complete equations would normally contain a term applicable to thermal diffusion. However, Baron (11) states that for Mach numbers less than five the effects of thermal diffusion can be neglected. In this thesis the largest Mach number considered was 3.5. Fay and Riddell (12) concur with this for an air equilibrium boundary layer at stagnation temperatures less than 18,000°R. Thus, even though the above statements may not apply to hydrogen, the thermal diffusion effects are neglected in all solutions presented in this dissertation, and the

appropriate terms are left out of the energy and species continuity equations.

For solving these equations, it is most convenient to transform them to total differential equations. Then they will be integrated by numerical techniques through the use of an electronic computer. The method of solution of the viscous flow region is left to Chapter IV.

Summary of Assumptions and Restrictions

1. An analysis will be performed only on the flow through the nozzle.

2. The flow will be independent of the arc operation.

3. The flow will have a uniform velocity into the nozzle, and it will be nonviscous.

4. The fluid will consist of a mixture of monatomic and diatomic gases of the same element.

5. All gases follow the perfect gas equation of state.

6. The inviscid core will be one-dimensional through the nozzle.

7. Thermodynamic equilibrium will be established upstream of the nozzle and it will continue in the subsonic portion of the nozzle.

8. The properties in the inviscid core will be calculated in the subsonic section as if the flow was pseudo-frozen.

9. The flow will be frozen in the supersonic portion of the nozzle.

10. No ionization products will be present.

11. The viscous flow will be laminar.

12. The boundary layer has zero thickness at the nozzle entrance, and starts to grow at that point.

13. The flow will not separate from the wall under any condition.

14. The boundary layer equations will represent the viscous flow.

15. Thermal diffusion effects will be neglected.

16. The no-slip boundary conditions are applicable to the flow.

CHAPTER IV

THE VISCOUS FLOW EQUATIONS

The solution of the viscous portion of the flow through the nozzle requires the simultaneous solution of Equations (3-1) through (3-4). These equations as stated are nonlinear partial differential equations which cannot be solved by the usual classical methods such as separation of variables, Laplace transforms, etc. They can readily be solved for fully developed pipe flow and couette flow where enough of the terms can be dropped to reduce the equations to ordinary differential equations.

Transformation of the Boundary Layer Equations*

Fortunately there are other circumstances under which these equations can be reduced to ordinary differential equations. Under these circumstances, the solutions are generally designated as "similarity solutions," the set of partial differential equations are reduced to ordinary differential equations by a transformation of the coordinate system in which the derivatives of the dependent variables become separable.

The proper transformation for this set of equations is the Lees-Dorodnitsyn transformations given by Dorrance (36). The appropriate new coordinates $(\bar{x}, \eta)$ are:

---

* In this chapter, the derivations are in essence those given by Dorrance (36), and they are presented here with modifications for completeness.

$$\eta = \frac{\rho_e \, u_e \, R}{(2 \, \bar{x})^{1/2}} \int_o^y \frac{\rho}{\rho_e} \, dy \qquad (4\text{-}1)$$

$$\bar{x} = \int_o^x \rho_e \, \mu_e \, u_e \, R^2 \, dx \qquad (4\text{-}2)$$

The properties with the subscript e are the free stream properties at the edge of the boundary layer and these properties along with the nozzle radius are a function of x only. The stream function, ψ (x, y), is chosen to satisfy continuity; thus, it can be defined by

$$\rho \, u \, R = \frac{\partial \psi(x,y)}{\partial y} \qquad (4\text{-}3)$$

and

$$\rho \, v \, R = \frac{\partial \psi(x,y)}{\partial x} \qquad (4\text{-}3a)$$

Now assume that the boundary layer equations have similar solutions. That is through the boundary layer, at any given x, u, I, and C_i are functions of η only, and they are the same function of η at all values of x. It will be discussed later, but this puts a severe restriction on the solutions. Therefore assume

$$\frac{u}{u_e} = f'(\eta) = \frac{df}{d\eta} \qquad (4\text{-}4)$$

$$\frac{I}{I_e} = g(\eta) \tag{4-4a}$$

$$\frac{C_i}{C_{i_e}} = Z_i(\eta) \tag{4-4b}$$

The functions $f(\eta)$, $g(\eta)$, and $Z_i(\eta)$ are functions only of η and the prime denotes differentiation with respect to η. The stream function is a function of both $\bar{x}$ and η. An adequate expression for ψ that will satisfy Equation (4-3) and global continuity is

$$\psi(x,y) = (2\,\bar{x})^{1/2}\, f(\eta) \tag{4-5}$$

Now apply the transformation equations, Equation (4-1) through (4-5) to the boundary layer Equations (3-1) through (3-4). Since there are many recurrent operations in the boundary layer equations, it is desirable to develop some useful operators. The first of these is

$$\frac{\partial}{\partial x} = \frac{\partial}{\partial \bar{x}} \frac{d\bar{x}}{dx} + \frac{\partial}{\partial \eta} \frac{\partial \eta}{\partial \bar{x}} \frac{d\bar{x}}{dx} \tag{4-6}$$

From Equation (4-2)

$$\frac{d\bar{x}}{dx} = \rho_e\, \mu_e\, u_e\, R^2 \tag{4-6a}$$

which yields when substituted into Equation (4-6)

$$\frac{\partial}{\partial x} = \rho_e \mu_e u_e R^2 \left[\frac{\partial}{\partial \bar{x}} + \frac{\partial}{\partial \eta}\frac{\partial \eta}{\partial \bar{x}}\right] \tag{4-6b}$$

Likewise, for the other coordinate

$$\frac{\partial}{\partial y} = \frac{\rho u_e R}{(2\bar{x})^{1/2}} \frac{\partial}{\partial \eta} \tag{4-6c}$$

Then

$$\frac{\partial \psi}{\partial \bar{x}} = \frac{f(\eta)}{(2\bar{x})^{1/2}} + (2\bar{x})^{1/2} f'(\eta) \frac{\partial \eta}{\partial \bar{x}} \tag{4-6d}$$

Combining Equation (4-6b), (4-6d) with Equation (4-3a) results in the following

$$\rho v = - \frac{\rho_e \mu_e u_e R}{(2\bar{x})^{1/2}} \left[f(\eta) + 4\bar{x} f'(\eta) \frac{\partial \eta}{\partial \bar{x}}\right] \tag{4-7}$$

Also

$$\rho u = \rho u_e f'(\eta) \tag{4-7a}$$

Finally

$$\rho u \frac{\partial}{\partial x} + \rho v \frac{\partial}{\partial y} = \rho_e \rho u_e^2 R^2 \mu_e \left[f'(\eta) \frac{\partial}{\partial \bar{x}} \right. \tag{4-8}$$

$$\left. - \frac{f(\eta)}{2\bar{x}} \frac{\partial}{\partial \eta} - f'(\eta) \frac{\partial \eta}{\partial \bar{x}} \frac{\partial}{\partial \eta} \right]$$

Another useful operator is

$$\frac{\partial}{\partial y} \left[Q \frac{\partial}{\partial y} \right] = \frac{\partial}{\partial \eta} \left[Q \frac{\rho u_e R}{(2\bar{x})^{1/2}} \frac{\partial}{\partial \eta} \right] \frac{\rho u_e R}{(2\bar{x})^{1/2}} \tag{4-9}$$

which reduces to

$$\frac{\partial}{\partial y} \left[Q \frac{\partial}{\partial y} \right] = \frac{\rho u_e^2 R^2}{2\bar{x}} \frac{\partial}{\partial \eta} \left[\rho Q \frac{\partial}{\partial \eta} \right] \tag{4-9a}$$

From the equation of motion for the inviscid core the following is obtained for the pressure gradient

$$\frac{dP}{dx} = - \rho_e u_e \frac{du_e}{dx} \tag{4-10}$$

which becomes in the new coordinate system

$$\frac{dP}{dx} = - \rho_e^2 u_e^2 \mu_e R^2 \frac{du_e}{d\bar{x}} \tag{4-11}$$

First apply these operators and transformations to the momentum boundary layer equation, Equation (3-2);

$$\rho_e \rho u_e^2 R^2 \mu_e \left[f'(\eta) \frac{\partial u_e f'(\eta)}{\partial \bar{x}} - \frac{f(\eta)}{2\bar{x}} - \frac{\partial u_e f'(\eta)}{\partial \eta} \right. \tag{4-12}$$

$$\left. - f'(\eta) \frac{\partial \eta}{\partial \bar{x}} \frac{\partial u_e f'(\eta)}{\partial \eta} \right] = - \rho_e^2 u_e^2 \mu_e R^2 \left[\frac{du_e}{d\bar{x}} \right]$$

$$+ \frac{\rho u_e^2 R^2}{2\bar{x}} \frac{\partial}{\partial \eta} \left(\rho \mu \frac{\partial u_e f'(\eta)}{\partial \eta} \right)$$

Define B, which is a function of η, by

$$B = \frac{\rho \mu}{\rho_e \mu_e} \tag{4-13}$$

Upon carrying out the indicated differentiation in Equation (4-12) and simplifying the momentum boundary layer equation becomes*

$$[B f'']' + f f' = \frac{2\bar{x}}{u_e} \frac{d u_e}{d\bar{x}} \left[(f')^2 - \frac{\rho_e}{\rho} \right] \tag{4-14}$$

Utilizing the same procedure for Equations (3-3), (3-4), the transformed species continuity equation becomes

---

* f, g, Z_i are functions of η only and after each of these terms the functional symbol (η) will be omitted.

$$\left[\frac{B}{S} Z_i'(\eta)\right]' + f Z_i' = \frac{2\bar{x}}{C_{i_e}} f' Z_i \frac{dC_{i_e}}{d\bar{x}} \qquad (4\text{-}15)$$

$$- \frac{2\bar{x} w_i}{\rho_e \rho u_e^2 R^2 u_e C_{i_e}}$$

and for the transformed energy equation

$$\left[\frac{B}{Pr} g'\right]' + f g' = \frac{2\bar{x}}{I_e} f' g \frac{dI_e}{d\bar{x}} + \left[\sum \frac{B}{S_i} h_i \left(\frac{1}{L_i} - 1\right)\right. \qquad (4\text{-}16)$$

$$\left.\frac{C_{i_e}}{I_e} Z_i'\right]' + \frac{u_e^2}{I_e}\left[\frac{B}{Pr}(1 - Pr) f' f''\right]'$$

It is convenient at this time to make the following definitions

$$D = \frac{2\bar{x}}{u_e} \frac{du_e}{d\bar{x}} \qquad (4\text{-}17)$$

$$E = \frac{2\bar{x}}{I_e} \frac{dI_e}{d\bar{x}} \qquad (4\text{-}17a)$$

$$F_i = \frac{h_i}{I_e} C_{i_e} \qquad (4\text{-}17b)$$

$$j = \frac{u_e^2}{I_e} \qquad (4\text{-}17c)$$

$$N_i = \frac{2\bar{x}}{C_{i_e}} \frac{dC_{i_e}}{d\bar{x}} \qquad (4\text{-}17d)$$

$$Q_i = \frac{2\bar{x}\,\omega_i}{\rho_e\,\rho\,u_e\,R^2\,C_{i_e}} \qquad (4\text{-}17e)$$

For the transformed boundary layer equations to be total differential equations, it is necessary that the terms D, E, F_i, j, N_i, and Q_i, which are defined in Equations (4-17), be a function only of η or constant. For the solution presented in this thesis many of these terms are identically zero.

Local similarity will be assumed in the nozzle; i.e., at each point along the nozzle the value of these parameters will be calculated and the boundary layer equations will be integrated with these values assumed constant. The validity of this assumption rests with comparisons of experimental measurements with analytical results, which have been favorable in many previous investigations.

Binary Mixture Simplification

Item 4 on page 28 states that this work will be restricted to an ideal binary gas mixture of atoms and molecules of the same element. Let α represent the mass fraction of atoms, and $1-\alpha$ will represent the mass fraction of molecules. The property of the atoms will be denoted by subscript A_1 and the molecular properties by subscript A_2. The following expressions hold

$$L_{A_1A_2} = L_{A_2A_1} \tag{4-18}$$

$$D_{A_1A_2} = D_{A_2A_1} \tag{4-18a}$$

$$Z_{A_2} = \frac{1-\alpha}{1-\alpha_e} = \left(\frac{1}{1-\alpha_e}\right)\left(1-\alpha_e\ Z_A\right) \tag{4-18b}$$

Upon differentiation with respect to η Equation (4-18b) becomes

$$Z'_{A_2} = -\frac{\alpha_e}{1-\alpha_e} Z'_A \tag{4-18c}$$

The term

$$\sum \frac{B}{S_i}\left(\frac{1}{L_i} - 1\right)\frac{h_i}{I_e} Z'_i\ C_{i_e}$$

in Equation (4-16) reduces to

$$\frac{B}{S}\left(\frac{1}{L} - 1\right)\left[\alpha_e \frac{h_A}{I_e} Z'_A + \left(1 - \alpha_e\right)\frac{h_{A_2}}{I_e}\left(-\frac{\alpha_e}{1-\alpha_e}\right) Z'_A\right] \tag{4-19}$$

$$= \frac{B}{S}\left(\frac{1}{L} - 1\right)\frac{\alpha_e}{I_e}\left(h_A - h_{A_2}\right) Z'_A$$

Since there are only two species present in the mixture only one

species continuity equation is required. The equation for the atoms is to be used.

The transformed total boundary layer equations with the appropriate constants from Equation (4-17) are given below. The simplified summation from Equation (4-19) is substituted in the energy equation, and the resultant equations are functions only of η with the prime signifying differentiation with respect to η.

1. Momentum

$$(B\ f'')' + f\ f'' = D\left[(f')^2 - \frac{\rho_e}{\rho}\right] \tag{4-20}$$

2. Species Continuity

$$\left(\frac{B}{S} Z_A'\right)' + f\ Z_A' = N_A\ f'\ Z_A - Q_A \tag{4-21}$$

3. Energy

$$\left(\frac{B}{Pr} g'\right)' + f\ g' = E\ f'\ g + \left[\frac{B}{S}\left(\frac{1}{L} - 1\right)\frac{\left(h_A - h_{A_2}\right)}{I_e}\ \alpha_e\ Z_A'\right]' \tag{4-22}$$

$$+ j\left[\frac{B}{Pr}\left(1 - Pr\right) f'\ f''\right]'$$

Frozen Boundary Layer

It will be shown in Chapter V that the Lewis Number of the binary gas mixture is close to one, even though it is a function of η across the boundary layer. Under this condition, if there is recombination in the gas phase it will have only a small effect on the magnitude of the heat transfer to the wall. Fay and Riddell (12) showed that for a catalytic wall the stagnation point heat transfer solution is independent of the reaction rate through the boundary layer. It will be shown later that the solution to the applicable equations is insensitive to the atomic concentration at the nozzle wall; i.e., the surface enthalpy and concentration gradients are not affected by the reaction rates in the gas phase.

Thus, it is reasonable to assume a frozen boundary layer, reaction rate of zero, in the gas phase and with the catalytic wall, reaction rate of infinity at the surface, since the nozzle for an engine will usually be constructed of metal which is catalytic to atomic recombination. This assumption of a frozen boundary layer permits an equation simplification without placing a serious restriction on the results obtained.

At the wall the concentration of each species is determined by the wall temperature, since thermodynamic equilibrium is established at the catalytic surface.

The nozzle radius is assumed to be much larger than the boundary layer thickness, therefore the enthalpy gradient at the edge of the thermal boundary layer is zero, thus no energy will be removed from the inviscid core. Therefore, $\frac{d I_e}{d\bar{x}}$ and the term E in Equation (4-22) is zero. The restriction of frozen flow in the inviscid core, as outlined

in Chapter III, requires that the N_A term in Equation (4-21) be zero, and the frozen boundary layer approximation requires the same of Q_A.

In solving the frozen boundary layer equations it is more convenient to work with the ideal gas stagnation enthalpy, rather than the total enthalpy. By removing the enthalpy of formation from the equations, the energy equation is simplified, thus facilitating its solution. Define a new variable

$$g_I = \frac{I_f}{I_{f_e}} \tag{4-23}$$

I_f is the frozen stagnation enthalpy which is for the binary mixture of atoms and molecules

$$I_f = \int_o^T \left[\alpha \left(C_{p_A} \right) + \left(1-\alpha \right) C_{p_{A_2}} \right] dT + \frac{u^2}{2} \tag{4-24}$$

It is desirable to introduce the simplification.

$$h_A - h_{A_2} = h_A^\circ \tag{4-25}$$

Equation (4-25) is exact when the specific heats of the two gases are the same. The following relation for g is obtained

$$g = g_I \frac{I_{f_e}}{I_e} + Z_A h_A^\circ \frac{\alpha_e}{I_e} \tag{4-26}$$

and for g'

$$g' = g'_I \frac{I_{f_e}}{I_e} + Z'_A \, h^o_A \frac{\alpha_e}{I_e} \tag{4-27}$$

Substitution of Equations (4-26) and (4-27) into Equation (4-22) and simplifying gives for the energy equation

$$\left(\frac{B}{Pr} g'_I\right)' \frac{I_{f_e}}{I_e} + f \, g'_I \frac{I_{f_e}}{I_e} + f \frac{h^o_A}{I_e} \alpha_e \, Z'_A = \tag{4-28}$$

$$- \left[\frac{B}{S} \frac{h^o_A \, \alpha_e \, Z'_A}{I_e}\right]' + j \left[\frac{B}{Pr} (1 - Pr) \, f' \, f''\right]'$$

The species continuity equation requires that the last term on the left of Equation (4-28) be equal to the first term on the right. It is convenient at this time to define

$$J = \frac{u_e^2}{I_{f_e}} \tag{4-29}$$

Summary of Equations

The complete set of equations applicable to the frozen boundary layer is:

1. Momentum

$$(B \, f'')' + f \, f'' = D \left[(f')^2 - \frac{\rho_e}{\rho}\right] \tag{4-30}$$

2. Species Continuity

$$\left(\frac{B}{S} Z_A'\right)' + f Z_A' = 0 \tag{4-31}$$

3. Energy

$$\left(\frac{B}{Pr} g_I'\right)' + f g_I' = J \left[\frac{B}{Pr} (1 - Pr) f' f''\right]' \tag{4-32}$$

Seven boundary conditions are required for the solution of the above three equations. It is desirable to have all boundary conditions at one boundary; however, for the nozzle solution this is impossible.

At $\eta = 0$

$$\left.\begin{aligned} f' &= 0 \\ f &= 0 \\ g_I &= g_{I_w} \\ Z_A &= Z_{Aw} \end{aligned}\right\} \tag{4-33}$$

As $\eta \to \infty$

$$\left.\begin{aligned} f' &\to 1 \\ g_I &\to 1 \\ Z_A &\to 1 \end{aligned}\right\} \tag{4-34}$$

If B is constant and D equal to zero then the solution of the momentum equation would be independent and once it was solved the species continuity and energy equations could be easily integrated by quadrature. However, B is a function of η across the boundary layer and its value cannot be assumed constant.

As mentioned previously, it will be assumed that local similarity exists through the nozzle. The pressure gradient parameter, D, and the viscous dissipation term, J, change slowly along the nozzle; however, the equations will be solved at every point with D and J assumed constant at their corresponding local values. It develops for nozzle flow that assuming D and J constant has only a very small effect on the enthalpy, velocity, and concentration profiles in the supersonic section of the nozzle.

To obtain a valid solution to the three non-linear total differential equations it is necessary to solve them simultaneously. This cannot be readily performed in closed form due to the complexity of the equations. The solution is of the two-point boundary value type since there are four boundary conditions at the wall and three boundary conditions at the edge of the boundary layer. A numerical solution is required and it is desirable to utilize the initial value technique to solve equations of this type. One initial value method is to have the three additional boundary conditions represented by unknowns, integrate across the boundary layer to the three final known boundary conditions, and then solve a set of equations simultaneously for the unknown terms. This is prohibitive since it would require the simultaneous solution of approximately 425 equations to obtain a solution of sufficient accuracy.

A modified initial value technique is used to solve Equations (4-30), (4-31), and (4-32) with the boundary conditions given in Equations (4-33) and (4-34). In the use of this technique, values are assumed for the three additional boundary conditions at the wall; the equations are then integrated numerically across the boundary layer, and a procedure is used to modify the initial assumed boundary conditions. New values are calculated. This process is continued until the boundary conditions at the outer edge are satisfied. The solution is presented in Chapter V.

CHAPTER V

NOZZLE FLOW SOLUTION

Introductory Remarks

The objective of this research is to analytically determine the performance of a small nozzle when it is supplied with a dissociated binary gas mixture at a high temperature with a pressure of one atmosphere. Since the nozzle flow is divided into two regions, an inviscid region where inertial forces predominate, and a viscous boundary layer region where the inertial and viscous forces are the same order of magnitude, two interdependent solutions are required.

Due to the dependency of the transport properties on temperature and concentration the complete solution is restricted to a particular nozzle with a specific working fluid. Values of D and J in Equations (4-30) and (4-31) and the free stream properties for the particular nozzle have to be determined from the inviscid solution. Thus, the applicable results for the boundary layer solutions are directly dependent on the properties of the flow obtained from the inviscid solution.

Solutions to the boundary layer equations for a range of values of D and J will be presented. However, these results will be restricted to a dissociated hydrogen working substance flowing through the nozzle and the specified boundary conditions at the wall.

Transport Properties

Before the species continuity, momentum and energy equations can

be integrated, it is necessary to define appropriate expressions for the transport coefficients which appear in the mass, momentum, and energy flux terms of those equations. The purpose of this section is to develop adequate equations for the coefficients of viscosity, diffusion, and thermal conductivity for a mixture of diatomic and monatomic hydrogen.

It is difficult to measure transport properties of a binary gas mixture at the high temperatures associated with a plasma jet nozzle. Very little experimental data are available, and it is necessary to determine analytically mathematical expressions for these properties at the temperatures encountered in the nozzle. The values of the transport coefficients derived in this section evolve indirectly from Enskog's solution to Boltzmann's equation for the singlet-velocity distribution function. Although the values determined for the transport coefficients cannot be experimentally verified, they will be sufficiently accurate to provide meaningful results to the nozzle solution. Later when better values are determined the results can be improved.

Viscosity

Of all the transport coefficients, viscosity is the one that has the most available data. Thus, it was felt that it was not necessary to depend entirely on analytical expressions for the viscosity coefficient when some of the data have been verified at low temperatures.

Spalding (38) presents values for the viscosity of H_2 and H up to 6000°R at low pressures. The values given are based on "Tables of Thermal Properties of Gases," National Bureau of Standards Circular 564,1955. A very simple expression fits his results very satisfactorily. For diatomic hydrogen

$$\mu_{H_2} = \left(\mu_{H_2}\right)_{1000°R} \left(\frac{T}{1000}\right)^{0.64} \tag{5-1}$$

and for monatomic hydrogen

$$\mu_H = \left(\mu_H\right)_{1000°R} \left(\frac{T}{1000}\right)^{0.64} \tag{5-2}$$

From this it develops that

$$\mu_H = \frac{\left(\mu_H\right)_{1000}}{\left(\mu_{H_2}\right)_{1000°R}} \mu_{H_2} \tag{5-3}$$

which reduces to

$$\mu_H = 1.21\ \mu_{H_2} \tag{5-4}$$

For a binary mixture Dorrance (36) states that the preferred expression for mixture viscosity is that proposed by Wilke, which reduces for dissociated hydrogen to

$$\mu = \frac{X_H\ \mu_H}{X_H + 1.26\ X_{H_2}} + \frac{X_{H_2}\ \mu_{H_2}}{X_{H_2} + 0.76\ X_H} \tag{5-5}$$

Spalding (38) suggests the use of the "Square-Root Rule," which is

for hydrogen

$$\mu = \frac{X_H \mu_H + \sqrt{2}\, X_{H_2} \mu_{H_2}}{X_H + \sqrt{2}\, X_{H_2}} \tag{5-6}$$

As shown by Equation (5-4), there is only 21 per cent variation in viscosity from pure H to pure H_2; thus the simpler expression

$$\mu = X_H \mu_H + X_{H_2} \mu_{H_2} \tag{5-7}$$

should give excellent results. As the mole fraction of monatomic hydrogen varies from zero to one there is less than 1 per cent variation in the values of viscosity between Equations (5-5), (5-6) and (5-7). Therefore Equation (5-7) will be used in this work for the mixture viscosity. When the expressions for the viscosity of monatomic hydrogen and diatomic hydrogen from Equations (5-1) and (5-2) are substituted into Equation (5-7), the results agree very closely with the values of viscosity given by King (37) up to a temperature of 9000°R.

In the viscous flow equations the viscosity shows up as a dimensionless ratio in the B term. The appropriate expression for μ/μ_e in terms of α and temperature is

$$\frac{\mu}{\mu_e} = \left(\frac{1 + 0.65\ \alpha}{1 + 0.65\ \alpha_e}\right)\left(\frac{1 + \alpha_e}{1 + \alpha}\right)\left(\frac{T}{T_e}\right)^{0.64} \tag{5-8}$$

Thermal Conductivity

From the Chapman-Enskog theory the thermal conductivity for a monatomic gas is given by (36)

$$K_i = \frac{15}{4} R_i \mu_i \tag{5-9}$$

which gives for monatomic hydrogen

$$K_H = 6.2 R_{H_2} \mu_{H_2} \tag{5-10}$$

For a diatomic gas

$$K = K' (Eu) \tag{5-11}$$

where K' is the value of the thermal conductivity assuming that Equation (5-9) applies and Eu is the Eucken factor to correct for the transfer of energy between the translational and the internal degrees of freedom for the diatomic molecule. The suggested Eucken factor (36) is given by

$$Eu = 0.115 + 0.354 \frac{C_p}{R} \tag{5-12}$$

Using Equations (5-11), (5-12) and the correct value for C_p, to be given later in this chapter, the thermal conductivity for diatomic hydrogen is

$$K_{H_2} = 6.3 R_{H_2} \mu_{H_2} \tag{5-13}$$

Upon comparing Equation (5-13) with Equation (5-10), it can be seen that sufficient accuracy is obtained by

$$K_{H_2} = K_H \tag{5-14}$$

Diffusion Coefficient

The coefficient of self-diffusion for H_2 is from Hirschfelder, Curtis and Bird (30)

$$D_{H_2H_2} = \frac{0.002628 \sqrt{\frac{T^3}{M_{H_2}}}}{P \sigma^2 \Omega^{(1,1)^*}} \tag{5-15}$$

The deviation of any particular molecular model from the idealized rigid-sphere model is given by $\Omega^{(1,1)^*}$ which is a function of the reduced temperature T^*. Where

$$T^* = \frac{kT}{\epsilon} \tag{5-16}$$

The molecule or atom cross section is given by Sigma.

For a binary mixture of H_2 and H

$$D_{HH_2} = \frac{0.0026280 \sqrt{\frac{T^3 \left[M_H + M_{H_2}\right]}{2\left[M_H M_{H_2}\right]}}}{P \sigma_{HH_2}^2 \Omega_{HH_2}^{(1,1)^*}} \tag{5-17}$$

The average values of σ_{HH_2} and $\frac{\varepsilon_{HH_2}}{k}$ are given by

$$\sigma_{HH_2} = \frac{\sigma_H + \sigma_{H_2}}{2} \tag{5-18}$$

$$\frac{\varepsilon_{HH_2}}{k} = \sqrt{\frac{\varepsilon_H}{k} + \frac{\varepsilon_{H_2}}{k}} \tag{5-19}$$

Values of $\frac{\varepsilon}{k}$ and σ are given in Table 4 for H and H_2. These values were obtained by King (37) from experimental data for viscosity.

Table 4. Force Constants for Transport Properties

Gas	σ in Angstroms	ε/k°K
H	2.497	99.8
H_2	2.729	86.1

The appropriate value of $\Omega^{(1,1)^*}$ is tabulated in Hirschfelder, et. al. (39). Utilizing the appropriate values in Equations (5-15) and (5-17) it is possible to obtain the binary diffusion coefficient of the mixture as a function of the self diffusion coefficient of hydrogen. This is

$$D_{HH_2} = 1.3\ D_{H_2H_2} \tag{5-20}$$

Upon comparing the Chapman-Enskog expression for the viscosity of hydrogen with that of the self diffusion coefficient of hydrogen, the following result is obtained

$$\frac{\mu_{H_2}}{\rho_{H_2} \mathcal{D}_{H_2H_2}} = 1.02 \frac{\bar{R}}{A^*} \tag{5-21}$$

where

$$A^* = \frac{\Omega^{(2,2)^*}}{\Omega^{(1,1)^*}} \tag{5-22}$$

Thus, an expression for the diffusion coefficient is obtained as a function of the viscosity of hydrogen, which is very convenient for determining the Schmidt number.

Schmidt Number

The Schmidt number for the mixture is a function of concentration and is given by

$$S = \frac{\mu}{\rho \, D_{HH_2}} \tag{5-23}$$

which becomes when the appropriate values are substituted in

$$S = \left(\frac{1 + 0.65\alpha}{1 + \alpha}\right) \frac{\mu_{H_2}}{1.3\ \rho\ D_{H_2H_2}} \tag{5-24}$$

The density of the mixture is

$$\rho = \frac{\rho_{H_2}}{1 + \alpha} \tag{5-25}$$

Thus

$$S = \frac{(1 + 0.65\alpha)}{(1.3)} S_{H_2} \tag{5-26}$$

At 500°R the Schmidt Number of hydrogen is 0.73 and at 9000°R it is

$$S_{H_2}{}_{9000} = S_{500} \frac{A^*_{500}}{A^*_{9000}} \tag{5-27}$$

From Hirschfelder (39) it can be seen that $A^*_{9000} \simeq A^*_{500}$ and the Schmidt number of hydrogen can be taken as 0.71 throughout the nozzle with excellent accuracy. Finally

$$S = (1 + 0.65\alpha)\ S_o \tag{5-28}$$

where

$$S_o = \frac{S_{H_2}}{1.3} \tag{5-29}$$

Prandtl Number

The specific heat of monatomic hydrogen is constant and at the temperatures encountered in the nozzle the specific heat of diatomic hydrogen is almost constant, since the vibrational mode is almost fully excited. The specific heat of the mixture is

$$C_P = \alpha C_{P_H} + (1 - \alpha) C_{P_{H_2}} \tag{5-30}$$

Using Equations (5-7), (5-10), (5-14) and (5-30) the Prandtl number as a function of composition is

$$P_r = \frac{(1 + 0.65\alpha)(1 + 0.13\alpha)}{(1 + \alpha)} \quad (0.7) \tag{5-31}$$

The Prandtl Number varies from 0.7 to 0.65 as α varies from 0.0 to 1.0. This can be considered a negligible change in comparison with the boundary layer assumptions; therefore, for the solutions the Prandtl Number will be assumed constant and equal to 0.675. It could be considered a variable parameter in the viscous flow solution, but it is thought that the contribution would be negligible. However, the Schmidt number must be considered variable since it has a wide range of values as the concentration changes.

Nozzle

Performance is the primary criteria for rating a nozzle for a rocket engine. For a small rocket engine of approximately one pound thrust it is especially important, and for every application there is an optimum nozzle selection. To obtain this optimum nozzle it would require a very thorough and extensive investigation. This research is concerned with evaluating the effects of friction and heat transfer on nozzle performance, and once the method is developed it is a simple matter to determine the optimum nozzle. Thus, at the present time it is necessary only to choose a nozzle for the purpose of illustrating the method; however, the nozzle chosen should have specifications that are in line with a particular application.

Since most low thrust engines will be operating in space, the optimum nozzle, when neglecting friction and heat transfer, would have a large expansion area ratio. However, this would require a long nozzle whose performance would be impaired when performing with these effects present.

The nozzle chosen for this solution has a convergence and divergence area ratio of four. The convergence half angle starts at approximately 45° and decreases to zero at the nozzle throat where x is 0.4 inches. The divergence half angle increases to 10° in 0.086 inches and then it remains constant until the nozzle exit. Dimensions of the nozzle chosen are given in Figure 3. The cross sectional area of the chamber at the nozzle entrance is much larger than the nozzle area at the entrance. The fluid properties entering the nozzle are:

1. A binary mixture of monatomic and diatomic hydrogen in chemi-

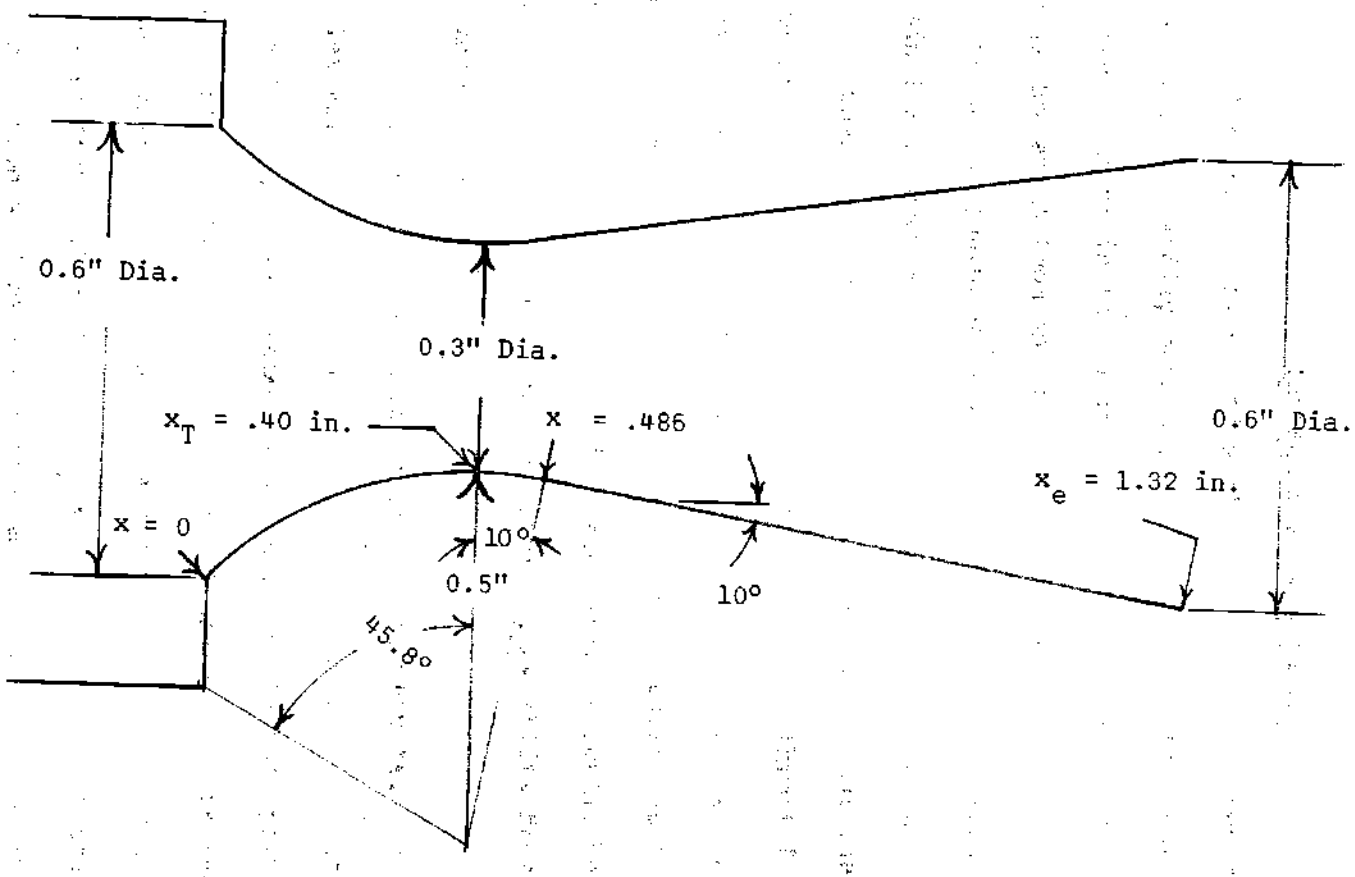

Figure 3. Nozzle.

cal equilibrium at 9000°R and one atmosphere pressure.

2. Uniform velocity profile with flow only in the axial direction.

3. Mass flow rate of 10^{-3} lb/sec.

Inviscous Flow Solution

The analytical solution of the undisturbed free stream through the nozzle is readily obtained by use of one-dimensional isentropic flow theory. Except in the vicinity of the nozzle entrance, there is only a small deviation from an axial velocity for the frictionless flow. This is due to the judicious choice of the particular nozzle, which has a very nominal area change with distance along the nozzle axis.

Chen (40) presents experimental evidence that thermodynamic equilibrium is maintained from the entrance to the throat for the flow of dissociated hydrogen through a nozzle similar to the one under analysis. He concludes that thermodynamic equilibrium exists as long as the time rate of change of the mixture's temperature is small, but when it becomes large in the vicinity of the throat the flow shifts from equilibrium to frozen.

To insure closer application of the results, the free stream properties will be computed assuming equilibrium flow in the entrance section up to the throat and frozen flow downstream of that point. The shifting equilibrium causes a change in composition due to the recombination and is accompanied by a release of energy. Concentration of the atoms will decrease from 0.95 at the nozzle entrance to 0.90 at the throat. This recombination will release sufficient energy to raise the ideal gas stag-

nation enthalpy from 43,950 Btu/lb to 48,170 Btu/lb. In effect, the atomic recombination causes an increase in the stagnation temperature.

Determination of the free stream properties in the nozzle converging section is very difficult when the flow is considered to be in equilibrium, since an iteration process is required. The flow in the entrance section will be treated as pseudo-frozen to facilitate the calculation of the flow properties. A suitable value of n is used for the polytropic process of the gas to account for the heat addition. The properties can then be calculated by use of the perfect gas relations using an average value of the concentration.

In solving for the free stream properties through the nozzle, an n of 1.25 is used in the converging section and a k of 1.629 is used in the diverging section (37). The free stream concentration of H is considered to be 0.93 in the converging section of the nozzle and 0.9 in the nozzle expansion. These values are used throughout in the viscous and inviscous solution.

It was anticipated that the boundary layer would cause a difference in the effective area seen by the frictionless fluid and the nozzle cross sectional area. This difference would lead to errors in determining the free stream properties and would require an iterative solution of both the viscous and inviscous portions of the flow. Fortunately this was not required since the boundary layer displacement thickness was very close to zero for the first 0.5 inch of the nozzle. At this point it started to grow and it became only 0.03 inch at the nozzle exit. Thus only a nominal correction is required in the vicinity of the nozzle exit.

Integration of the compressible flow equations is required for determining the values of D along the nozzle. As shown by Shapiro (33), it is easy to arrive at expressions for the fluid properties as a function of Mach number; but it is difficult to obtain the Mach number as an explicit function of area or x. When integration with respect to x is required it is performed graphically.

All of the free stream properties are made dimensionless by dividing them by their respective properties at the nozzle throat. This dimensionless property is denoted by a bar.

Applying the one-dimensional compressible flow equations to Equation (4-17), D as a function of x in the x, y coordinate system becomes

$$D = \frac{\int_o^x \bar{T}_e^{0.64}\, dx}{A\, \bar{T}_e^{0.64}} \left[\frac{2}{(\bar{M}^2 - 1)} \frac{d\bar{A}}{dx}\right] \qquad (5\text{-}32)$$

Equation (4-29) is repeated for J:

$$J = \frac{u_e^2}{I_{fe}} \qquad (4\text{-}29)$$

Substitution of the dimensionless properties in Equation (4-2) for $\bar{x}$ gives

$$\bar{x} = \int_o^x \rho_{et}\, \bar{\rho}_e\, \mu_{et}\, \bar{\mu}_e\, u_{et}\, \bar{u}_e\, R_t^2\, \bar{R}^2\, dx \qquad (5\text{-}33)$$

ρ_{et}, μ_{et}, u_{et}, and R_t are independent of x and from the global continuity equation for steady flow

$$\bar{\rho}_e \, \bar{u}_e \, \bar{R}^2 = 1 \tag{5-34}$$

Equation (5-3) then reduces to

$$\bar{x} = \frac{\dot{m}}{\pi} \mu_{et} \int_o^x \bar{\mu}_e \, dx \tag{5-35}$$

Rearrangement of Equation (5-8) for $\bar{\mu}_e$ with constant α_e and substituting into Equation (5-35) gives

$$\bar{x} = \frac{\dot{m}}{\pi} \mu_{et} \int_o^x \bar{T}_e^{\,0.64} \, dx \tag{5-36}$$

Within the conditions imposed on the particular nozzle

$$\mu_{et} = 29.2 \times 10^{-6} \frac{\text{lb}}{\text{ft-sec}} \tag{5-37}$$

and

$$\dot{m} = 10^{-3} \text{ lbm/sec} \tag{5-38}$$

D and J are shown as a function of x in Figure 4. The discontinuity in the curve for D is due to the shift from equilibrium to frozen

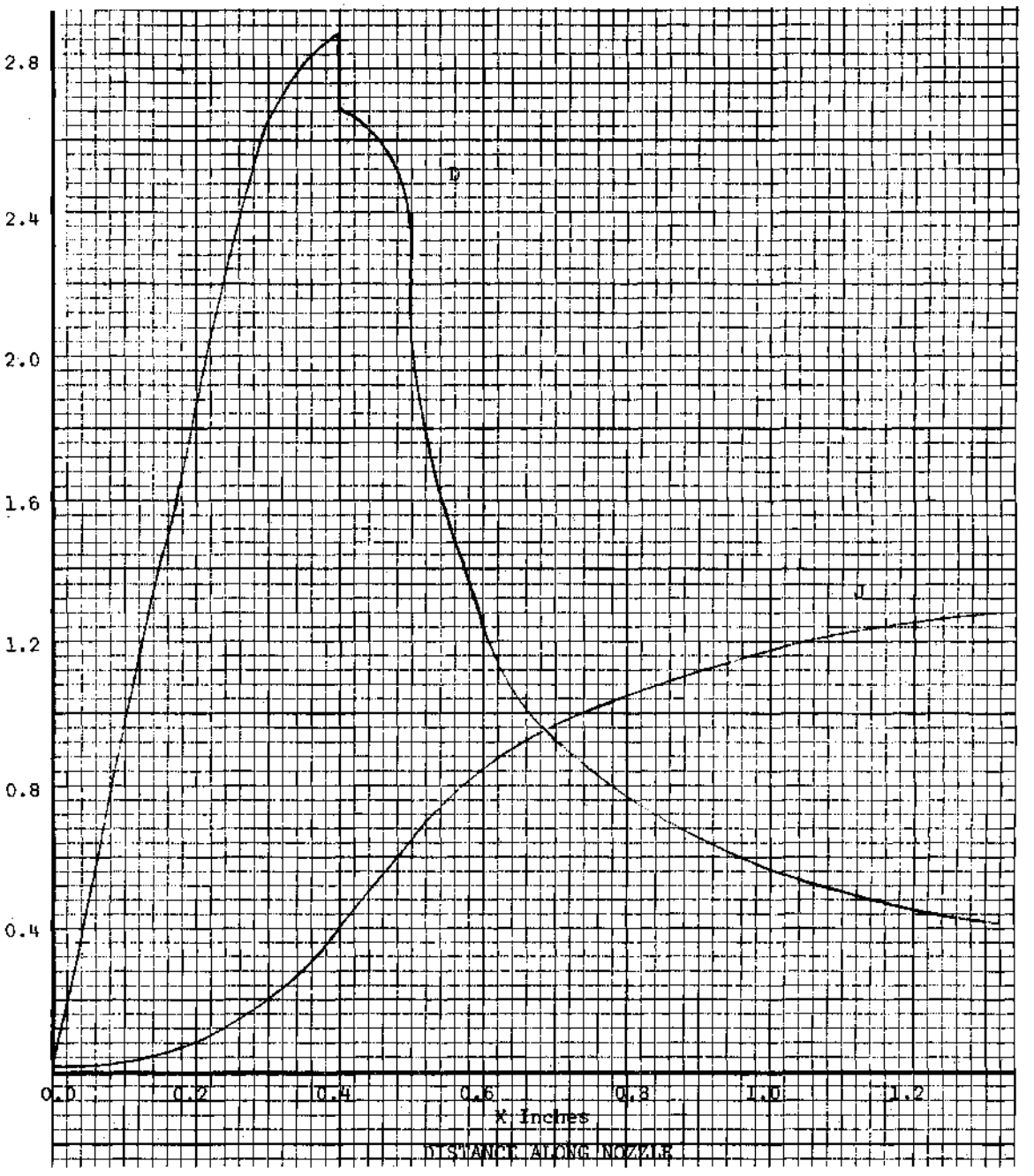
2.8
2.4
2.0
1.6
1.2
0.8
0.4
D
J
0.0
0.2
0.4
0.6
0.8
1.0
1.2
X Inches
DISTANCE ALONG NOZZLE

flow at the nozzle throat.

Viscous Flow

Prior to entering the nozzle the flow is uniform and there are no velocity gradients. Upon entering the nozzle the fluid that contacts the nozzle wall is decelerated to zero velocity. At this point the flow is broken down into two regions, the inviscous region and the viscous or boundary layer region.

Solving for the properties in the boundary layer requires the simultaneous solution of Equations (4-30), (4-31), and (4-32) with the boundary conditions at the wall, Equation (4-33) and the free stream boundary conditions, Equation (4-34). Integration of the three equations is performed numerically by use of the Runge-Kutta method. An initial value technique is utilized which requires assuming the values of three additional boundary conditions at the wall. Values are assumed at the wall for f_w'', g_{Iw}', and Z_{Aw}' .

Keeping track of the solution and the associated equations is readily accomplished with the Runge-Kutta technique which makes it desirable for use on electronic computers. When applying it to a second or higher order equation it is usually desirable to break them up into first order equations, again simplifying the accounting procedure. The three total differential equations for the viscous flow are first broken down into seven first order equations. Equation (4-30) for momentum is a third order equation and it is changed into three first order equations. Equations (4-31) and (4-32) for species continuity and energy are both second order equations and each of them convert to two first order equations.

The seven first order differential equations are:

$$f''' = \frac{D}{B}\left[(f')^2 - \frac{\rho_e}{\rho}\right] - \frac{f''}{B}(B' + f) \tag{5-39}$$

$$f'' = \frac{d(f')}{d\eta} \tag{5-40}$$

$$f' = \frac{df}{d\eta} \tag{5-41}$$

$$g_I'' = J(1 - Pr)\left[\frac{B'}{B} f' f'' + (f'')^2 + f' f'''\right] - \left[B' + f\,Pr\right]\frac{g_I'}{B} \tag{5-42}$$

$$g_I' = \frac{d\,g_I}{d\eta} \tag{5-43}$$

$$Z_A'' = Z_A'\left[\frac{S'}{S} - \frac{B'}{B} - \frac{f\,S}{B}\right] \tag{5-44}$$

$$Z_A' = \frac{d}{d\,\eta}(Z_A) \tag{5-45}$$

It is necessary to have B', B, $\frac{\rho_e}{\rho}$, and S as functions of f'', f', f, g_I', g_I, Z_A', and Z_A in order to successfully carry out the required integrations. Recalling Equation (4-13) for B,

$$B = \frac{\rho\,\mu}{\rho_e \mu_e} \tag{4-13}$$

Equation (5-8) is an applicable expression for $\frac{\mu}{\mu_e}$ as a function of α and

T. Applying the perfect gas equation of state to the mixture gives

$$\frac{\rho}{\rho_e} = \left(\frac{1 + \alpha_e}{1 + \alpha}\right) \frac{T_e}{T} \tag{5-46}$$

Thus,

$$B = \left(\frac{1 + 0.65\ \alpha}{1 + 0.65\ \alpha_e}\right)\left(\frac{1 + \alpha_e}{1 + \alpha}\right)^2\left(\frac{T_e}{T}\right)^{0.36} \tag{5-47}$$

An assumption for the value of $C_{p_{H_2}}$ is required to reduce Equation (5-47). The frozen ideal gas static enthalpy is given by

$$h_f = [\alpha\ C_{p_H} + (1 - \alpha)\ C_{p_{H_2}}]\ T \tag{5-48}$$

C_{p_H} is constant at 4.92 Btu/lb°R, but $C_{p_{H_2}}$ is a function of T, and a suitable average value has to be chosen for Equation (5-48), the integral portion of Equation (4-24), to apply. For the ranges to temperature involved in the nozzle, the vibration mode of diatomic hydrogen is partially excited. However, a suitable average value from 0°R to the temperature in the nozzle is 3.9 Btu/lb°R. Thus

$$\frac{T_e}{T} = \left(\frac{3.86 + \alpha}{3.86 + \alpha_e}\right) \frac{h_{f_e}}{h_f} \tag{5-49}$$

Also note that

$$\frac{I_{f_e}}{h_{f_e}} = \frac{2}{2-J} \tag{5-50}$$

Rearrangement of Equations (5-50) and (5-49) with Equation (5-47) and recalling that $\alpha = \alpha_e Z_A$ gives

$$B = \left(\frac{1 + \alpha_e}{1 + \alpha_e Z_A}\right)^2 \left(\frac{1 + 0.65\ \alpha_e Z_A}{1 + 0.65\ \alpha_e}\right) \left(\frac{3.86 + \alpha_e Z_A}{3.86 + \alpha_e}\right)^{0.36} \tag{5-51}$$

$$\left(\frac{2 - J}{2\ g_I - J\ (f')^2}\right)^{0.36}$$

Differentiation of the above with respect to η and rearranging gives

$$B' = B \left[\left(\frac{0.65}{1 + 0.65\ \alpha_e Z_A} + \frac{0.36}{3.86 + \alpha_e Z_A} - \frac{2}{1 + \alpha_e Z_A}\right) \frac{\alpha_e Z'_A}{1}\right. \tag{5-52}$$

$$\left. - \frac{0.72\ (g'_I - J\ f'\ f'')}{2\ g_I - J\ (f')^2}\right]$$

Likewise rearrangement of Equation (5-46) gives

$$\frac{\rho}{\rho_\theta} = \left(\frac{1 + \alpha_e Z_A}{1 + \alpha_e}\right) \left(\frac{3.86 + \alpha_e}{3.86 + \alpha_e Z_A}\right) \frac{2\ g_I - J\ (f')^2}{2 - J} \tag{5-53}$$

Equation (5-28) becomes

$$S = (1 + 0.65\ \alpha_e\ Z_A)\ S_o \tag{5-54}$$

In addition to solving the viscous equations for f", f', f, g_I', g_I, Z_A', and Z_A it is desirable to solve for the displacement and momentum thickness. Also, it is necessary to integrate the value of $\frac{\rho_e}{\rho}$ across the boundary to revert from the $\bar{x}$, η coordinate system to the x, y coordinate system.

Equation (4-1) is

$$\eta = \frac{\rho_e\ u_e\ R}{(2\bar{x})^{1/2}} \int_o^y \frac{\rho}{\rho_e}\, dy \tag{4-1}$$

Rearranging and solving for y

$$y = Y \int_o^\eta \frac{\rho_e}{\rho}\, d\eta \tag{5-55}$$

where

$$Y = \frac{(2\bar{x})^{1/2}}{\rho_e\ u_e\ R} \tag{5-56}$$

which becomes for this nozzle in known terms with x in inches

$$Y = 0.123\ R \left(\int_o^x \bar{T}_e^{\,0.64}\ dx \right) \tag{5-57}$$

The displacement thickness, δ^*, is given by

$$\delta^* = Y \int_0^\eta \left(\frac{\rho_e}{\rho} - f' \right) d\eta \qquad (5\text{-}58)$$

and the momentum thickness, θ, is

$$\theta = Y \int_0^\eta (1 - f') f' \, d\eta \qquad (5\text{-}59)$$

Integration of the Viscous Flow Equations

Numerical analysis is readily applied to the solution of differential equations of the initial value type; i.e., where all of the boundary conditions occur at the point of initiation of the integration. The problem under consideration is of the two point boundary value type, where seven first order differential equations have to be solved simultaneously. To solve them by the initial value techniques requires seven boundary conditions at the wall. Only four boundary conditions are known at the wall which are from Equation (4-33)

$$\begin{array}{ll} f = 0 & f' = 0 \\ \eta = 0 & \\ g_I = g_{Iw} & Z_A = Z_{Aw} \end{array} \qquad (4\text{-}33)$$

It is necessary to determine three more boundary conditions at the wall, f''_w, Z'_{Aw}, and g'_{Iw}, such that when the integration is carried

out the three known conditions at the boundary layer's edge will be satisfied. The boundary conditions at the boundary layer's edge are

$$\begin{aligned} \eta &\to \infty & g_I &\to 1 \\ f' &\to 1 & Z_A &\to 1 \end{aligned} \tag{4-34}$$

When the same coordinate system used in this research is applied to the momentum equation for an incompressible isothermal fluid, Blausius' solution for the flat plate will lead to a value of f' of 0.99 at η equal to 3.5. In order to insure that the solution to the additional energy and species continuity equations will not be restricted, the equations were integrated out to a value of η of 7. In the integrations, this value was shown to be adequate, since the maximum value of η for an f' of 0.99 was 4.33. This particular integration was for both D and J zero, and for most of the integrations this value of η was less than 4. Then, the upper limit for integration, ∞ in Equation (4-34), can be replaced by 7. An example of the computer program used to solve these equations is given in Appendix B, and a discussion of the Runge-Kutta method is given in Appendix C.

Usually it is impossible to assume initial values of f''_w, Z'_{Aw}, and g'_{Iw} that would give the values in Equation (4-34) on the first attempt. The method followed is to guess the three values and then integrate across the boundary layer. For reasonable accuracy and to conserve time on the computer, a $\Delta\eta$ of 0.05 is chosen, thus 140 points are taken

across the boundary layer. It is desirable to have the values of f, f', f'', g_I, g_I', Z_A, Z_A' and the integral portions of Equations (5-55), (5-58) and (5-59) only for steps of η of 0.2, so the corresponding values are to be stored in an array while the integrations are performed on the computer.

With the assumed values of f_w'', g_{Iw}' and Z_{Aw}', two difficulties could arise on the first integration since the bounds of Equation (4-34) cannot be guaranteed if the values are out of range. It is always necessary that

$$2\, g_I > J\, (f')^2 \tag{5-60}$$

However, if the initial value of f_w'' is too large, this can be violated and the operation

$$\left(\frac{2 - J}{2\, g_I - J\, (f')^2}\right)^{0.36}$$

in Equation (5-51) cannot be performed since the term within the bracket becomes negative or infinite. Also in order to be within range for the iteration, it is desirable to keep f' positive. A technique is incorporated in the program to raise the value of f_w'' if f' becomes negative, and to lower its value if Equation (5-61) is violated. This modification is repeated until integration can be completed without f_e' being negative or

$$(f'_e)^2 > \frac{2\, g_I}{J}$$

After the first integration is completed the values of f'_e, g_{Ie}, Z_{Ae} are compared with Equation (4-34) to see if they agree within tolerances of 0.0001 for small values of D and J and 0.001 for the larger values, to conserve computer time. If this tolerance is not satisfied, three more integrations are carried out with changes in the values of the assumed boundary conditions. For each of these three integrations, one of the assumed boundary conditions is changed by the value of the influence coefficient, IC. Let f''_w, g'_{Iw}, Z'_{Aw}, f'_{e1}, g_{Ie1}, and Z_{Ae_1} be the values arrived at for the first complete integration. Then, for the second integration

$$f''_{w_1} = f''_w + IC \tag{5-61}$$

while g'_{Iw} and Z_{Aw} remain unchanged. This will give values of f'_{e2}, g_{Ie2}, and Z_{Ae2} at $\eta = 7$. For the third integration f''_w and Z'_{Aw} are used and

$$g'_{w2} = g'_w + IC \tag{5-62}$$

leading to values of f'_{e3}, g'_{Ie3}, and Z_{Ae3}. For the last integration before an iteration to new values is performed

$$Z'_{Aw3} = Z'_{Aw} + IC \tag{5-63}$$

It is apparent that

$$\frac{\partial f'_e}{\partial f''_w} \approx \frac{f'_{e_2} - f'_{e_1}}{IC} \tag{5-64}$$

$$\frac{\partial f'_e}{\partial g'_{Iw}} \approx \frac{f'_{e_3} - f'_{e_1}}{IC} \tag{5-65}$$

and

$$\frac{\partial f'_e}{\partial Z'_{Aw}} = \frac{f'_{e_4} - f'_{e_1}}{IC} \tag{5-66}$$

Likewise, similar expressions can be written for g_{Ie} and Z_{Ae}. Now it can approximately be stated that the desired change in the conditions at the boundary layer edge is

$$df'_e = \frac{\partial f'_e}{\partial f''_w} df''_w + \frac{\partial f'_e}{\partial g'_{Iw}} dg'_{Iw} + \frac{\partial f'_e}{\partial Z'_{Aw}} dZ'_{Aw} \tag{5-67}$$

$$dg_{Ie} = \frac{\partial g_{Ie}}{\partial f''_w} df''_w + \frac{\partial g_{Ie}}{\partial g'_{Iw}} dg'_{Iw} + \frac{\partial g_{Ie}}{\partial Z_{Aw}} dZ'_{Aw} \tag{5-68}$$

$$dZ_{Ae} = \frac{\partial Z_{Ae}}{\partial f''_w} df''_w + \frac{\partial Z_{Ae}}{\partial g'_{Iw}} dg'_{Iw} + \frac{\partial Z_{Ae}}{\partial Z_{Aw}} dZ'_{Aw} \tag{5-69}$$

From the known conditions it is desired to have

$$df'_e = 1 - f'_{el} \tag{5-70}$$

$$dg_{Ie} = 1 - g_{Ie} \tag{5-71}$$

$$dZ_{Ae} = 1 - Z_{Ae} \tag{5-72}$$

Three algebraic Equations (5-67), (5-68) and (5-69) contain three unknowns, df''_w, dg'_{Iw} and dZ'_{Aw}, which can readily be obtained by solving them simultaneously. Thus the new values of f''_w, g'_{Iw}, and Z'_{Aw} will be obtained by adding the respective values of df''_w, dg'_{Iw} and dZ'_{Aw} to the values used for the first successful integration.

The above procedure is repeated until the desired accuracy on Equation (4-34) is satisfied. When this occurs the answers are printed out and the solution proceeds to the next value of D and J. The assumed values for the boundary conditions for the second combination of D and J are the values that gave the correct result to the first set. Therefore, when the assumed values of f''_w, g'_{Iw} and Z'_{Aw} are read into the program they are used only once.

IC was chosen to be 10^{-4} for the earlier solutions with small D and J, but for the larger values of D and J it was necessary to decrease IC to 10^{-6} for rapid convergence of the solution. For D = J = 0 an IC of 10^{-4} was adequate since $\frac{\partial f'_e}{\partial f''_w} = 2.81$, but at values of D = 2.7 and J = 0.6, $\frac{\partial f'_e}{\partial f''_w}$ had increased to 13,970 making it necessary to decrease

IC to 10^{-6}.

Convergence of the solution was also aided by the lower values of IC. As an example, 26 complete iterations, or 105 integrations, were required at D = 2.7 and J = 0.2 where $\frac{\partial f'_e}{\partial f''_w} = 4{,}560$ for IC = 10^{-4}; but when D was increased to 2.9 and IC reduced to 10^{-6} only 4 iterations were required for a solution even though $\frac{\partial f'_e}{\partial f'_w}$ had increased to 7,540.

General Results

For more generality, the integration of the viscous flow equations was not limited to the values of D and J required for the particular nozzle considered. A total of 65 integrations were carried out for various values of D, J, g_{Iw}, and Z_{Aw}. In the majority of the solutions, g_{Iw} was taken as 0.4 and Z_{Aw} as 0.05; however, other values were used to determine their effects on the overall nozzle performance.

A summary of all the solutions is given in Table 5 of Appendix D where values of f''_w, g'_{Iw}, Z'_{Aw}, δ^*_I and θ_I are tabulated for all of the solutions. δ^*_I and θ_I are the integral portions of Equations (5-58) and (5-59), respectively. A tabulation of 24 representative integrations across the boundary layer is given in Tables 6, 7 and 8. In these tables values of f, f', f'', g_I, g'_I, Z_A, Z'_A are given for values of η between 0.0 and 7.0.

Typical variations of the velocity, velocity gradient, enthalpy, enthalpy gradient, concentration, and concentration gradient profiles are given in Figure 5, 6, and 7 where these quantities are plotted for three different extremes of boundary conditions.

The boundary conditions at the wall, and the dimensionless dis-

placement thickness, are plotted in Figures 8, 9, and 10. Plots of f''_w, Z'_{Aw}, and δ_I^* are given as functions of D and J for $g_{Iw} = 0.4$ and $Z_{Aw} = 0.5$.

When changing the boundary conditions all of the solutions seem to revolve around g'_{Iw} which is almost constant; therefore, no plot of g_{Iw} is given. For the 65 integrations, g'_{Iw} ranged from 0.1107 to 0.1381 while f''_w varied from 0.1928 to 0.6981. Variation of Z'_{Aw} was intermediate, from 0.1013 to 0.2268. Strong effects of g_I and g'_I on B, B', and $\frac{\rho_e}{\rho}$ are probably the reason that there is very little change allowed in g'_{Iw} between the various boundary conditions. This can be seen in Figure 6 where the enthalpy gradient profile for D = 1.2, J = 0.2 is the same for $g_{Iw} = 0.4$ as for $g_{Iw} = 0.1$.

Consideration of variable properties across the boundary layer exerted some very interesting effects on the integration results. With constant values of Pr, S, B and ρ the quantities f''', g''_I, and Z''_I are all zero at the wall and become negative immediately as the integration proceeds from the wall, and they will remain negative across the boundary layer. Equation (5-39) for f''' contains a term $\frac{-f'' B'}{B}$, Equation (5-42) for g''_I contains a term $\frac{-B'}{B} g'_I$ and Equation (5-44) for Z'_A contains a term $\left(\frac{S'}{S} - \frac{B'}{B}\right) Z'_A$ when variable properties are considered. From the investigation of Equations (5-51), (5-52), and (5-54) it is apparent that all of these terms are positive at the wall since f'', g'_I, Z'_A have positive values at the wall; thus it is necessary for f''_w, g'_I, and Z'_A to obtain their maximum values at some point other than the wall, and then to decrease in order to reach zero at the bounary layer's edge. For large values of D and J, f''_w reaches its maximum value by $\eta = 0.2$, but a larger η is required before g'_I and Z'_A reach their maximum values.

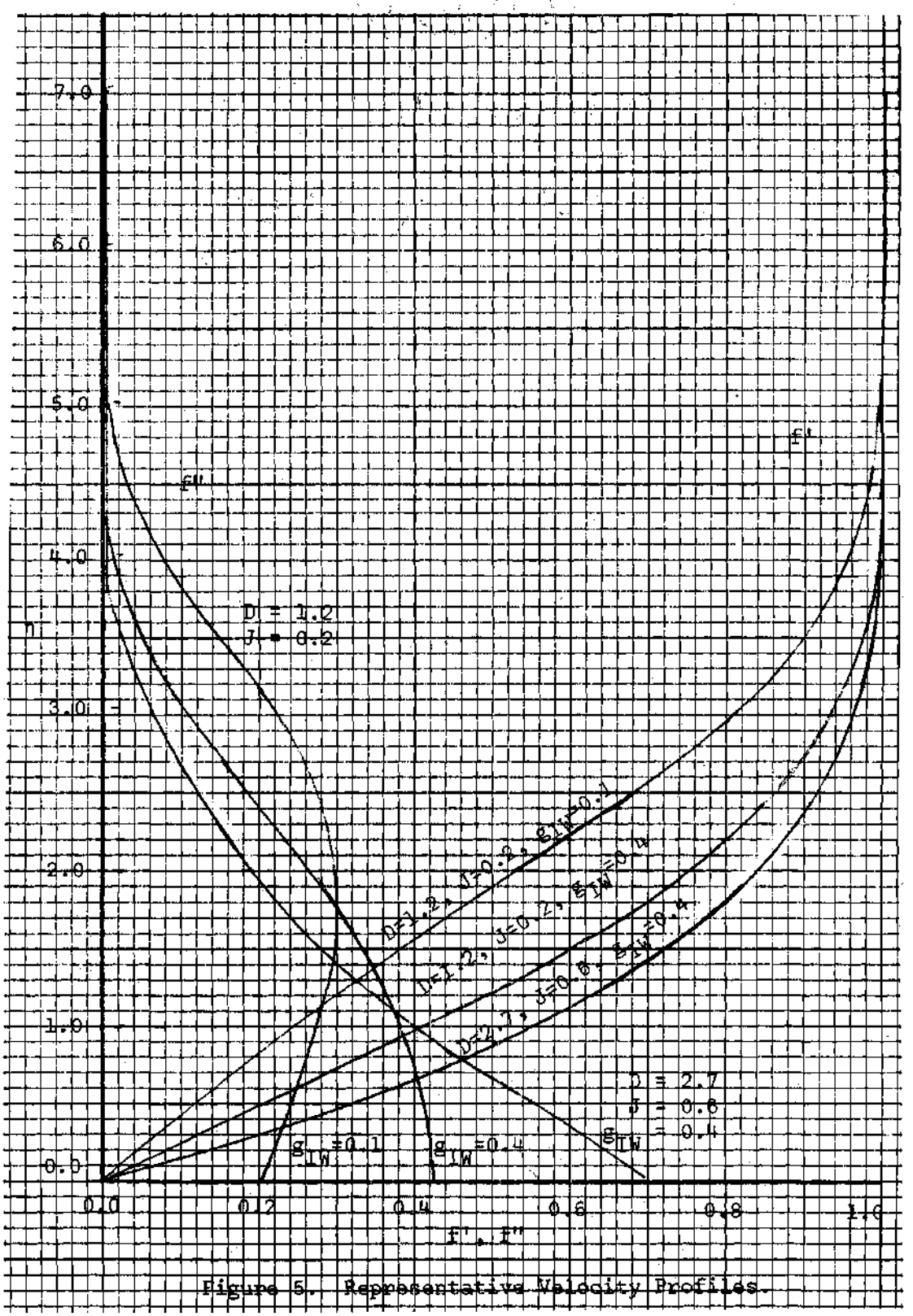

Figure 5. Representative Velocity Profiles.

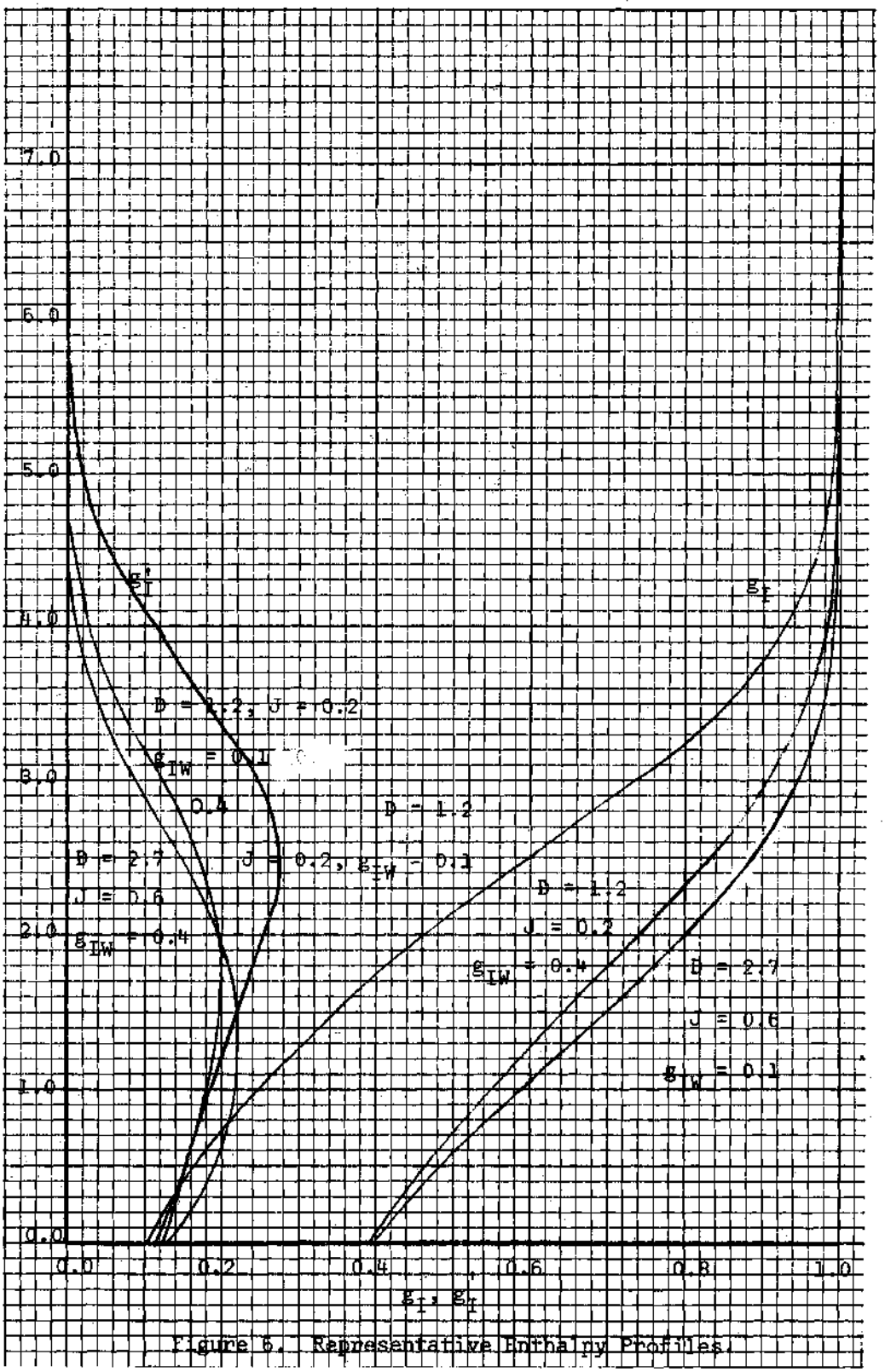

Figure 6. Representative Enthalpy Profiles.

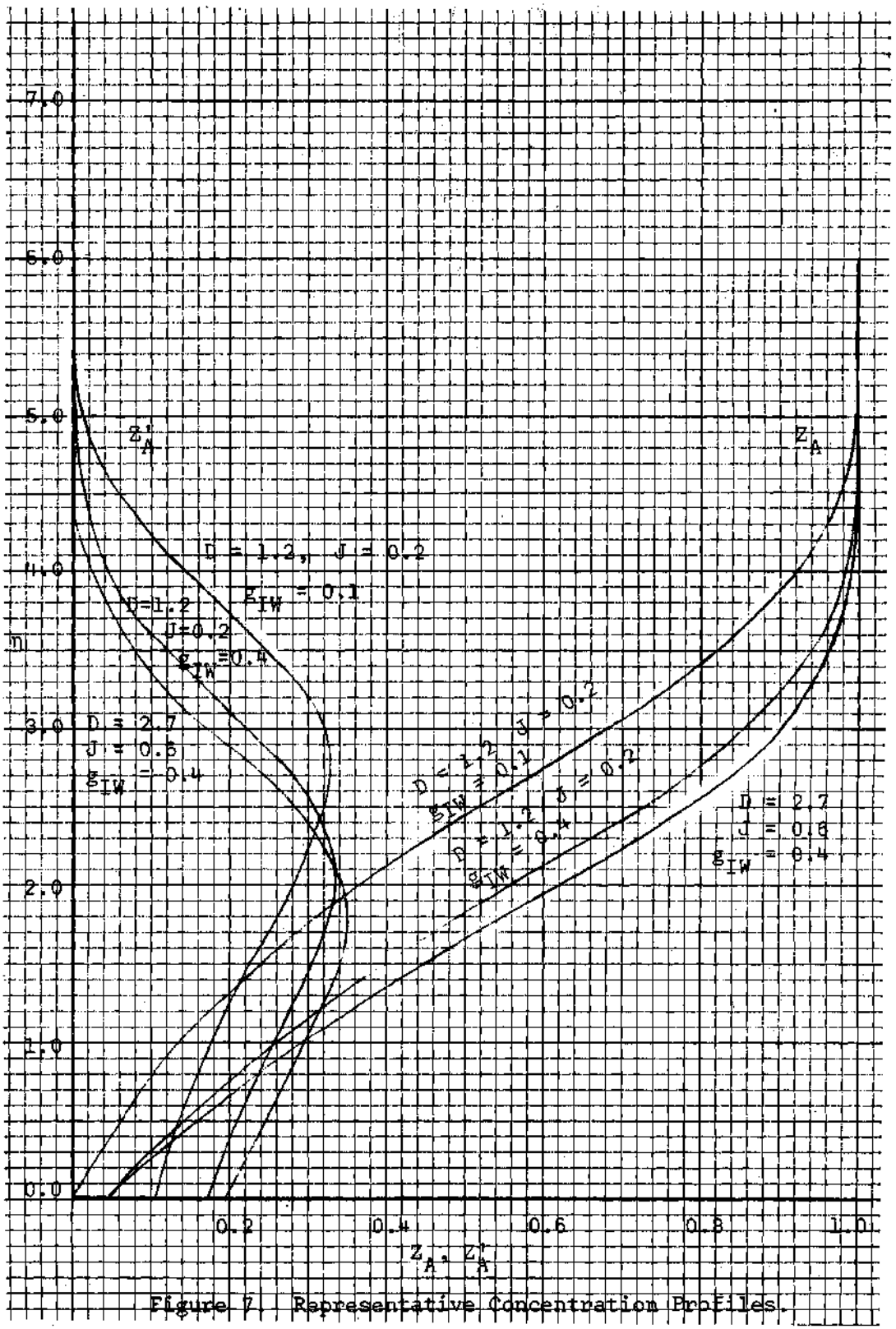

Figure 7. Representative Concentration Profiles.

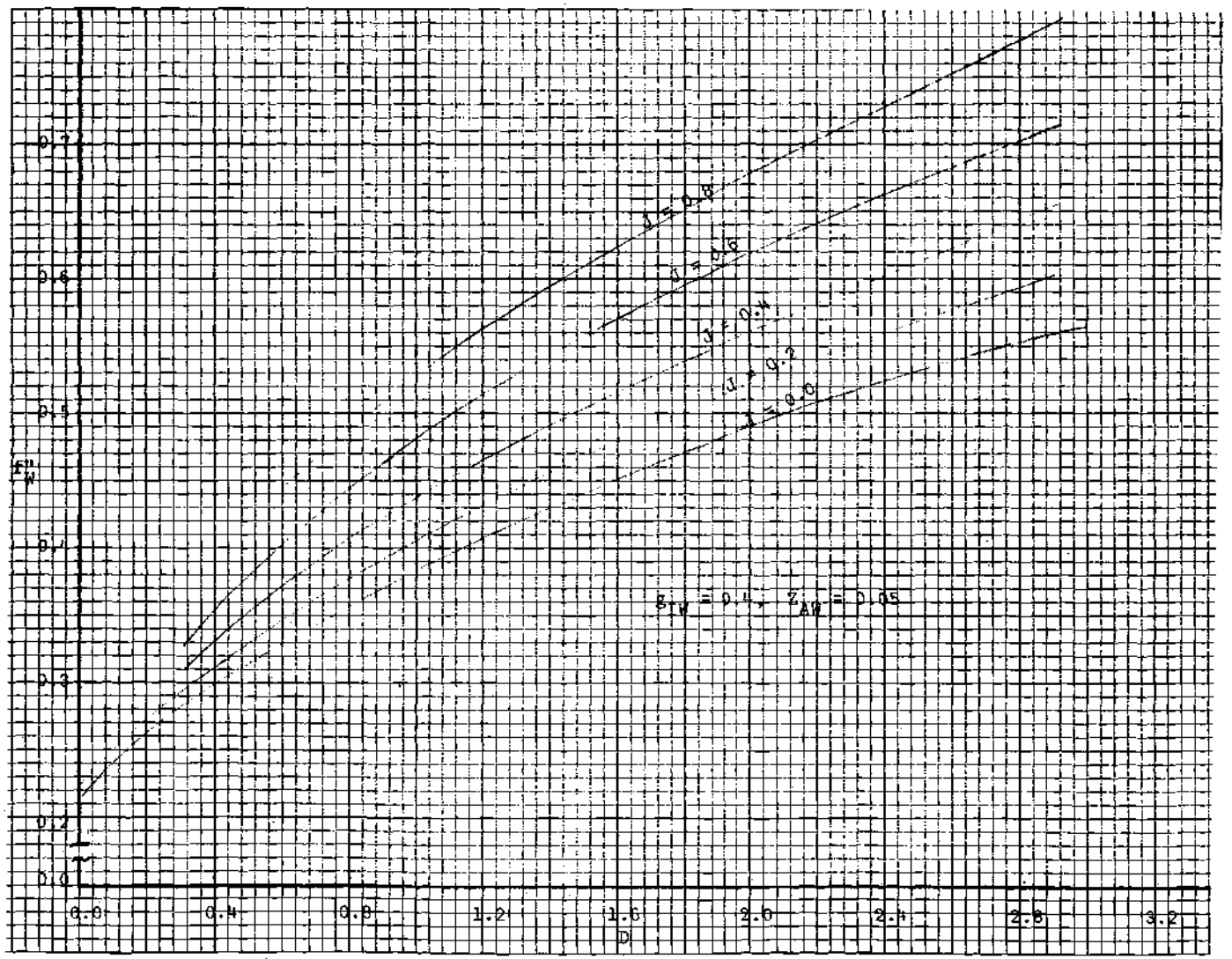

Figure 8. Velocity Gradient at the Wall as a Function of D and J.

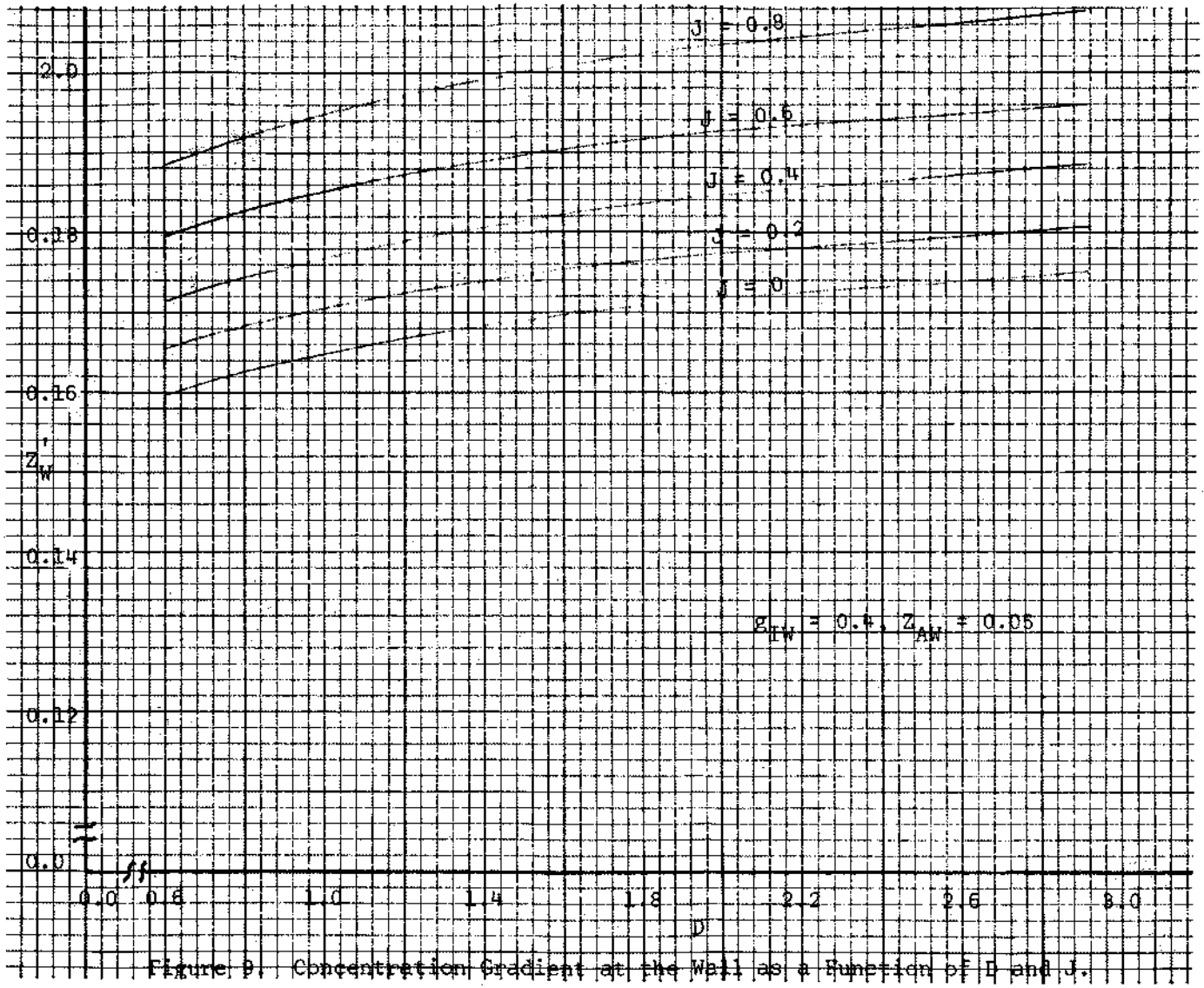

Figure 9. Concentration Gradient at the Wall as a Function of D and J.

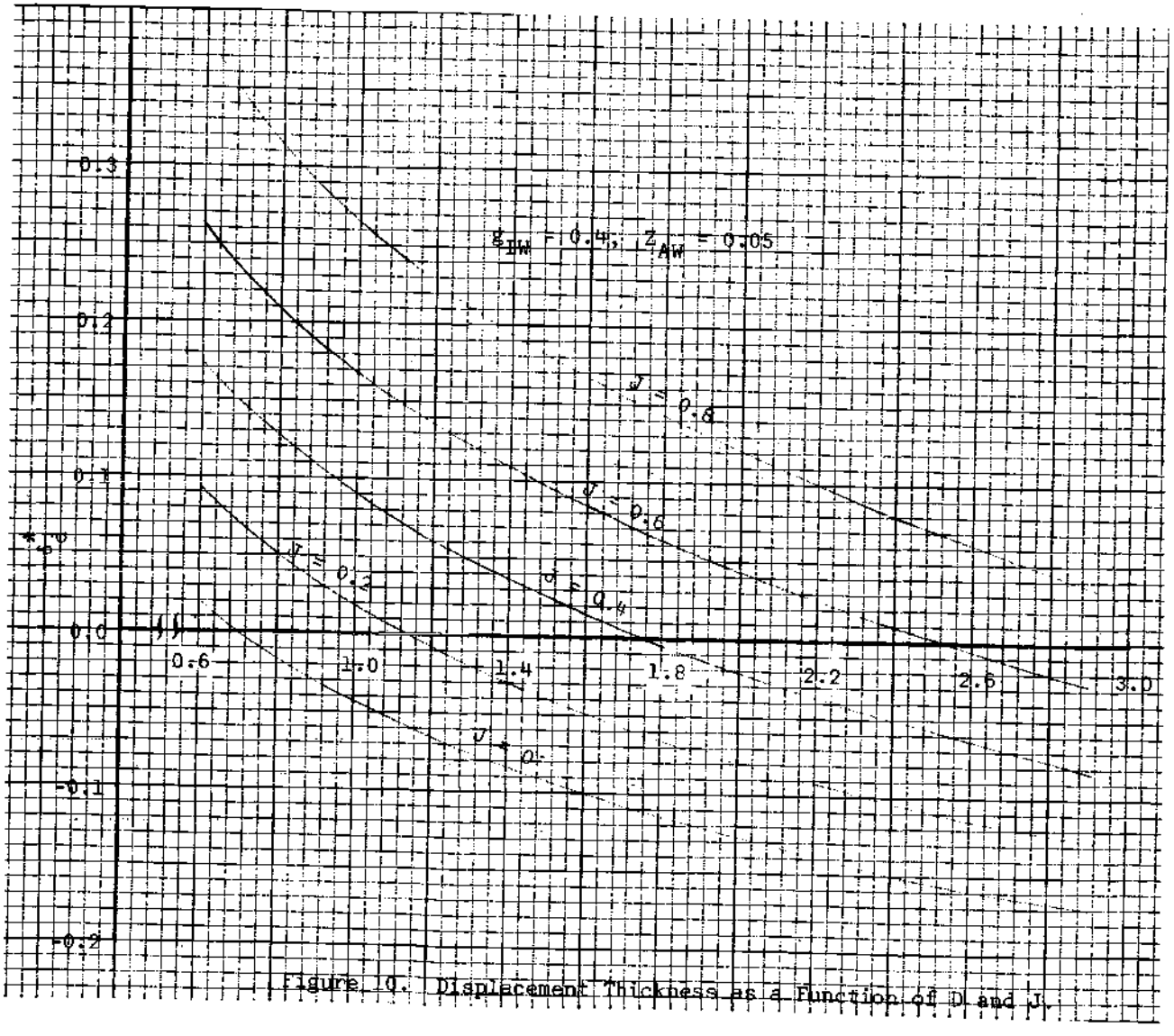

Figure 10. Displacement Thickness as a Function of D and J.

Dorrance (36) shows that for D = J = 0, the wall gradients can be evaluated by

$$f''_w = \frac{0.47}{B^{1/2}} \tag{5-73a}$$

$$g'_{Iw} = \frac{0.47}{B^{1/2}} P_r^{1/3} (1 - g_{Iw}) \tag{5-73b}$$

$$Z'_{Aw} = \frac{0.47\ S^{1/3}}{B^{1/2}} (1 - Z_{Aw}) \tag{5-73c}$$

It is obvious that the above expression would be true if B were constant across the boundary layer. However, as explained above, the consideration of variable properties require that the maximum gradients be at some point other than the wall; therefore, the gradients given by Equation (5-73) would be expected to be too large, since the gradients increase from the wall, pass through a maximum, and then decrease to zero at the boundary layer's edge. The values calculated at D = J = 0 were 0.77 of the values given by using B_w in Equation (5-73).

An attempt was made to find a simple expression of f''_w as a function of D and J. Unfortunately, this endeavor was unsuccessful; however, interpolation and extrapolation can be used successfully to obtain a great deal of information from a few calculations.

Another interesting result of considering variable properties is negative boundary layer displacements. In certain cases, when the effects of increased density are greater than the effects of reduced velocity in

the boundary layer, negative displacement thicknesses are the result. In all cases, the ratio of displacement thickness to boundary layer thickness is less than that for the incompressible case. The significance of a negative displacement thickness is that the mass flow rate per unit area is greater through the boundary layer than it is in the free stream. Larger momentum thicknesses are the result when the displacement thickness is small or negative.

Energy is transmitted to the wall by two methods. There is heat transfer to the wall by conduction, and monatomic hydrogen is recombining at the surface. The frozen boundary layer approximation and the catalytic surface assumption require that all reassociation take place at the surface. Therefore, the concentration of atoms at the surface is determined by the temperature of the surface. By performing an energy balance, see for an example Dorrance (36), the total energy transferred to the surface per unit area is

$$- \dot{q}_w = K \left.\frac{\partial T}{\partial y}\right]_w + \rho D_{HH_2} \left[h_H \frac{\partial \alpha}{\partial y} + h_{H_2} \frac{\partial (1 - \alpha)}{\partial y} \right]_w \tag{5-74}$$

which becomes in the $\bar{x}$, η plane

$$- \dot{q}_w = \frac{\mu_e}{Y} B_w \frac{I_{fe}}{Pr} \left[g_I' + \frac{L(h_H - h_{H_2})}{I_{fe}} \alpha_e Z_A' \right]_w \tag{5-75}$$

The heat transfer in terms of enthalpy is

$$- \dot{q}_w = \frac{h_I \, (I_{fe} - I_{fw})}{C_{p_w}} \tag{5-76}$$

Define the Nusselt number by

$$Nu = \frac{h_I \, x_I}{K_w} \tag{5-77}$$

For the characteristic length in the Nusselt number, x_I is chosen for convenience as

$$x_I = \frac{(2\bar{x})^{1/2}}{\rho_w \, u_e \, R} \tag{5-78}$$

Equating the right hand sides of Equations (5-75) and (5-76), solving for h_I and substituting it along with Equation (5-78) into Equation (5-77) gives for the Nusselt number

$$Nu = \frac{1}{1 - g_{Iw}} \left[g_I' + A \, Z_A' \right]_w \tag{5-79}$$

A is the amplification factor for the heat transfer due to the atomic recombination at the surface. A is given by

$$A = \left. \frac{L(h_H - h_{H_2}) \, \alpha_e}{I_{fe}} \right]_w \tag{5-80}$$

The bracketed term on the right of Equation (5-79) is plotted in Figure

11 for two values of A, and it shows that Nu is in essence independent of D and only slightly dependent on J.

Newton's law of viscosity for laminar flow is

$$\tau_w = \mu_w \left.\frac{\partial u}{\partial y}\right)_w \tag{5-81}$$

which becomes in the $\bar{x}$, η coordinates

$$\tau_w = \frac{\rho_w \mu_w u_e^2 R}{(2\bar{x})^{1/2}} f''_w \tag{5-82}$$

The coefficient of friction based on x is

$$C_{fx} = \frac{2 \tau_w}{\rho_w u_e^2} \tag{5-83}$$

Substituting for τ_w from Equation (5-82) gives

$$C_{fx} = \frac{2 f''_w}{R_e} \tag{5-84}$$

where

$$R_e = \frac{\rho_w u_e X_I}{\mu_w} \tag{5-85}$$

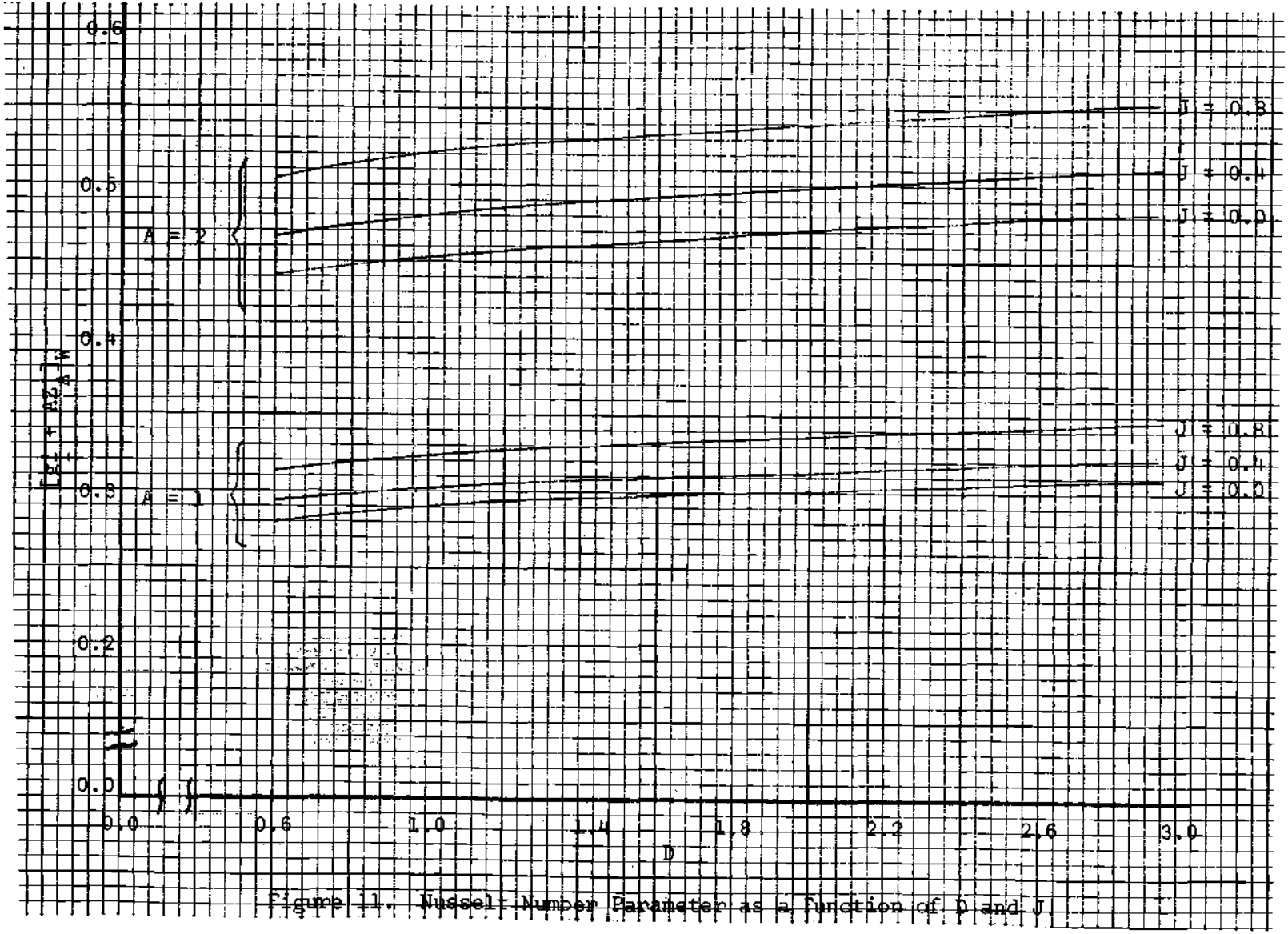

Figure 11. Nusselt Number Parameter as a Function of D and J.

Particular Nozzle Solution

From the general results given in the previous section, the solution for the values of D and J given in Figure 4 for the particular nozzle illustrated in Figure 3 is obtained. The correct value for each point along the nozzle was determined by interpolation and extrapolation from the general results. For the particular solution discussed in this section g_{Iw} was taken as 0.4 and Z_{Aw} was taken as 0.05. This would correspond to a constant wall temperature of 4680°R, which is possible with a tungsten nozzle.

Illustrated in Figure 12 is the range of values of B_w through the nozzle. Figure 13 illustrates the values of f''_w, g'_{Iw}, Z'_{Aw} and θ_I through the nozzle. Values of Y for converting from the $\bar{x}$, η planes to the real plane is given in Figure 14. The momentum boundary layer thickness divided by the nozzle radius is also given in Figure 14. Figure 15 shows results for both δ_I^* and δ^*.

For the particular nozzle under discussion, the heat transfer rate per unit area is

$$- \dot{q}_w = 0.167 \frac{B_w \bar{\mu}_e}{Y} (g'_I + 2.28\, Z'_A)_w \qquad (5\text{-}86)$$

The heat transfer rate in Equation (5-86) is in units of Btu/in^2-sec and the variation of heat transfer through the nozzle is given in Figure 16.

Nozzle performance, or overall engine performance, is reduced by the friction and heat transfer to the nozzle wall. At the nozzle exit, the momentum thickness is 0.017 inches which causes an 11 per cent reduction in the thrust from that calculated for an identical nozzle with

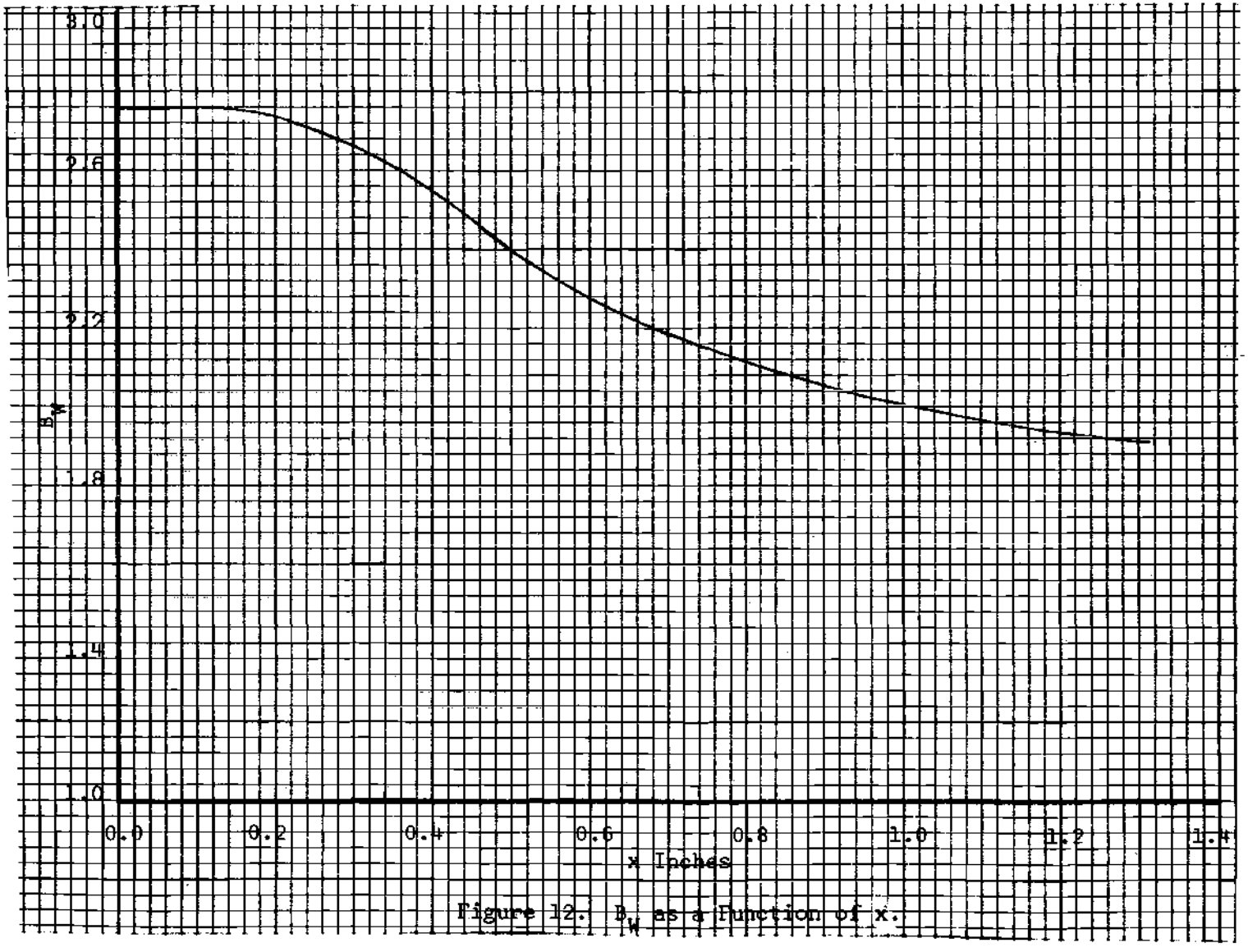

Figure 12. B_W as a Function of x.

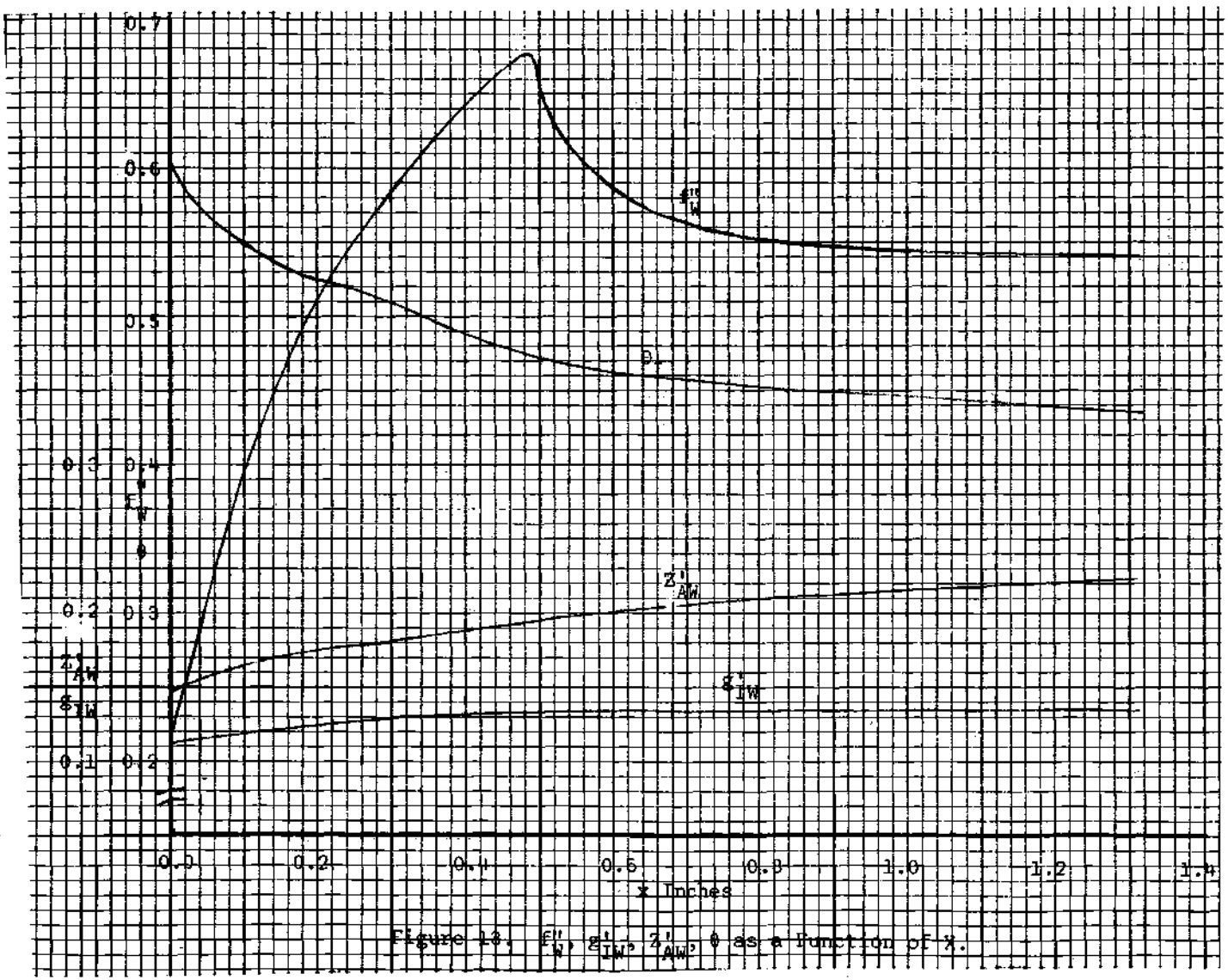

Figure 13. f''_w, g'_{Iw}, z'_{Aw}, θ as a Function of χ.

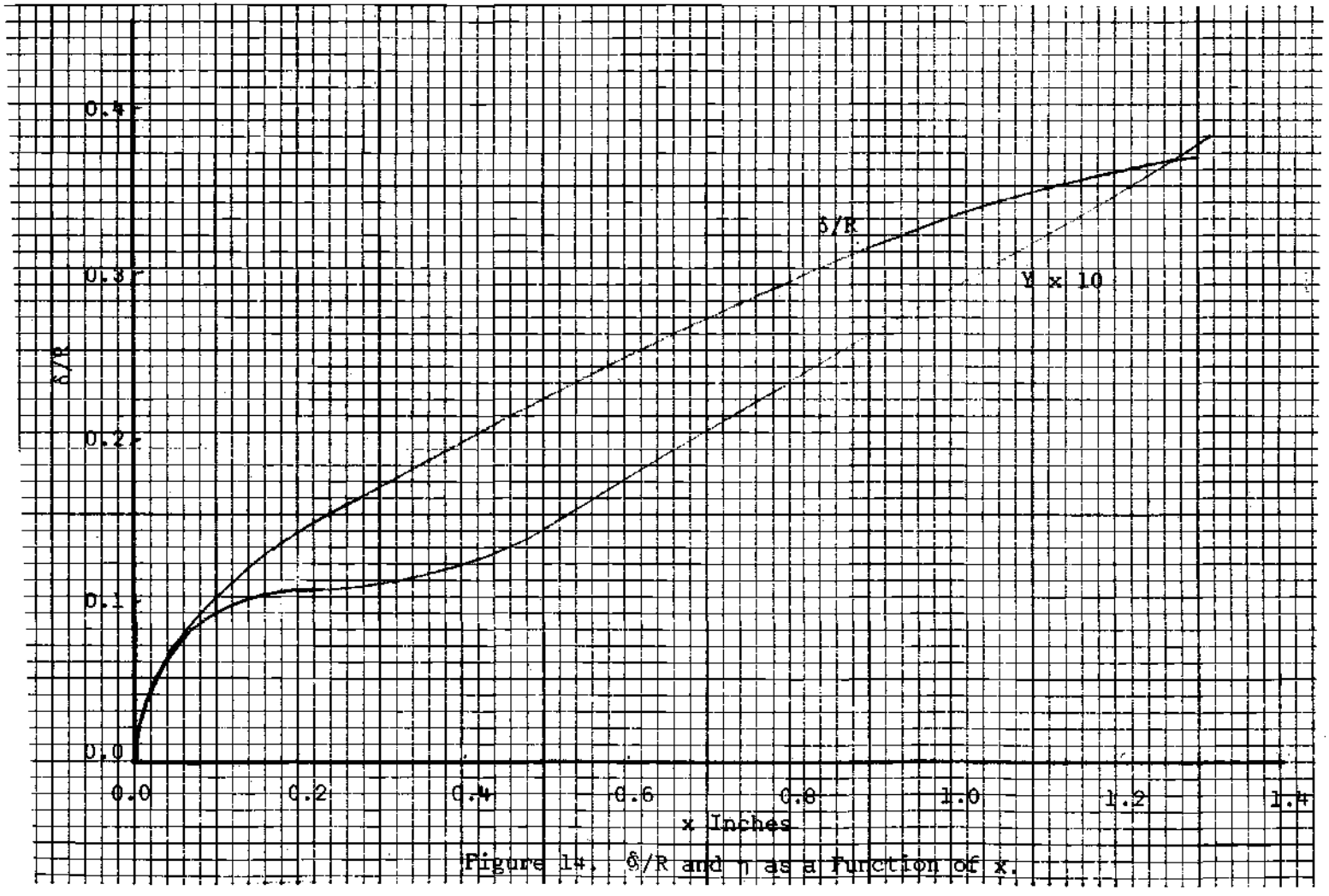

Figure 14. δ/R and η as a Function of x.

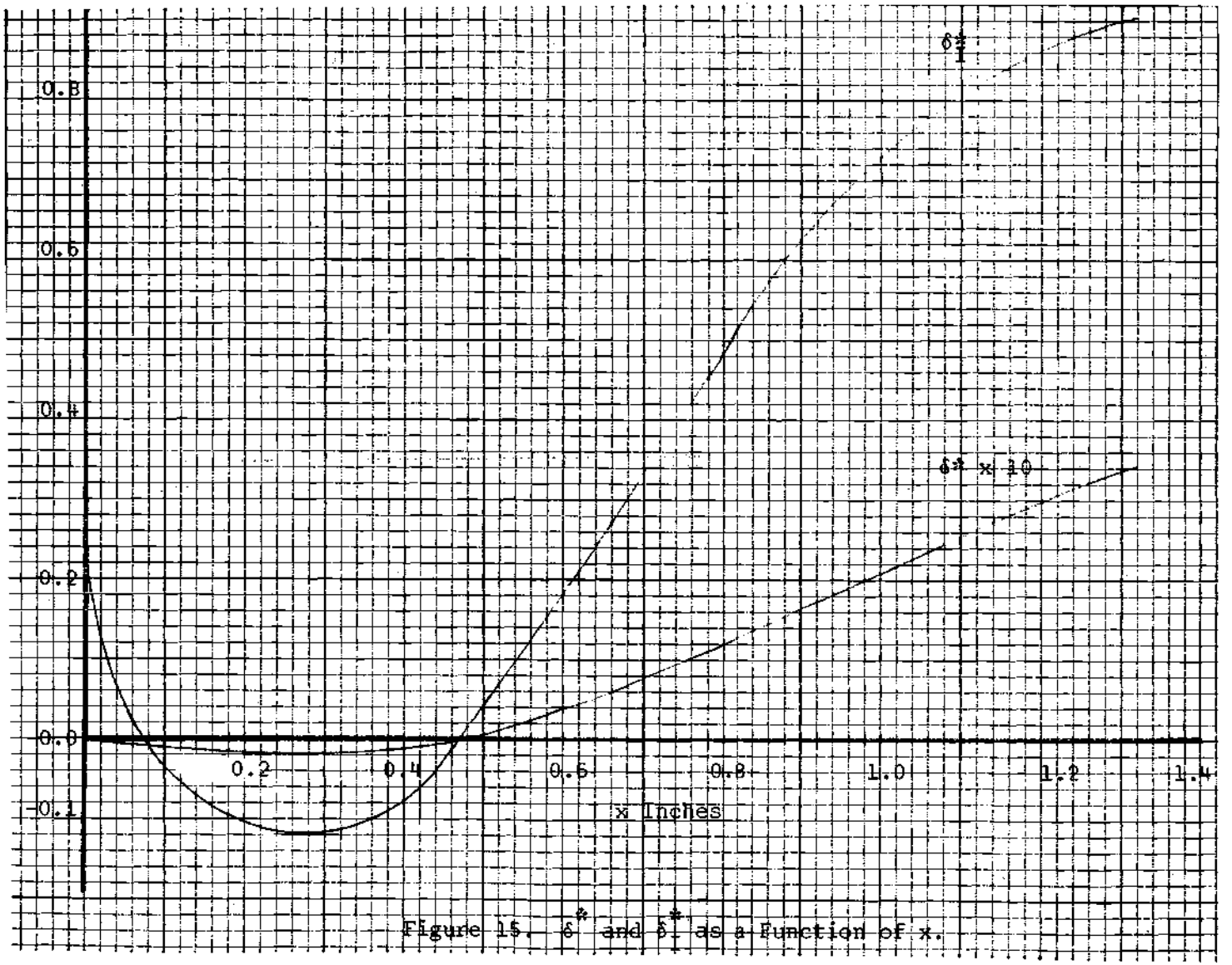

Figure 15. δ^* and δ_1^* as a Function of x.

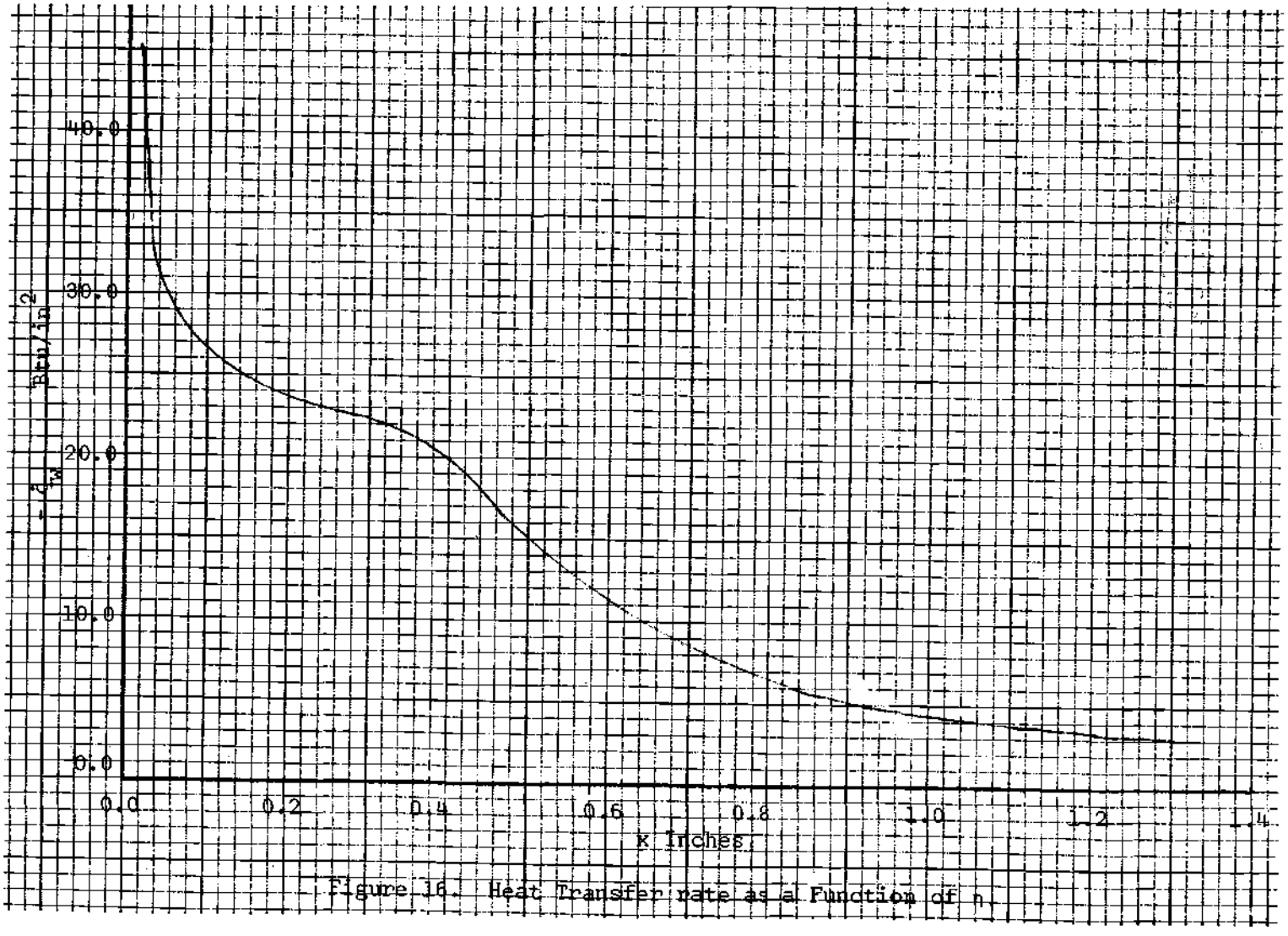

Figure 16. Heat Transfer rate as a Function of n

identical inviscous flow properties, but neglecting heat transfer and friction.

CHAPTER VI

DISCUSSION

Results of this analysis indicate that friction and heat transfer can account for at least a 10 per cent reduction in the specific impulse of a small nozzle. When it is realized that all of the other irreversibilities have been eliminated from the analysis, this is within the proper range when the results of actual plasma jet engines are considered.

Items not accounted for in this analysis were the turbulence and swirl required for good mixing in the arc chamber, and the fact that in most arc jets the arc is attached through the nozzle throat. Thus the gas is well on its way to complete expansion before it receives all of its energy from the arc. These items will account for a large increase in losses due to friction and heat transfer, and it accounts for the poor performance to date for all tested plasma jet engines. It indicates that considerable work is needed in optimizing the thrust chambers for the small engines.

At this time it is desirable to discuss the effect of various assumptions on the overall applicability of the analysis.

1. Local Similarity--Unfortunately the conditions within the nozzle are such that total similarity cannot be used. To obtain an analysis, local similarity was assumed. As can be seen from Figure 13, 0.2 inches from the nozzle entrance to the exit there is little variation f''_w, and almost no change in Z'_{Aw} and g'_{Iw}. Even though f''_w has a large

variation when D and J change, investigation of Figure 13 shows that g'_{Iw} and Z'_{Aw} are almost constant through the nozzle; therefore, when this method is used to calculate heat transfer, excellent results should be obtained. In general, this is reiterated by Figure 11. Therefore, the local similarity assumption appears to be within reason.

2. $g_{Iw} = 0.4$ --By reducing g_{Iw} to 0.1 the conditions for total similarity could be realized from the analysis, since the variation of f''_w would be reduced by a factor of 7. However, this would be an unrealistic restriction since the heat transfer rate would be increased and the performance would suffer due to a 2.6 per cent larger momentum thickness at the nozzle exit.

Equation (5-75) illustrates the increase in heat transfer when g_{Iw} is reduced from 0.4 to 0.1. Under this boundary condition Z_{Aw} would be reduced about 40 per cent. Every other term in Equation (5-75) would remain constant except B_w which would be increased by approximately 74 per cent. Thus, it would result in a heat transfer rate increase of about 20 per cent.

3. Catalytic Wall--This appears to be an excellent assumption since a large increase in Z_{Aw} results in insignificant effects on all other terms, except the heat transfer. However, increasing Z_{Aw} from 0.05 to 0.15 decreases the heat transfer only about 9 per cent.

4. Boundary Layer Assumption--In Appendix A in arriving at the boundary layer equations it was assumed that δ was an order of magnitude less than R. Figure 14 shows the variation of the ratio $\frac{\delta}{R}$ throughout the nozzle. When consideration is given to the small size of the displacement thickness it appears to be an excellent justification. There

is almost no mass crossing the edge of the boundary layer, except at the nozzle exit.

5. Accuracy of Numerical Results--The inherent error of the Runge-Kutta method is discussed in Appendix C. As a check on the accuracy and method of solution, a solution was obtained for $D = J = 0$, $\alpha_e = \alpha_w = 0$, $B = 1$, and $g_{Iw} = g_{Ie} = 1$. The classical Blausius' solution was obtained, and the results agreed to the fifth place. The results were the same regardless of the initial assumed value of f''_w; convergence of the solution was rapid.

Conclusions and Recommendations

It is felt that this work is an important step in understanding the performance of small nozzles with high velocity dissociated gases flowing through them. Although the effect of dissociation is to increase the heat transfer rate to the wall by a factor of 3, over a single species, with modern materials this can be readily accomplished in the design, and it does not limit the application to small engines.

One favorable result is that the friction and heat transfer effects do not completely stifle the development of small engines of this type, since their effects reduce the thrust only by 11 per cent. However, when comparing performance of engines of this type the actual performance suffers much greater in comparison to the theoretical performance. This would indicate that much work is needed in solving the thrust chamber irreversibilities, where a lot of turbulence is induced by swirl in the thrust chamber to aid the mixing of the gases heated by the arc, and the

arc being struck through the throat.

An excellent method to extend this work is described by Kunz (41). He has developed a procedure whereby the results of this analysis could be experimentally verified. This should be initiated as soon as possible after the necessary high temperature gas generator becomes available.

It should be pointed out that the results of this work are just one step in selecting an optimum nozzle for a small engine. In any application there will be an optimum expansion ratio, expansion angle and thrust chamber. More details of the complete application would have to be available before this is attempted.

APPENDIX A

BOUNDARY LAYER EQUATIONS

In this Appendix, the equations are presented in cylindrical coordinates even though the final boundary layer equations are used in the body coordinate system. This is an acceptable procedure for problems of this type and any introduced error is neglected.

The applicable boundary layer equations are derived from the complete momentum, energy, continuity, and species continuity equations below. Within the boundary layer the viscous and inertial forces are the same order of magnitude, while outside the boundary layer the inertial forces dominate.

Flow is steady through the nozzle which is axially symmetrical. There will be no change in the properties with respect to time and angular variation, and in the equations these terms will be omitted. In the cylindrical coordinate system used the coordinate along the axis is z where r is the radial coordinate, and the velocity in their respective directions is v_z and v_r. The fundamental equations (44) are:

1. Global Continuity

$$\frac{\partial(\rho v_r)}{\partial r} + \frac{\partial(\rho v_z r)}{\partial z} = 0 \qquad \text{(A-1)}$$

2. Axial Momentum

$$\rho v_z \frac{\partial v_z}{\partial z} + \rho v_r \frac{\partial v_z}{\partial r} = \frac{-\partial P}{\partial z} + \frac{\partial}{\partial z}\left(\mu\left[2\frac{\partial v_z}{\partial z}\right.\right. \qquad \text{(A-2)}$$

$$\left.\left. - 2/3\left(\frac{1}{r}\frac{\partial v_r\, r}{\partial r} + \frac{\partial v_z}{\partial z}\right)\right]\right) + \frac{1}{r}\frac{\partial}{\partial r}\left[\mu_r\left(\frac{\partial v_r}{\partial z} + \frac{\partial v_z}{\partial r}\right)\right]$$

3. Radial Momentum

$$\rho v_z \frac{\partial v_r}{\partial z} + \rho v_r \frac{\partial v_r}{\partial r} = \frac{-\partial P}{\partial r} + \frac{\partial}{\partial r}\left(\mu\left[2\frac{\partial v_r}{\partial r} - 2/3\left(\frac{1}{r}\frac{\partial r\, v_r}{\partial r}\right.\right.\right. \qquad \text{(A-3)}$$

$$\left.\left.\left. + \frac{\partial v_z}{\partial z}\right)\right]\right) + \frac{\partial}{\partial z}\left[\mu\left(\frac{\partial v_r}{\partial z} + \frac{\partial v_z}{\partial r}\right)\right] + 2\frac{\mu}{r}\left(\frac{\partial v_r}{\partial r} - \frac{v_r}{r}\right)$$

4. Species Continuity

$$\rho\, v_z\left(\frac{\partial C_i}{\partial z} + v_r\frac{\partial C_i}{\partial r}\right) = \frac{1}{r}\frac{\partial}{\partial r}\left[\rho r\left(D_i\frac{\partial C_i}{\partial r} + D_i^T\frac{C_i}{T}\frac{\partial T}{\partial r}\right)\right] \qquad \text{(A-4)}$$

$$+ \frac{\partial}{\partial z}\left[\rho\left(D_i\frac{\partial C_i}{\partial z} + \frac{C_i}{T}D_i^T\frac{\partial T}{\partial z}\right)\right] + w_i$$

5. Energy

$$\rho\left(v_z\frac{\partial h}{\partial z} + v_r\frac{\partial h}{\partial r}\right) = \frac{1}{r}\frac{\partial}{\partial r}\left(K_r\frac{\partial T}{\partial r}\right) + \frac{\partial}{\partial z}\left(K\frac{\partial T}{\partial z}\right) \qquad \text{(A-5)}$$

$$+ \sum \left(\frac{1}{r} \frac{\partial}{\partial r} \left[\rho r \, h_i \left(D_i \frac{\partial C_i}{\partial r} + \frac{C_i}{T} D_i^T \frac{\partial T}{\partial r} \right) \right] + \right.$$

$$\left. \frac{\partial}{\partial z} \left[\rho \, h_i \left(D_i \frac{\partial C_i}{\partial z} + \frac{C_i}{T} D_i^T \frac{\partial T}{\partial z} \right) \right] \right) + v_r \frac{\partial P}{\partial r} + v_z \frac{\partial P}{\partial z} +$$

$$\mu \left[2 \left(\frac{\partial v_z}{\partial z} \right)^2 + 2 \left(\frac{\partial v_r}{\partial r} \right)^2 + \left(\frac{\partial v_r}{\partial z} + \frac{\partial v_r}{\partial r} \right)^2 + 2 \frac{v_r^2}{r^2} \right.$$

$$\left. - 2/3 \left(\frac{\partial v_r}{\partial r} + \frac{\partial v_z}{\partial z} + \frac{v_r}{r} \right)^2 \right]$$

For a mixture of n species, n-1 species continuity equations have to be satisfied in addition to the usual global continuity equation.

The first step is to reduce the equations to their applicable boundary layer form by an order analysis; thus reducing their complexity and facilitating their solution. Let δ be a measure of the boundary layer thickness, and let L be the characteristic length of the nozzle. Now L is an order of magnitude greater than δ since the boundary layer region is a thin layer next to the nozzle wall. Before the order analysis can be applied the equations have to be put in dimensionless form.

The center line axial velocity will be used to make dimensionless all velocities and L will be used likewise for length. The other properties will be made dimensionless by use of their respective main stream properties. The dimensionless properties will be noted by a bar and the

order of magnitude will be symbolized by 0 ( ).

Define order one by,

$$0\,(1) = L/L \tag{A-6}$$

and order delta bar by,

$$0(\bar{\delta}) = \frac{\delta}{L} \tag{A-6a}$$

The resultant non-dimensional properties are $\bar{z}$, $\bar{r}$, $\bar{v}_z$, $\bar{v}_r$, $\bar{\rho}$, $\bar{P}$, $\bar{T}$, $\bar{h}$, $\bar{\mu}$, $\bar{D}_i$, and $\bar{K}$, all of which have an order (1) except $\bar{v}_r$ which has order $(\bar{\delta})$. The derivatives of properties with respect to $\bar{z}$ and $\bar{r}$ are required from continuity to be

$$\frac{\partial}{\partial \bar{z}} = 0(1) \tag{A-7}$$

$$\frac{\partial}{\partial \bar{r}} = 0\left(\frac{1}{\bar{\delta}}\right) \tag{A-7a}$$

$$\frac{\partial^2}{\partial \bar{r}^2} + 0\left(\frac{1}{\bar{\delta}^2}\right) \tag{A-7b}$$

The large value of the derivative with respect to $\bar{r}$ is because of large gradients across the thin boundary layer.

The thermal diffusion coefficient appears in Equations (A-4) and

(A-5). The thermal effect as discussed in Chapter III is much less than the mass diffusion effect; therefore, the thermal diffusion coefficient will be dropped from the equations that follow.

In each of the Equations (A-2) through (A-5) at least one term of the following form appears

$$\frac{1}{r}\frac{\partial}{\partial r}\left(rQ\,\frac{\partial}{\partial r}\right) = \frac{Q_o}{L^2}\left[\frac{1}{\bar{r}}\frac{\partial}{\partial \bar{r}}\left(\bar{r}\bar{Q}\,\frac{\partial}{\partial \bar{r}}\right)\right] \qquad \text{(A-8)}$$

Carrying out the differentiation indicated and performing an order analysis on the right side of Equation (A-8) results in

$$\frac{1}{Q_o L^2}\left[\frac{1}{\bar{r}}\frac{\partial}{\partial \bar{r}}\left(\bar{r}\bar{Q}\,\frac{\partial}{\partial \bar{r}}\right)\right] = \frac{Q_o}{L^2}\underbrace{\left(\frac{\bar{r}}{\bar{r}}\frac{\partial}{\partial \bar{r}}\right)}_{O(1)}\left[\underbrace{\bar{Q}\left(\frac{\partial}{\partial \bar{r}}\right)}_{O\left(\frac{1}{\bar{\delta}^2}\right)} + \underbrace{\frac{\bar{Q}}{\bar{r}}\left[\frac{\partial}{\partial \bar{r}}\right]}_{O\left(\frac{1}{\bar{\delta}}\right)}\right] \qquad \text{(A-8a)}$$

The second term on the right side of Equation (A-8a) is an order of magnitude less than the first term. The second term will be neglected in the following analysis and in each instance that an expression of the form of the left side of Equation (A-8) appears it will be written

$$\frac{1}{r}\ \frac{\partial}{\partial r}\left(rQ\ \frac{\partial}{\partial r}\right) = \frac{\partial}{\partial r}\left[Q\left(\frac{\partial}{\partial r}\right)\right] \qquad \text{(A-8b)}$$

The axial momentum equation, Equation (A-2), becomes, with the order of each term indicated below it,

$$\underset{O(1)}{\bar{\rho}\ \bar{v}_z}\ \underset{O(1)}{\frac{\partial \bar{v}_z}{\partial \bar{z}}} + \underset{O(1)}{\bar{\rho}\ \bar{v}_r}\ \underset{O(1)}{\frac{\partial \bar{v}_z}{\partial \bar{r}}} = \underset{O(1)}{\frac{-P_o}{\rho_o\ U_o^{\,2}}}\ \underset{O(1)}{\frac{\partial \bar{P}}{\partial \bar{z}}} \qquad \text{(A-9)}$$

$$+\ \underset{O(\bar{\delta}^2)}{\frac{\mu_o}{\rho_o\ U_o\ L}} \left\{ \underset{O(1)}{\frac{\partial}{\partial \bar{z}}} \left(\underset{O(1)}{\bar{\mu}} \left[\underset{O(1)}{2\ \frac{\partial \bar{v}_z}{\partial \bar{z}}} - 2/3 \left(\underset{O(1)}{\frac{1}{\bar{r}}\ \frac{\partial \bar{r}\ \bar{v}_r}{\partial \bar{r}}} + \underset{O(1)}{\frac{\partial \bar{v}_z}{\partial z}} \right) \right] \right) \right.$$

$$\left. + \underset{O(1)}{\frac{\partial}{\partial \bar{r}}} \left[\underset{O(1)}{\mu\ \frac{\partial \bar{v}_z}{\partial \bar{r}}} \right] \right\}$$

The order of the left side of Equation (A-9) is one; therefore, the right side must have the same order of magnitude. For the viscous forces to be of comparable order as the inertial forces the Reynolds number, $\frac{\rho_o\ U_o\ L}{\mu_o}$, must be of the order $\frac{1}{\bar{\delta}^2}$. Neglecting all of the viscous terms of the order less than $\frac{1}{\bar{\delta}^2}$ the axial momentum equation becomes

$$\rho\ v_z\ \frac{\partial v_z}{\partial z} + \rho\ v_r\ \frac{\partial v_z}{\partial r} = -\ \frac{\partial P}{\partial z} + \frac{\partial}{\partial r}\left[\mu\ \frac{\partial v_z}{\partial r}\right] \qquad \text{(A-10)}$$

Applying the same method to the radial momentum equation, Equation (A-3), and neglecting all terms of $O(\bar{\delta})$ or less results in

$$\frac{\partial \bar{P}}{\partial \bar{r}} = O(\bar{\delta}) \tag{A-11}$$

Thus pressure will vary only in the axial direction, and at any station along the nozzle the pressure is constant across the boundary layer. The $\left(\frac{\partial P}{\partial z}\right)$ term in Equation (A-10) can be replaced with $\left(\frac{dP}{dz}\right)$.

When put in the dimensionless form the species continuity equation is

$$\underset{O(1)}{\bar{\rho}\ \bar{v}_z \frac{\partial C_i}{\partial \bar{z}}} + \underset{O(1)}{\bar{\rho}\ \bar{v}_r \frac{\partial C_i}{\partial \bar{r}}} = \underset{O(\bar{\delta}^2)}{\frac{D_{i_o}}{U_o L}} \left\{ \underset{O\left(\frac{1}{\bar{\delta}}\right)}{\left[\frac{\partial}{\partial \bar{r}}\left(\bar{\rho}\ \bar{D}_i \frac{\partial C_i}{\partial \bar{r}}\right)\right]} + \underset{O(1)}{\left[\frac{\partial}{\partial \bar{z}}\left(\bar{\rho}\ \bar{D}_i \frac{\partial C_i}{\partial \bar{z}}\right)\right]} \right\} + \underset{O(1)}{\frac{w_i L}{\rho_o U_o}} \tag{A-12}$$

The product of the Reynolds number and Schmidt number, $\frac{U_o L}{D_{i_o}}$, has an order of magnitude of $\left(\frac{1}{\bar{\delta}^2}\right)$. From the momentum equation the Reynolds number must have an order $\left(\frac{1}{\bar{\delta}^2}\right)$ and the Schmidt number for gases is very close to one. Again neglecting terms of order $(\bar{\delta})$ or less the species continuity equation for the boundary layer becomes

$$\rho\, v_z \frac{\partial C_i}{\partial z} + \rho\, v_r \frac{\partial C_i}{\partial r} = \frac{\partial}{\partial r}\left[\rho\, D_i \frac{\partial C_i}{\partial r}\right] + w_i \qquad \text{(A-13)}$$

The energy equation, Equation (A-5), takes the following form when it is made dimensionless

$$\bar{\rho}\, \bar{v}_z \frac{\partial \bar{h}}{\partial \bar{z}} + \bar{\rho}\, \bar{v}_r \frac{\partial \bar{h}}{\partial \bar{r}} = \frac{K_o\, T_o}{\rho_o\, U_o\, h_o\, L}\left[\frac{\partial}{\partial \bar{r}}\left(\bar{K} \frac{\partial \bar{T}}{\partial \bar{r}}\right)\right. \qquad \text{(A-14)}$$

$$O(1) \qquad O(1) \qquad O(\bar{\delta}^2) \qquad O\left(\frac{1}{\bar{\delta}^2}\right)$$

$$\left. + \frac{\partial}{\partial \bar{z}}\left(\bar{K} \frac{\partial \bar{T}}{\partial \bar{z}}\right)\right] + \frac{D_{i_o}}{U_o\, L}\left\{\sum\left[\frac{\partial}{\partial \bar{r}}\left[\bar{\rho}(\bar{h}_i)\, \bar{D}_i \frac{\partial C_i}{\partial \bar{r}}\right]\right.\right.$$

$$O\left(\bar{\delta}^2\right) \qquad O\left(\frac{1}{\bar{\delta}^2}\right)$$

$$\left.\left. + \frac{\partial}{\partial \bar{z}}\left[\bar{\rho}\, (\bar{h}_i - \bar{h}_{i^o})\, \bar{D}_i \frac{\partial C_i}{\partial \bar{r}}\right]\right]\right\} + \frac{P_o}{\rho_o\, h_o}\left(\bar{v}_r \frac{\partial \bar{P}}{\partial \bar{r}} + \bar{v}_z \frac{\partial \bar{P}}{\partial \bar{z}}\right)$$

$$O(1) \qquad O(1) \quad O\left(\bar{\delta}^2\right) \quad O(1)$$

$$+ \frac{\mu_o\, U_o}{\rho_o\, L\, h_o}\, \bar{\mu}\left[2\left(\frac{\partial \bar{v}_z}{\partial \bar{z}}\right)^2 + 2\left(\frac{\partial \bar{v}_r}{\partial \bar{r}}\right)^2 + \left(\frac{\partial \bar{v}_r}{\partial \bar{z}} + \frac{\partial \bar{v}_z}{\partial \bar{r}}\right)^2\right.$$

$$O\left(\bar{\delta}^2\right) \qquad O(1) \qquad O(1) \qquad O(1) \quad O\left(\frac{1}{\bar{\delta}^2}\right)$$

$$+ 2\left(\frac{\bar{v}_r}{\bar{r}}\right)^2 - 2/3\left(\frac{\partial \bar{v}_r}{\partial \bar{r}} + \frac{\partial \bar{v}_z}{\partial \bar{z}} + \frac{\bar{v}_r}{\bar{r}}\right)^2 \Bigg\}$$

$$O(\bar{\delta}^2) \qquad O(1) \quad O(1) \quad O(\bar{\delta}^2)$$

Note the order of magnitude of the following terms that appear in Equation (A-14)

$$\frac{K_o T_o}{\rho_o U_o h_o L} = \frac{1}{Re \times Pr} \qquad \text{(A-14a)}$$

$$O(\bar{\delta}^2)$$

$$\frac{D_{i_o}}{U_o L} = \frac{1}{Re \times S} \qquad \text{(A-14b)}$$

$$O(\bar{\delta}^2)$$

$$\frac{P_o}{P_o h_o} = \frac{R_o}{C_p} \qquad \text{(A-14c)}$$

$$O(1)$$

$$\frac{\mu_o U_o}{\rho_o L h_o} = \frac{1}{Re} \times \frac{R_o M^2}{C_v} \qquad \text{(A-14d)}$$

$$O(\bar{\delta}^2)$$

After neglecting terms of an order of magnitude of $\bar{\delta}$ or less the energy equation takes the form

$$\rho v_z \frac{\partial h}{\partial z} + \rho v_r \frac{\partial h}{\partial r} = \frac{\partial}{\partial r}\left(K \frac{\partial T}{\partial r}\right) \qquad \text{(A-15)}$$

$$+ \sum \left(\frac{\partial}{\partial r} \left[\rho (h_i) D_i \frac{\partial C_i}{\partial r} \right] \right) + \mu \left(\frac{\partial v_z}{\partial r} \right)^2 + v_z \frac{\partial P}{\partial z}$$

For the flow through a nozzle it is much more convenient to have a coordinate system for the flow very close to the wall, rather than the cylindrical coordinate system. Thus a change will be made to coordinates x, distance along nozzle wall, and y, distance normal to the nozzle wall. The velocity components will be u and v in the x and y direction respectively. This coordinate system is illustrated in Figure 17.

If the boundary layer thickness is small in comparison with the nozzle radius then r in the global continuity equation, when applied to the boundary layer, can be replaced with R, the nozzle radius.

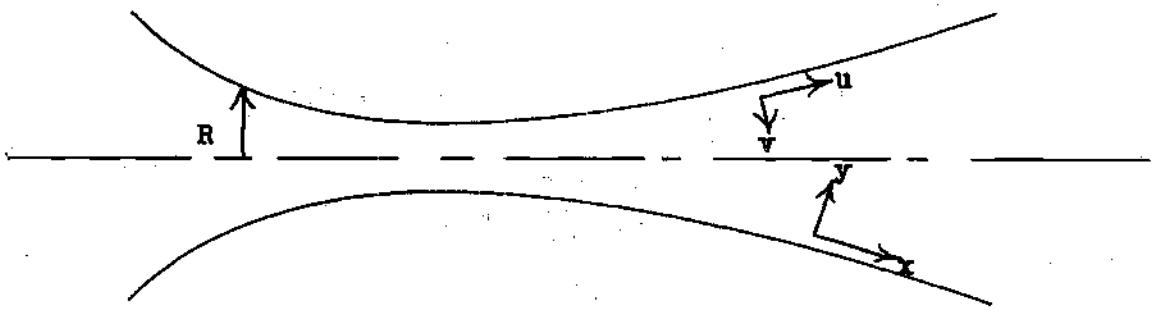

Figure 17. Nozzle Coordinate System.

Before writing the boundary layer equations in final form it is

desirable to further modify the energy boundary layer equation, Equation (A-15). This equation written in the final coordinate system is

$$\rho\, u\, \frac{\partial h}{\partial x} + \rho\, v\, \frac{\partial h}{\partial y} = \frac{\partial}{\partial y}\left(K\frac{\partial T}{\partial y}\right) + \sum\left(\frac{\partial}{\partial y}\left[\rho\, h_i\, D_i\, \frac{\partial C_i}{\partial y}\right]\right) + \mu\left(\frac{\partial u}{\partial y}\right)^2 + u\, \frac{dP}{dx} \qquad \text{(A-15a)}$$

It can be shown very readily that

$$\frac{\partial T}{\partial y} = \frac{1}{\bar{C}_p}\left[\frac{\partial h}{\partial y} - \sum h_i\, \frac{\partial C_i}{\partial y}\right] \qquad \text{(A-16)}$$

$\bar{C}_p$ is the average specific heat of the mixture. If the momentum equation is multiplied by u, added to Equation (A-15a), and Equation (A-16) is substituted for $\frac{\partial T}{\partial y}$ in Equation (A-15a), the final form of the energy boundary layer equation will be obtained after rearrangement. This equation is given below, Equation (A-20).

The resultant boundary layer equations in the final coordinate system are:

1. Global Continuity

$$\frac{\partial(\rho u R)}{\partial x} + \frac{\partial(\rho v R)}{\partial y} = 0 \qquad \text{(A-17)}$$

2. Momentum

$$\rho\ u\ \frac{\partial u}{\partial x} + \rho\ v\ \frac{\partial u}{\partial y} = \frac{-dP}{dx} + \frac{\partial}{\partial y}\left[\mu\ \frac{\partial u}{\partial y}\right] \qquad \text{(A-18)}$$

3. Species Continuity

$$\rho\ u\ \frac{\partial C_i}{\partial x} + \rho\ v\ \frac{\partial C_i}{\partial y} = \frac{\partial}{\partial y}\left[\rho\ D_i\ \frac{\partial C_i}{\partial y}\right] + w_i \qquad \text{(A-19)}$$

4. Energy Equation

$$\rho\ u\ \frac{\partial I}{\partial x} + \rho\ v\ \frac{\partial I}{\partial y} = \frac{\partial}{\partial y}\left(\frac{u}{Pr}\ \frac{\partial I}{\partial y}\right) + \frac{\partial}{\partial y}\left[\mu\left(1 - \frac{1}{Pr}\right)\ \frac{\partial \frac{u^2}{2}}{\partial y}\right] \qquad \text{(A-20)}$$

$$+ \frac{\partial}{\partial y}\left\{\sum\left[\left(\rho\ D_i\ h_i\right)\left(1 - \frac{1}{L_i}\right)\ \frac{\partial C_i}{\partial y}\right]\right\}$$

APPENDIX B

Computer Program

Solution to the viscous flow equations was performed on the Burroughs B5000 Electronic Computer at the Rich Electronic Computer Center on the Georgia Institute of Technology Campus. The computer program is given below in the Algol language as it was read into the computer.

All of the information up to the first procedure declaration relates to the type of variables, program output and the output format. The six real procedures relate to useful functions used in the numerical integration. The density viscosity product, density and the derivative with respect to η of the density viscosity product are calculated in the first three procedures, respectively, during the numerical integration. f''', g_I', and Z_A'' are calculated, respectively, in the next three procedures.

Simultaneous solution of the seven first order differential equations is carried out in the PROCEDURE WSS( ) which ends at the label GOOF:, page 117. The next line after GOOF: is for reading in known properties and boundary conditions, and the second line is for the value of the influence coefficient.

Assumed values for the three unknown boundary conditions at the wall, f_w'', g_{Iw}', Z_{Aw}', are placed in the program on the third card after the label GOOF:. These values are used only once and within the computation they are modified to give the appropriate solution. The values of

J or D for the computation are put into the program on the next line. In the particular program shown the calculation is carried for 15 values of J from 0.0 to 1.4 in equal steps of 0.1 each. The first BEGIN after GOOF: starts the calculation and in this case it is for D held constant at 0.9 for the 15 values of J.

The procedure call WSS( ) starts the numerical solution and it goes to completion if the value of f' stays within reasonable bounds. If not then it automatically stops the calculation and modifies the value of f''_w until the calculation on f' stays within the bounds. The ninth and tenth line after the label REPEAT: on page 118 provide the test for values of f', g_I, and Z_A at the edge of the boundary layer.

If these values meet the test then the solution to the various profiles are printed out and the next value of J is used and the calculation is started over. If the tests are not met then the iterative procedure is initiated and f''_w, g'_{Iw}, Z'_{Aw} are modified accordingly and new values are calculated to meet the required conditions on f', g_I, and Z_A at the boundary layer's edge. This iterative procedure is continued until the appropriate tests are satisfied and the correct solution is printed out.

The initial assumed values of f''_w, Z'_{Aw}, and g'_{Iw} are used only once; in this case for J = 0. When the calculation proceeds to the next higher J, or D, its first solution uses the values of f''_w, Z'_{Aw} and g'_{Iw} that has given the correct solution for the current value of J, or D.

Only capital letters of the English alphabet are used in the Algol language thus a change in symbols from those used in text is necessary. The required changes are tabulated below:

A for α_e	F for f	F1 for f'
F2 for f"	F3 for f'"	F2W for f''_w
F1E for f'_∞	G for g_I	G1 for g'_I
G1W for g'_{Iw}	GE for $g_{I\infty}$	Z for Z_A
Z1 for Z'_A	N for n	Dn for Δn

Program For Nozzle Solution

```
BEGIN    FILE IN BOW1 (1,10); FILE OUT BOW2 1 (1,15)                    ;
COMMENT  WS SHEPARD REAL GAS NOZZLE                                     ;
         INTEGER I,K; REAL A,D,F2W,F1E,F1EF,F1EG,F1EZ,GW,G1W,GE,GEF,GEG,
         GEZ,J,PR,SO,Z1W,ZE,ZEF,ZEG,ZEZ,ZW,DN,IC,DF1E,DGE,DZE,FF,FG,FZ,
         GG,GZ,GF,ZZ,ZF,ZG,DF,DG,DZ,DD,D1,D2,D3,D4,D5,D6,D7,D8,D9,F1,G  ;
         REAL ARRAY EN,EF,EF1,EF2,EG,EG1,EZ,EZ1,EC,EE,EH,EB[0:55]       ;
         LABEL REPEAT, PRINT                                            ;
MONITOR  BOW2 (F1E,F1EF,F1EG,F1EZ,GE,GEF,GEG,GEZ,ZE,ZEF,ZEG,ZEZ)        ;
LIST     OUT3 (F1,G)                                                    ;
LIST     OUT2 (F2W,G1W,Z1W)                                             ;
LIST     BUT(FOR I ← 1 STEP 1 UNTIL 35 DO [EN[I],EF[I],EF1[I],EF2[I],
         EG[I],EG1[I],EZ[I],EZ1[I],EC[I],EE[I],EH[I],EB[I]])           ;
LIST     TITL2 (D,J,A,PR,GW,ZW,F2W,G1W,Z1W)                             ;
FORMAT   FMT3 ("F1  =",F8.6,", G  =",F8.6)                              ;
FORMAT   FMT2 ("F2W = ",F8.6,", G1W = ",F8.6,", Z1W = ",F8.6,X74)       ;
FORMAT   FMT(F3.1, 11F9.4)                                              ;
FORMAT   DUMM(X120)                                                     ;
FORMAT   TITL(X12,"gOLUTION TO MOMENTUM, ENERGY, AND SPECIES CONTINUIT",
```

```
        "Y EQUATIONS FOR NOZZLE FLOW."/X20,"D = ",F5.3,", J = ",F5.3,
        ", A = ",F4.2,", PR = ",F5.3,", GW = ",F4.2,", ZW = ",F4.2,/
        X30,"F2W = ",F7.5,", G1W = ",F7.5,", Z1W = ",F7.5,//X1,
        "N",X6,"F",X8,"DF",X6,"D2F",X7,"G",X8,"DG",X7,"Z",X8,"DZ",X7,
        "Y",X7,"DIS",X5,"MOM",X7,"B"//)                                  ;
REAL PROCEDURE DVP(A,F1,G,J,Z); VALUE A,F1,G,J,Z; REAL A,F1,G,J,Z        ;
BEGIN REAL VIS; VIS ← (((1+A)*2)/(((3.86+A)*0.36)x(1+0.65xA))) x
        (((1+0.65xAxZ)x((3.86+AxZ)*0.36))/((1+AxZ)*2))x(((2-J)/
        (2xG-Jx(F1*2)))*0.36) ; DVP ← VIS ; END DVP                      ;
REAL PROCEDURE DQ(A,F1,G,J,Z) ; VALUE A,F1,G,J,Z; REAL A,F1,G,J,Z        ;
BEGIN   REAL RHO ; RHO ← ((3.86+A)/(1+A)) x ((1 + AxZ)/(3.86 + AxZ))
        x ((2xG - J x (F1*2))/(2 - J)) ; DQ ← RHO ; END DQ               ;
REAL PROCEDURE DER(A,F1,F2,G,G1,J,Z,Z1) ; VALUE A,F1,F2,G,G1,J,Z,Z1      ;
        REAL A,F1,F2,G,G1,J,Z,Z1                                         ;
BEGIN   REAL DDVP ;  DDVP ← (0.65/(1+0.65xAxZ) + 0.36/(3.86 + AxZ) -
        2/(1+AxZ)) x A x(Z1) -(0.72 x (G1-JxF1xF2))/(2xG - J x (F1*2));
        DER ← DDVP ; END DER                                             ;
REAL PROCEDURE DDF(A,D,F,F1,F2,G,G1,J,Z,Z1)                              ;
        VALUE A,D,F,F1,F2,G,G1,J,Z,Z1                                    ;
        REAL A,D,F,F1,F2,G,G1,J,Z,Z1                                     ;
BEGIN   REAL B,B1,DR,MOM                                                 ;
        B ← DVP(A,F1,G,J,Z)                                              ;
        B1 ← DER(A,F1,F2,G,G1,J,Z,Z1) x B                                ;
        DR ← DQ(A,F1,G,J,Z)                                              ;
        MOM ← (D/B)x ((F1*2) - DR) - ((F2/B) x (B1 + F))                 ;
        DDF ← MOM   ; END DDF                                            ;
```

```
REAL PROCEDURE DDG(A,F,F1,F2,F3,G,G1,J,PR,Z,Z1)                    ;
        VALUE A,F,F1,F2,F3,G,G1,J,PR,Z,Z1                          ;
        REAL A,F,F1,F2,F3,G,G1,J,PR,Z,Z1                           ;
BEGIN   REAL B,B1,ENE;  B ← DVP(A,F1,G,J,Z)                        ;
        B1 ← DER(A,F1,F2,G,G1,J,Z,Z1) x B                          ;
        ENE ← (Jx(1-PR)) x ((B1/B)xF1xF2 + (F2*2)+F1xF3) -
        ((B1+FxPR) x (G1/B)) ;   DDG ← ENE   ; END DDG             ;
REAL PROCEDURE DDZ(A,F,F1,F2,G,G1,J,SO,Z,Z1)                       ;
        VALUE A,F,F1,F2,G,G1,J,SO,Z,Z1                             ;
        REAL A,F,F1,F2,G,G1,J,SO,Z,Z1                              ;
BEGIN   REAL B,B1,S,S1,SPE ;  B ← DVP(A,F1,G,J,Z)                  ;
        B1 ← DER(A,F1,F2,G,G1,J,Z,Z1) x B                          ;
        S ← SOx(1+0.65xAxZ) ; S1 ← 0.65 x A x Z1 x SO              ;
        SPE ← Z1x((S1/S) -(B1/B) -(FxS/B))                         ;
        DDZ ← SPE ;   END DDZ                                      ;
PROCEDURE WSS(A,D,DN,F2W,GW,G1W,J,PR,SO,ZW,Z1W,EN,EF,EF1,EF2,EG,F1,G,
        EG1,EZ,EZ1,EC,EE,EH,EB)                                    ;
        VALUE A,D,DN,F2W,GW,G1W,J,PR,SO,ZW,Z1W                     ;
        REAL A,D,DN,F2W,GW,J,PR,SO,ZW,Z1W,F1,G,G1W                 ;
        REAL ARRAY EN,EF,EF1,EF2,EG,EG1,EZ,EZ1,EC,EE,EH,EB[0]      ;
BEGIN   INTEGER I,K ; REAL F,F2,F3,G1,Z,Z1,N,C,E,H,DR1,DR2,DR3,
        DR4,P1,P2,P3,P4,Q1,Q2,Q3,Q4,R1,R2,R3,R4,T1,T2,T3,T4,U1,U2,
        U3,U4,V1,V2,V3,V4,W1,W2,W3,W4,L1,L2,L3,L4,M1,M2,M3,M4,
        X1,X2,X3,X4  ;   LABEL GOOF                                ;
        F ← 0 ; F1 ← 0; F2 ← F2W ; G ← GW ; G1 ← G1W ; Z ← ZW      ;
        Z1 ← Z1W ; C ← 0 ;  E ← 0 ;  H ← 0 ; K ← 0 ; I ← 1         ;
```

```
          FOR N ← 0 STEP DN UNTIL  7.0 DO
BEGIN     P1 ← F1 x DN                                                    ;
          Q1 ← F2 x DN                                                    ;
          R1 ← DDF(A,D,F,F1,F2,G,G1,J,Z,Z1) x DN                          ;
          T1 ← G1 x DN                                                    ;
          U1 ← DDG(A,F,F1,F2,(R1/DN),G,G1,J,PR,Z,Z1) x DN                 ;
          V1 ← Z1  x DN                                                   ;
          W1 ← DDZ(A,F,F1,F2,G,G1,J,SO,Z,Z1) x DN                         ;
          DR1 ← DQ(A,F1,G,J,Z)                                            ;
          L1 ← DR1  x DN                                                  ;
          M1 ← (DR1-F1)  x DN                                             ;
          X1 ← (1-F1)xF1xDN                                               ;
          P2 ← (F1 + Q1/2) x DN                                           ;
          Q2 ← (F2 + R1/2) x DN                                           ;
          R2 ← DDF(A,D,F+P1/2,F1+Q1/2,F2+R1/2,G+T1/2,G1+U1/2,J,Z+V1/2,
               Z1+W1/2) x DN                                              ;
          T2 ← (G1 + U1/2) x DN                                           ;
          U2 ← DDG(A,F+P1/2,F1+Q1/2,F2+R1/2,(R2/DN),
                    G+T1/2,G1+U1/2,J,PR,Z+V1/2,Z1+W1/2) x DN               ;
          V2 ← (Z1 + W1/2) x DN                                           ;
          W2 ← DDZ(A,F+P1/2,F1+Q1/2,F2+R1/2,G+T1/2,
               G1+U1/2,J,SO,Z+V1/2,Z1+W1/2) x DN                          ;
          DR2 ← DQ(A,F1 + Q1/2,G + T1/2,J, Z + V1/2)                      ;
          L2 ← DR2 x DN                                                   ;
          M2 ← (DR2 - (F1 + Q1/2)) x DN                                   ;
          X2 ← (1- F1 - Q1/2) x (F1 + Q1/2) xDN                           ;
```

```
P3 ← (F1 + Q2/2) x DN                                                    ;
Q3 ← (F2 + R2/2) x DN                                                    ;
R3 ← DDF(A,D,F+P2/2,F1+Q2/2,F2+R2/2,G+T2/2,
     G1+U2/2,J,Z+V2/2,Z1+W2/2) x DN                                      ;
T3 ← (G1 + U2/2) x DN                                                    ;
U3 ← DDG(A,F+P2/2,F1+Q2/2,F2+R2/2,(R3/DN),
     G+T2/2,G1+U2/2,J,PR,Z+V2/2,Z1+W2/2) x DN                            ;
V3 ← (Z1 + W2/2) x DN                                                    ;
W3 ← DDZ(A,F+P2/2,F1+Q2/2,F2+R2/2,G+T2/2,
     G1+U2/2,J,SO,Z+V2/2,Z1+W2/2) x DN                                   ;
DR3 ← DQ(A,F1 + Q2/2,G + T2/2,J,Z + V2/2)                                ;
L3 ← DR3 x DN                                                            ;
M3 ← (DR3 - F1 - Q2/2) x DN                                              ;
X3 ← (1 - F1 - Q2/2) x (F1 + Q2/2) x DN                                  ;
P4 ← (F1 + Q3) x DN                                                      ;
Q4 ← (F2 + R3) x DN                                                      ;
R4 ← DDF(A,D,F+P3,F1+Q3,F2+R3,G+T3,G1+U3,J,Z+V3,Z1+W3) x DN              ;
T4 ← (G1 + U3) x DN                                                      ;
U4 ← DDG(A,F+P3,F1+Q3,F2+R3,R4/DN,G+T3,G1+U3,J,
     PR,Z+V3,Z1+W3) x DN                                                 ;
V4 ← (Z1 + W3) x DN                                                      ;
W4 ← DDZ(A,F+P3,F1+Q3,F2+R3,G+T3,G1+U3,J,SO,Z+V3,Z1+W3) x DN             ;
DR4 ← DQ(A,F1 + Q3, G + T3, J, Z + V3)                                   ;
L4 ← DR4 x DN                                                            ;
M4 ← (DR4 - F1 - Q3) x DN                                                ;
X4 ← (1-F1 - Q3) x (F1 + Q3) x DN                                        ;
```

```
        F ← F  + (P1 + 2xP2 + 2xP3 + P4)/6                              ;
        F1 ← F1 + (Q1 + 2xQ2 + 2xQ3 + Q4)/6                             ;
        F2 ← F2 + (R1 + 2xR2 + 2xR3 + R4)/6                             ;
        G ← G  + (T1 + 2xT2 + 2xT3 + T4)/6                              ;
        G1 ← G1 + (U1 + 2xU2 + 2xU3 + U4)/6                             ;
        Z ← Z + (V1 + 2xV2 + 2xV3 + V4)/6                               ;
        Z1 ← Z1 + (W1 + 2xW2 + 2xW3 + W4)/6                             ;
        C ← C + (L1 + 2xL2 + 2xL3 + L4)/6                               ;
        E ← E + (M1 + 2xM2 + 2xM3 + M4)/6                               ;
        H ← H + (X1 + 2xX2 + 2xX3 + X4)/6                               ;
        IF (J x F1*2 + 0.1) > 2 x G THEN GO TO GOOF                     ;
        IF F1 < 0  THEN GO TO GOOF                                      ;
        K ← K + 1                                                       ;
        IF (K MOD 4)= 0  THEN
BEGIN   EN[I]←N+DN; EF[I] ← F; EF1[I] ← F1; EF2[I] ← F2; EG[I] ← G       ;
        EG1[I] ← G1; EZ[I] ← Z; EZ1[I] ← Z1; EC[I] ← C ;  EE[I] ← E     ;
        EH[I] ← H; EB[I] ← DVP(A,F1,G,J,Z); I ← I + 1                   ;
        END;   END                                                      ;
GOOF:   END WSS                                                         ;
        DN ← 0.05; A ← 0.9; GW ← 0.4; ZW ← 0.05; PR ← 0.675; SO ← 0.545 ;
        IC ← 0.0001                                                     ;
        F2W ← 0.380   ; G1W ← 0.120   ; Z1W ← 0.160                     ;
        FOR J ← 0.0 STEP 0.1 UNTIL 1.4 DO
BEGIN   D ← 0.9                                                         ;
REPEAT: WRITE (BOW2, FMT2, OUT2)                                        ;
        WSS(A,D,DN,F2W,GW,G1W,J,PR,SO,ZW,Z1W,EN,EF,EF1,EF2,EG,F1,G,
```

```
EG1,EZ,EZ1,EC,EE,EH,EB)                                                    ;
WRITE (BOW2, FMT3, OUT3)                                                   ;
IF (J x F1*2 + 0.1) > 2 x G THEN BEGIN
F2W ← F2W - 0.005; GO TO REPEAT ;  END                                     ;
IF F1 < 0  THEN BEGIN F2W ← F2W + 0.005 ; GO TO REPEAT ; END               ;
F1E ← EF1[35] ; GE ← EG[35] ; ZE ← EZ[35]                                  ;
DF1E ← 1 - F1E ; DGE ← 1 - GE ; DZE ← 1 - ZE                               ;
IF (ABS(DF1E) < 0.0001 AND ABS(DGE) < 0.0001
AND ABS(DZE) < 0.0001) THEN GO TO PRINT                                    ;
F2W ← F2W + IC                                                             ;
WRITE (BOW2, FMT2, OUT2)                                                   ;
WSS(A,D,DN,F2W,GW,G1W,J,PR,SO,ZW,Z1W,EN,EF,EF1,EF2,EG,F1,G,
EG1,EZ,EZ1,EC,EE,EH,EB)                                                    ;
IF (J x F1*2 + 0.1) > 2 x G THEN BEGIN
F2W ← F2W - 0.005; GO TO REPEAT ; END                                      ;
IF F1 < 0  THEN BEGIN F2W ← F2W + 0.005 ; GO TO REPEAT ; END               ;
F1EF ← EF1[35] ; GEF ← EG[35] ; ZEF  ←  EZ[35]                             ;
F2W ← F2W - IC ; G1W ← G1W + IC                                            ;
WRITE (BOW2, FMT2, OUT2)                                                   ;
WSS(A,D,DN,F2W,GW,G1W,J,PR,SO,ZW,Z1W,EN,EF,EF1,EF2,EG,F1,G,
EG1,EZ,EZ1,EC,EE,EH,EB)                                                    ;
IF (J x F1*2 + 0.1) > 2 x G THEN BEGIN
F2W ← F2W - 0.005; GO TO REPEAT ;  END                                     ;
IF F1 < 0  THEN BEGIN F2W ← F2W + 0.005 ; GO TO REPEAT ; END               ;
F1EG ← EF1[35] ; GEG ← EG[35] ; ZEG ← EZ[35]                               ;
G1W ← G1W - IC ; Z1W ← Z1W + IC                                            ;
```

```
        WRITE (BOW2, FMT2, OUT2)                                          ;
        WSS(A,D,DN,F2W,GW,G1W,J,PR,SO,ZW,Z1W,EN,EF,EF1,EF2,EG,F1,G,
        EG1,EZ,EZ1,EC,EE,EH,EB)                                           ;
        IF (J x F1*2 + 0.1) > 2 x G THEN BEGIN
        F2W ← F2W - 0.005; GO TO REPEAT ;  END                            ;
        IF F1 < 0  THEN BEGIN F2W ← F2W + 0.005 ; GO TO REPEAT ; END      ;
        F1EZ ← EF1[35] ; GEZ ← EG[35] ; ZEZ ← EZ[35]                      ;
        FF ← F1EF - F1E ;  FG ← F1EG - F1E ; FZ ← F1EZ - F1E              ;
        GG ← GEG - GE ; GZ ← GEZ - GE ; GF ← GEF - GE                     ;
        ZZ ← ZEZ - ZE ; ZF ← ZEF - ZE ; ZG ← ZEG - ZE                     ;
        D1 ← (GG x ZZ) - (GZ x ZG)                                        ;
        D2 ← (GZ x ZF) - (GFxZZ) ; D3 ← (GFxZG)- (GGxZF)                  ;
        D4 ← (FZxZG)- (FGxZZ) ; D5 ← (FFxZZ) -(FZxZF)                     ;
        D6 ← (FGxZF)- (FFxZG) ; D7 ← (FGxGZ) - (FZxGG)                    ;
        D8 ← (FZxGF) - (FFxGZ)  ;     D9 ← (FFxGG) - (FGxGF)              ;
        DD ← (D1xFF) + (D2xFG) + (D3xFZ)                                  ;
        DF ← (IC/DD) x ((D1xDF1E) + (D4xDGE) + (D7xDZE))                  ;
        DG ← (IC/DD) x ((D2xDF1E) + (D5xDGE) + (D8xDZE))                  ;
        DZ ← (IC/DD) x ((D3xDF1E) + (D6xDGE) + (D9xDZE))                  ;
        F2W ← F2W + DF                                                    ;
        G1W ← G1W + DG                                                    ;
        Z1W ← Z1W + DZ - IC                                               ;
        GO TO REPEAT                                                      ;
PRINT:  WRITE (BOW2 [PAGE], DUMM)                                         ;
        WRITE (BOW2, TITL, TITL2)                                         ;
        WRITE (BOW2, FMT, BUT); WRITE (BOW2 [PAGE], DUMM); END; END.
```

APPENDIX C

RUNGE-KUTTA METHOD FOR NUMERICAL SOLUTION OF DIFFERENTIAL EQUATIONS

For the numerical solution of a differential equation of the form $y' = f(x,y)$ with a boundary condition $y(x_o) = y_o$ the fourth order Runge-Kutta method (43) gives

$$y(n + 1) = y(n) + 1/6\ [K(1,n) + 2K(2,n) + 2K(3,n) + K(4,n)] \qquad \text{(C-1)}$$

where

$$K(1,n) = h\ f\ [nh, y(n)] \qquad \text{(C-2)}$$

$$K(2,n) = h\ f\ [(n + \tfrac{1}{2})h, y(n) + \tfrac{1}{2}K(1,n)] \qquad \text{(C-3)}$$

$$K(3,n) = h\ f\ [(n + \tfrac{1}{2})h, y(n) + \tfrac{1}{2}K(2,n)] \qquad \text{(C-4)}$$

$$K(4,n) = h\ f\ [(n + 1)h, y(n) + K(3,n)] \qquad \text{(C-5)}$$

h is the step size for each integration.

The main advantage of this method is that it is readily adapted to

a system of equations. For the solution of the boundary layer equations it was necessary to write them in the form of seven first order equations. No special starting techniques are required and it proceeds in an orderly fashion. Before a quantity is needed in the integration of any term it has already been calculated in the integration of another term, etc. It is necessary to determine each step for all seven equations before proceeding to the next step of any integration.

It does have one disadvantage, the determination of the error in integration, and it has no checks and balances. For a simple differential equation the local error, ε, is

$$\varepsilon \cong \sigma(h^5) \tag{C-6}$$

The upper bound on the total accumulative error is approximately 140 times this since 140 steps were used in the integration. Therefore, with a step size of 0.05 in η the total error for one simple differential equation is

$$\varepsilon_t \cong 140\ (.05)^5 \tag{C-7}$$

or

$$\varepsilon_t \cong 5 \times 10^{-5} \tag{C-8}$$

This does not mean that the error in integrating Equations (5-39), (5-42), and (5-44) is going to be less than Equation (C-8). However,

Equations (5-40), (5-41), (5-43), and (5-45) are simple and their total error will be much less than Equation (C-8).

It can be anticipated that the total accumulative error for the integration of the seven equations should be less than 0.1 per cent, which would occur at the edge of the boundary layer.

APPENDIX D

TABULATED AND GRAPHICAL RESULTS

Table 5 Boundary conditions, δ_I^* and θ_I for all solutions.

Table 6a-h Momentum Equation Solutions f, f', f".

Table 7a-l Energy and Species Continuity Solutions g_I, g_I', Z_A, Z_A'.

Table 8 Complete solutions for D = J = 0.

Table 5. Displacement and Momentum Thickness, Velocity, Enthalpy and Concentration Gradients

J	D	g_w	Z_w	f''_w	g'_{Iw}	Z'_{Aw}	δ^*_I	θ_I
0.0	0.0	0.4	0.05	0.2181	0.1117	0.1483	0.2139	0.6064
0.0	0.6	0.4	0.05	0.3297	0.1203	0.1599	0.0194	0.5655
0.0	0.9	0.4	0.05	0.3702	0.1227	0.1632	-0.0291	0.5554
0.0	1.2	0.4	0.05	0.4057	0.1246	0.1657	-0.0651	0.5481
0.1	0.0	0.4	0.05	0.2209	0.1116	0.1502	0.2675	0.6029
0.1	0.6	0.4	0.05	0.3393	0.1207	0.1627	0.0559	0.5581
0.1	0.9	0.4	0.05	0.3819	0.1231	0.1660	0.0014	0.5479
0.1	1.2	0.4	0.05	0.4192	0.1250	0.1687	-0.0370	0.5402
0.2	0.0	0.4	0.05	0.2238	0.1115	0.1522	0.3263	0.5990
0.2	0.3	0.4	0.05	0.2957	0.1174	0.1605	0.1741	0.5686
0.2	0.6	0.4	0.05	0.3497	0.2094	0.1655	0.0900	0.5514
0.2	0.9	0.4	0.05	0.3947	0.1235	0.1691	0.0338	0.5400
0.2	1.2	0.4	0.05	0.4340	0.1254	0.1719	-0.0074	0.5318
0.2	1.5	0.4	0.05	0.4691	0.1270	0.1741	-0.0392	0.5257
0.2	1.8	0.4	0.05	0.5013	0.1284	0.1760	-0.0648	0.5210
0.2	2.1	0.4	0.05	0.5311	0.1295	0.1776	-0.0863	0.5170
0.2	2.3	0.4	0.05	0.5499	0.1302	0.1786	-0.0995	0.5140
0.2	2.5	0.4	0.05	0.5680	0.1308	0.1794	-0.1108	0.5120
0.2	2.7	0.4	0.05	0.5853	0.1314	0.1802	-0.1193	0.5121
0.2	2.9	0.4	0.05	0.6021	0.1319	0.1810	-0.1298	0.5092
0.3	0.6	0.4	0.05	0.3613	0.1214	0.1686	0.1292	0.5436
0.3	0.9	0.4	0.05	0.4087	0.1240	0.1724	0.0686	0.5316
0.3	1.2	0.4	0.05	0.4501	0.1260	0.1753	0.0245	0.5231
0.4	0.6	0.4	0.05	0.3740	0.1219	0.1720	0.1715	0.5353
0.4	0.9	0.4	0.05	0.4243	0.1245	0.1760	0.1059	0.5227
0.4	1.2	0.4	0.05	0.4680	0.1266	0.1791	0.0580	0.5133
0.4	2.7	0.4	0.05	0.6357	0.1327	0.1882	-0.0694	0.4908
0.5	0.6	0.4	0.05	0.3881	0.1225	0.1757	0.2174	0.5265
0.5	0.9	0.4	0.05	0.4416	0.1252	0.1799	0.1462	0.5132
0.5	1.2	0.4	0.05	0.4879	0.1273	0.1832	0.0951	0.5039
0.6	0.6	0.4	0.05	0.4040	0.1232	0.1798	0.2671	0.5168
0.6	0.9	0.4	0.05	0.4609	0.1260	0.1842	0.1899	0.5032
0.6	1.2	0.4	0.05	0.5101	0.1281	0.1876	0.1339	0.4929
0.6	2.7	0.4	0.05	0.6981	0.1343	0.1976	-0.0105	0.4707
0.7	0.6	0.4	0.05	0.4219	0.1241	0.1843	0.3202	0.5058
0.7	0.9	0.4	0.05	0.4827	0.1269	0.1890	0.2374	0.4924
0.7	1.2	0.4	0.05	0.5353	0.1291	0.1926	0.1768	0.4817
0.8	0.6	0.4	0.05	0.4422	0.1251	0.1892	0.3826	0.4959

Table 5. Displacement and Momentum Thickness, Velocity, Enthalpy and Concentration Gradients (Continued)

J	D	g_w	Z_w	f''_w	g'_{Iw}	Z'_{Aw}	δ^*_I	θ_I
0.8	0.9	0.4	0.05	0.5076	0.1281	0.1943	0.2895	0.4808
0.8	1.2	0.4	0.05	0.5639	0.1303	0.1980	0.2243	0.4705
0.9	0.6	0.4	0.05	0.4657	0.1264	0.1948	0.4495	0.4839
0.9	0.9	0.4	0.05	0.5362	0.1294	0.2002	0.3469	0.4683
0.9	1.2	0.4	0.05	0.5969	0.1316	0.2042	0.2757	0.4577
1.0	0.6	0.4	0.05	0.4931	0.1278	0.2011	0.5243	0.4709
1.0	0.9	0.4	0.05	0.5697	0.1309	0.2069	0.4107	0.4549
1.1	0.9	0.4	0.05	0.6092	0.1328	0.2146	0.4823	0.4403
1.2	0.6	0.4	0.05	0.5645	0.1319	0.2168	0.7066	0.4407
1.2	0.9	0.4	0.05	0.6570	0.1352	0.2235	0.5641	0.4241
1.3	0.6	0.4	0.05	0.6130	0.1347	0.2268	0.8210	0.4232
0.0	1.2	0.1	0.00	0.1928	0.1107	0.1013	-0.4223	0.6536
0.1	1.2	0.1	0.00	0.1984	0.1117	0.1031	-0.4019	0.6475
0.2	1.2	0.1	0.00	0.2045	0.1127	0.1050	-0.3807	0.6405
0.3	1.2	0.1	0.00	0.2111	0.1139	0.1071	-0.3582	0.6332
0.4	1.2	0.1	0.00	0.2185	0.1152	0.1094	-0.3341	0.6254
0.5	1.2	0.1	0.00	0.2266	0.1166	0.1118	-0.3096	0.6161
0.6	1.2	0.1	0.00	0.2356	0.1182	0.1145	-0.2804	0.6085
0.7	1.2	0.1	0.00	0.2458	0.1110	0.1174	-0.2503	0.5993
0.8	1.2	0.1	0.00	0.2573	0.1220	0.1207	-0.2176	0.5892
0.9	1.2	0.1	0.00	0.2705	0.1243	0.1243	-0.1819	0.5784
1.0	1.2	0.1	0.00	0.2858	0.1270	0.1285	-0.1417	0.5664
1.0	0.6	0.1	0.05	0.2511	0.1282	0.1254	-0.0169	0.5664
1.0	0.6	0.2	0.00	0.3284	0.1361	0.1572	0.1674	0.5402
1.0	0.6	0.3	0.00	0.4027	0.1337	0.1804	0.3472	0.5088
1.0	0.6	0.4	0.10	0.5153	0.1330	0.2022	0.5340	0.4620
1.0	0.6	0.4	0.15	0.5374	0.1381	0.2021	0.5429	0.4536

Table 6a. Momentum Equation Solutions: f, f', f"

$g_{Iw} = 0.4$, $Z_{Aw} = 0.05$, $J = 0.2$

	D = 0.0			D = 0.6			D = 1.2		
	f	f'	f"	f	f'	f"	f	f'	f"
0.0	0.0000	0.0000	0.2238	0.0000	0.0000	0.3497	0.0000	0.0000	0.4339
0.2	0.0046	0.0460	0.2360	0.0070	0.0706	0.3558	0.0087	0.0866	0.4312
0.4	0.0186	0.0944	0.2489	0.0283	0.1422	0.3604	0.0346	0.1722	0.4250
0.6	0.0425	0.1456	0.2623	0.0640	0.2146	0.3633	0.0775	0.2563	0.4155
0.8	0.0770	0.1994	0.2760	0.1142	0.2874	0.3642	0.1370	0.3382	0.4029
1.0	0.1224	0.2560	0.2895	0.1789	0.3601	0.3626	0.2126	0.4173	0.3874
1.2	0.1795	0.3152	0.3022	0.2582	0.4322	0.3581	0.3036	0.4930	0.3690
1.4	0.2487	0.3767	0.3133	0.3517	0.5031	0.3500	0.4095	0.5647	0.3479
1.6	0.3303	0.4403	0.3217	0.4593	0.5720	0.3378	0.5292	0.6319	0.3240
1.8	0.4249	0.5052	0.3261	0.5803	0.6379	0.3209	0.6619	0.6941	0.2974
2.0	0.5324	0.5704	0.3253	0.7142	0.7000	0.2990	0.8065	0.7507	0.2683
2.2	0.6530	0.6348	0.3179	0.8600	0.7572	0.2722	0.9618	0.8013	0.2370
2.4	0.7862	0.6971	0.3029	1.0167	0.8086	0.2410	1.1266	0.8455	0.2042
2.6	0.9316	0.7555	0.2801	1.1830	0.8534	0.2066	1.2996	0.8830	0.1709
2.8	1.0881	0.8086	0.2501	1.3575	0.8911	0.1708	1.4794	0.9139	0.1384
3.0	1.2546	0.8552	0.2147	1.5390	0.9218	0.1358	1.6647	0.9385	0.1082
3.2	1.4296	0.8943	0.1764	1.7258	0.9456	0.1036	1.8544	0.9574	0.0815
3.4	1.6118	0.9258	0.1384	1.9168	0.9635	0.0758	2.0473	0.9714	0.0591
3.6	1.7995	0.9499	0.1034	2.1109	0.9763	0.0531	2.2427	0.9814	0.0413
3.8	1.9913	0.9675	0.0736	2.3071	0.9851	0.0358	2.4397	0.9882	0.0279
4.0	2.1861	0.9797	0.0500	2.5047	0.9909	0.0232	2.6378	0.9928	0.0181
4.2	2.3829	0.9879	0.0323	2.7033	0.9946	0.0145	2.8367	0.9957	0.0114
4.4	2.5810	0.9930	0.0200	2.9025	0.9969	0.0088	3.0360	0.9975	0.0070
4.6	2.7800	0.9961	0.0118	3.1020	0.9983	0.0051	3.2356	0.9986	0.0042
5.0	3.1791	0.9989	0.0036	3.5016	0.9995	0.0016	3.6353	0.9996	0.0014
6.0	4.1788	1.0000	0.0001	4.5014	1.0000	0.0001	4.6352	1.0000	0.0001
7.0	5.1788	1.0000	0.0000	5.5014	1.0000	0.0000	5.6353	1.0001	0.0000

Table 6b. Momentum Equation Solutions: f, f', f''

$g_{Iw} = 0.4$, $Z_{Aw} = 0.05$, $J = 0.2$

	D = 1.8			D = 2.3			D = 2.9		
	f	f'	f''	f	f'	f''	f	f'	f''
0.0	0.0000	0.0000	0.5013	0.0000	0.0000	0.5499	0.0000	0.0000	0.6021
0.2	0.0100	0.0991	0.4887	0.0109	0.1080	0.5586	0.0118	0.1174	0.5700
0.4	0.0394	0.1951	0.4708	0.0429	0.2110	0.5008	0.0465	0.2275	0.5301
0.6	0.0877	0.2872	0.4488	0.0949	0.3080	0.4685	0.1023	0.3291	0.4858
0.8	0.1540	0.3744	0.4236	0.1656	0.3982	0.4335	0.1775	0.4217	0.4401
1.0	0.2372	0.4564	0.3961	0.2537	0.4813	0.3975	0.2703	0.5052	0.3954
1.2	0.3362	0.5328	0.3671	0.3577	0.5572	0.3616	0.3790	0.5800	0.3530
1.4	0.4499	0.6032	0.3372	0.4761	0.6261	0.3267	0.5018	0.6467	0.3139
1.6	0.5771	0.6676	0.3068	0.6076	0.6880	0.2931	0.6372	0.7058	0.2783
1.8	0.7165	0.7259	0.2759	0.7509	0.7434	0.2608	0.7837	0.7582	0.2457
2.0	0.8670	0.7780	0.2447	0.9046	0.7924	0.2296	0.9400	0.8043	0.2155
2.2	1.0273	0.8238	0.2133	1.0674	0.8353	0.1992	1.1050	0.8445	0.1869
2.4	1.1961	0.8633	0.1820	1.2383	0.8721	0.1697	1.2774	0.8791	0.1594
2.6	1.3722	0.8966	0.1513	1.4159	0.9032	0.1411	1.4563	0.9083	0.1329
2.8	1.5543	0.9239	0.1221	1.5992	0.9287	0.1140	1.6404	0.9323	0.1076
3.0	1.7414	0.9456	0.0953	1.7870	0.9489	0.0891	1.8289	0.9515	0.0844
3.2	1.9322	0.9622	0.0718	1.9784	0.9645	0.0673	2.0207	0.9663	0.0638
3.4	2.1260	0.9746	0.0521	2.1725	0.9761	0.0490	2.2151	0.9772	0.0465
3.6	2.3218	0.9834	0.0365	2.3686	0.9843	0.0344	2.4114	0.9851	0.0327
3.8	2.5191	0.9894	0.0247	2.5661	0.9901	0.0233	2.6090	0.9905	0.0222
4.0	2.7174	0.9935	0.0162	2.7645	0.9939	0.0153	2.8075	0.9941	0.0145
4.2	2.9164	0.9961	0.0103	2.9636	0.9964	0.0097	3.0066	0.9965	0.0092
4.4	3.1158	0.9977	0.0063	3.1630	0.9979	0.0060	3.2060	0.9980	0.0057
4.6	3.3155	0.9987	0.0038	3.3627	0.9989	0.0036	3.4057	0.9988	0.0034
5.0	3.7151	0.9996	0.0012	3.7625	0.9998	0.0013	3.8055	0.9997	0.0011
6.0	4.7150	1.0000	0.0000	4.7625	1.0003	0.0003	4.8054	1.0001	0.0002
7.0	5.7150	0.9999	0.0000	5.7630	1.0007	0.0005	5.8056	1.0003	0.0003

Table 6c. Momentum Equation Solutions: f, f', f"

$g_{Iw} = 0.4$, $Z_{Aw} = 0.05$, $J = 0.0$

	D = 0.6			D = 0.9			D = 1.2		
	f	f'	f"	f	f'	f"	f	f'	f"
0.0	0.0000	0.0000	0.3297	0.0000	0.0000	0.3702	0.0000	0.0000	0.4057
0.2	0.0066	0.0666	0.3361	0.0074	0.0744	0.3731	0.0081	0.0811	0.4048
0.4	0.0267	0.1344	0.3416	0.0298	0.1491	0.3741	0.0324	0.1617	0.4011
0.6	0.0605	0.2031	0.3458	0.0671	0.2239	0.3732	0.0727	0.2414	0.3949
0.8	0.1080	0.2726	0.3485	0.1193	0.2983	0.3702	0.1289	0.3195	0.3861
1.0	0.1695	0.3424	0.3492	0.1863	0.3718	0.3647	0.2004	0.3957	0.3748
1.2	0.2450	0.4121	0.3475	0.2679	0.4440	0.3565	0.2869	0.4693	0.3608
1.4	0.3343	0.4812	0.3426	0.3638	0.5142	0.3452	0.3879	0.5398	0.3441
1.6	0.4374	0.5489	0.3340	0.4734	0.5818	0.3304	0.5026	0.6067	0.3245
1.8	0.5537	0.6145	0.3209	0.5963	0.6461	0.3118	0.6303	0.6694	0.3019
2.0	0.6829	0.6770	0.3029	0.7316	0.7063	0.2892	0.7701	0.7273	0.2764
2.2	0.8242	0.7353	0.2798	0.8785	0.7615	0.2626	0.9208	0.7797	0.2480
2.4	0.9767	0.7885	0.2517	1.0358	0.8111	0.2325	1.0816	0.8263	0.2172
2.6	1.1393	0.8357	0.2195	1.2025	0.8543	0.1998	1.2509	0.8665	0.1851
2.8	1.3106	0.8762	0.1849	1.3371	0.8909	0.1660	1.4277	0.9003	0.1527
3.0	1.4893	0.9096	0.1498	1.5584	0.9208	0.1330	1.6106	0.9277	0.1216
3.2	1.6740	0.9362	0.1165	1.7450	0.9443	0.1025	1.7984	0.9491	0.0934
3.4	1.8633	0.9565	0.0869	1.9357	0.9620	0.0759	1.9899	0.9653	0.0690
3.6	2.0562	0.9713	0.0621	2.1295	0.9749	0.0540	2.1842	0.9771	0.0491
3.8	2.2515	0.9817	0.0426	2.3254	0.9840	0.0370	2.3805	0.9853	0.0337
4.0	2.4486	0.9887	0.0281	2.5228	0.9900	0.0245	2.5782	0.9908	0.0224
4.2	2.6469	0.9932	0.0179	2.7213	0.9940	0.0156	2.7767	0.9944	0.0143
4.4	2.8458	0.9961	0.0110	2.9203	0.9965	0.0096	2.9759	0.9967	0.0089
4.6	3.0452	0.9978	0.0065	3.1198	0.9980	0.0058	3.1754	0.9981	0.0054
5.0	3.4447	0.9993	0.0021	3.5193	0.9994	0.0019	3.5749	0.9994	0.0018
6.0	4.4445	1.0000	0.0001	4.5191	1.0000	0.0001	4.5748	1.0000	0.0001
7.0	5.4445	1.0000	0.0000	5.5191	1.0000	0.0000	5.5748	1.0001	0.0000

Table 6d. Momentum Equation Solutions: f, f', f''

$g_{Iw} = 0.4$, $Z_{Aw} = 0.05$, $J = 0.6$

	D = 0.6			D = 0.9			D = 1.2		
	f	f'	f''	f	f'	f''	f	f'	f''
0.0	0.0000	0.0000	0.4040	0.0000	0.0000	0.4609	0.0000	0.0000	0.5101
0.2	0.0081	0.0813	0.4083	0.0092	0.0921	0.4590	0.0102	0.1013	0.5014
0.4	0.0325	0.1631	0.4098	0.0368	0.1833	0.4524	0.0403	0.2001	0.4865
0.6	0.0734	0.2450	0.4080	0.0824	0.2727	0.4415	0.0900	0.2955	0.4662
0.8	0.1305	0.3261	0.4029	0.1457	0.3596	0.4263	0.1582	0.3863	0.4416
1.0	0.2037	0.4059	0.3939	0.2260	0.4430	0.4072	0.2442	0.4719	0.4135
1.2	0.2927	0.4834	0.3808	0.3226	0.5222	0.3844	0.3466	0.5516	0.3827
1.4	0.3969	0.5579	0.3633	0.4346	0.5965	0.3581	0.4644	0.6248	0.3497
1.6	0.5156	0.6284	0.3411	0.5608	0.6652	0.3284	0.5961	0.6913	0.3151
1.8	0.6479	0.6940	0.3141	0.7002	0.7277	0.2958	0.7404	0.7508	0.2793
2.0	0.7928	0.7538	0.2828	0.8515	0.7834	0.2608	0.8959	0.8030	0.2428
2.2	0.9490	0.8069	0.2479	1.0131	0.8319	0.2242	1.0611	0.8479	0.2063
2.4	1.1151	0.8528	0.2107	1.1837	0.8731	0.1873	1.2346	0.8856	0.1707
2.6	1.2896	0.8912	0.1730	1.3619	0.9069	0.1514	1.4149	0.9163	0.1370
2.8	1.4710	0.9221	0.1367	1.5460	0.9338	0.1181	1.6007	0.9406	0.1062
3.0	1.6580	0.9461	0.1038	1.7349	0.9544	0.0886	1.7908	0.9591	0.0795
3.2	1.8491	0.9639	0.0756	1.9274	0.9696	0.0640	1.9840	0.9727	0.0574
3.4	2.0432	0.9767	0.0528	2.1225	0.9803	0.0445	2.1796	0.9823	0.0399
3.6	2.2395	0.9854	0.0355	2.3193	0.9877	0.0298	2.3767	0.9889	0.0267
3.8	2.4372	0.9912	0.0229	2.5174	0.9925	0.0192	2.5750	0.9933	0.0173
4.0	2.6358	0.9948	0.0143	2.7162	0.9956	0.0120	2.7740	0.9961	0.0108
4.2	2.8350	0.9971	0.0086	2.9155	0.9975	0.0072	2.9734	0.9978	0.0066
4.4	3.0346	0.9984	0.0050	3.1151	0.9986	0.0042	3.1730	0.9988	0.0039
4.6	3.2343	0.9992	0.0028	3.3149	0.9992	0.0024	3.3728	0.9994	0.0022
5.0	3.6342	0.9998	0.0008	3.7148	0.9998	0.0007	3.7727	0.9999	0.0007
6.0	4.6342	1.0001	0.0001	4.7147	1.0000	0.0000	4.7728	1.0002	0.0001
7.0	5.6342	1.0001	0.0000	5.7147	1.0000	0.0000	5.7731	1.0004	0.0002

Table 6e. Momentum Equation Solutions: f, f', f"

$g_{Iw} = 0.4, \quad Z_{Aw} = 0.05$

	D = 0.6 J = 1.3			D = 0.9 J = 1.2			D = 1.2 J = 0.9		
	f	f'	f"	f	f'	f"	f	f'	f"
0.0	0.0000	0.0000	0.6123	0.0000	0.0000	0.6570	0.0000	0.0000	0.5969
0.2	0.0122	0.1218	0.6025	0.0130	0.1295	0.6357	0.0118	0.1178	0.5790
0.4	0.0485	0.2402	0.5794	0.0514	0.2533	0.6002	0.0468	0.2309	0.5510
0.6	0.1079	0.3528	0.5457	0.1138	0.3689	0.5543	0.1038	0.3377	0.5154
0.8	0.1891	0.4578	0.5034	0.1983	0.4746	0.5017	0.1814	0.4368	0.4747
1.0	0.2904	0.5538	0.4552	0.3029	0.5694	0.4458	0.2779	0.5273	0.4308
1.2	0.4099	0.6397	0.4031	0.4254	0.6529	0.3892	0.3917	0.6090	0.3856
1.4	0.5456	0.7149	0.3495	0.5633	0.7252	0.3339	0.5209	0.6816	0.3404
1.6	0.6952	0.7795	0.2962	0.7147	0.7867	0.2813	0.6638	0.7452	0.2960
1.8	0.8567	0.8336	0.2449	0.8773	0.8379	0.2322	0.8184	0.8001	0.2530
2.0	1.0280	0.8777	0.1970	1.0493	0.8798	0.1873	0.9832	0.8466	0.2120
2.2	1.2071	0.9127	0.1537	1.2287	0.9132	0.1472	1.1565	0.8851	0.1735
2.4	1.3925	0.9395	0.1160	1.4140	0.9391	0.1123	1.3368	0.9162	0.1382
2.6	1.5825	0.9595	0.0845	1.6039	0.9585	0.0829	1.5225	0.9406	0.1067
2.8	1.7759	0.9793	0.0592	1.7971	0.9726	0.0591	1.7126	0.9591	0.0796
3.0	1.9717	0.9836	0.0400	1.9927	0.9825	0.0406	1.9059	0.9728	0.0574
3.2	2.1691	0.9901	0.0259	2.1899	0.9892	0.0269	2.1014	0.9824	0.0398
3.4	2.3676	0.9942	0.0162	2.3882	0.9935	0.0172	2.2986	0.9890	0.0267
3.6	2.5667	0.9968	0.0097	2.5872	0.9963	0.0106	2.4969	0.9933	0.0172
3.8	2.7662	0.9983	0.0056	2.7866	0.9979	0.0063	2.6958	0.9961	0.0108
4.0	2.9660	0.9991	0.0031	2.9863	0.9989	0.0036	2.8952	0.9978	0.0065
4.2	3.1658	0.9996	0.0016	3.1861	0.9994	0.0020	3.0949	0.9988	0.0038
4.4	3.3658	0.9998	0.0008	3.3860	0.9997	0.0011	3.2947	0.9994	0.0021
4.6	3.5658	0.9999	0.0004	3.5860	0.9999	0.0005	3.4946	0.9997	0.0012
5.0	3.9657	1.0000	0.0000	3.9860	1.0000	0.0001	3.8946	0.9999	0.0003
6.0	4.9657	0.9999	-0.0002	4.9860	1.0000	0.0000	4.8946	1.0000	0.0000
7.0	5.9655	0.9997	-0.0002	5.9860	1.0000	-0.0001	5.8946	1.0001	0.0000

Table 6f. Momentum Equation Solutions: f, f', f"

$g_{Iw} = 0.4, \quad Z_{Aw} = 0.05$

	D = 2.7 J = 0.2			D = 2.7 J = 0.4			D = 2.7 J = 0.6		
	f	f'	f"	f	f'	f"	f	f'	f"
0.0	0.0000	0.0000	0.5853	0.0000	0.0000	0.6357	0.0000	0.0000	0.6981
0.2	0.0115	0.1144	0.5569	0.0125	0.1237	0.5997	0.0137	0.1352	0.6515
0.4	0.0453	0.2222	0.5210	0.0489	0.2393	0.5543	0.0534	0.2598	0.5928
0.6	0.0999	0.3225	0.4806	0.1076	0.3451	0.5040	0.1168	0.3720	0.5291
0.8	0.1737	0.4144	0.4384	0.1863	0.4408	0.4524	0.2013	0.4714	0.4654
1.0	0.2651	0.4978	0.3964	0.2832	0.5262	0.4023	0.3045	0.5584	0.4055
1.2	0.3723	0.5730	0.3560	0.3961	0.6019	0.3554	0.4239	0.6340	0.3512
1.4	0.4938	0.6404	0.3181	0.5233	0.6686	0.3126	0.5574	0.6994	0.3032
1.6	0.6280	0.7005	0.2830	0.6630	0.7272	0.2739	0.7031	0.7557	0.2611
1.8	0.7735	0.7538	0.2504	0.8137	0.7784	0.2388	0.8592	0.8041	0.2240
2.0	0.9291	0.8008	0.2197	0.9740	0.8229	0.2067	1.0243	0.8456	0.1909
2.2	1.0934	0.8418	0.1906	1.1425	0.8612	0.1766	1.1970	0.8807	0.1606
2.4	1.2654	0.8770	0.1624	1.3181	0.8937	0.1482	1.3761	0.9099	0.1325
2.6	1.4439	0.9068	0.1352	1.4996	0.9206	0.1214	1.5606	0.9338	0.1066
2.8	1.6278	0.9312	0.1094	1.6860	0.9424	0.0965	1.7493	0.9527	0.0831
3.0	1.8161	0.9507	0.0857	1.8762	0.9594	0.0742	1.9414	0.9673	0.0626
3.2	2.0078	0.9657	0.0648	2.0695	0.9722	0.0550	2.1360	0.9780	0.0454
3.4	2.2021	0.9768	0.0472	2.2649	0.9816	0.0393	2.3324	0.9856	0.0317
3.6	2.3983	0.9848	0.0331	2.4619	0.9882	0.0270	2.5301	0.9909	0.0214
3.8	2.5958	0.9903	0.0225	2.6600	0.9926	0.0180	2.7286	0.9944	0.0139
4.0	2.7943	0.9940	0.0147	2.8589	0.9955	0.0115	2.9278	0.9966	0.0087
4.2	2.9933	0.9963	0.0093	3.0582	0.9974	0.0072	3.1272	0.9980	0.0053
4.4	3.1928	0.9978	0.0057	3.2578	0.9985	0.0043	3.3269	0.9988	0.0031
4.6	3.3924	0.9987	0.0034	3.4576	0.9992	0.0026	3.5267	0.9993	0.0017
5.0	3.7921	0.9995	0.0010	3.8574	0.9998	0.0008	3.9265	0.9997	0.0004
6.0	4.7918	0.9996	-0.0003	4.8574	1.0001	0.0002	4.9262	0.9996	-0.0003
7.0	5.7912	0.9991	-0.0008	5.8576	1.0004	0.0003	5.9256	0.9991	-0.0008

Table 6g. Momentum Equation Solutions: f, f', f"

$g_{Iw} = 0.4$, D = 0.6, J = 1.0

	$Z_{Aw} = 0.05$			$Z_{Aw} = 0.15$		
	f	f'	f"	f	f'	f"
0.0	0.0000	0.0000	0.4931	0.0000	0.0000	0.5374
0.2	0.0099	0.0987	0.4928	0.0107	0.1071	0.5327
0.4	0.0394	0.1967	0.4862	0.0427	0.2126	0.5201
0.6	0.0884	0.2928	0.4735	0.0955	0.3147	0.5002
0.8	0.1563	0.3857	0.4548	0.1683	0.4122	0.4736
1.0	0.2424	0.4743	0.4306	0.2600	0.5038	0.4413
1.2	0.3457	0.5576	0.4013	0.3694	0.5884	0.4041
1.4	0.4650	0.6345	0.3674	0.4948	0.6651	0.3629
1.6	0.5990	0.7043	0.3296	0.6348	0.7334	0.3191
1.8	0.7462	0.7662	0.2891	0.7876	0.7927	0.2739
2.0	0.9050	0.8198	0.2469	0.9513	0.8429	0.2288
2.2	1.0736	0.8650	0.2047	1.1242	0.8843	0.1853
2.4	1.2504	0.9018	0.1641	1.3045	0.9173	0.1452
2.6	1.4338	0.9308	0.1269	1.4906	0.9427	0.1098
2.8	1.6223	0.9529	0.0944	1.6811	0.9616	0.0799
3.0	1.8145	0.9690	0.0674	1.8748	0.9751	0.0560
3.2	2.0095	0.9802	0.0463	2.0708	0.9843	0.0377
3.4	2.2064	0.9878	0.0305	2.2684	0.9905	0.0245
3.6	2.4045	0.9928	0.0194	2.4669	0.9944	0.0153
3.8	2.6034	0.9958	0.0118	2.6660	0.9968	0.0092
4.0	2.8027	0.9977	0.0070	2.8655	0.9982	0.0054
4.2	3.0024	0.9987	0.0040	3.0653	0.9991	0.0030
4.4	3.2022	0.9993	0.0022	3.2651	0.9995	0.0017
4.6	3.4021	0.9997	0.0012	3.4651	0.9998	0.0009
5.0	3.8020	0.9999	0.0003	3.8650	0.9999	0.0002
6.0	4.8020	1.0000	0.0000	4.8650	1.0000	0.0000
7.0	5.8020	1.0000	0.0000	5.8650	1.0000	0.0000

Table 6h. Momentum Equation Solutions: f, f', f"

$g_{Iw} = 0.1$, $Z_{Aw} = 0.0$, D = 1.2

	J = 0.2			J = 0.6			J = 1.0		
	f	f'	f"	f	f'	f"	f	f'	f"
0.0	0.0000	0.0000	0.2045	0.0000	0.0000	0.2356	0.0000	0.0000	0.2858
0.2	0.0042	0.0426	0.2216	0.0048	0.0491	0.2554	0.0059	0.0596	0.3095
0.4	0.0173	0.0886	0.2376	0.0199	0.1020	0.2729	0.0241	0.1235	0.3282
0.6	0.0398	0.1376	0.2524	0.0459	0.1581	0.2880	0.0555	0.1906	0.3420
0.8	0.0725	0.1894	0.2658	0.0833	0.2170	0.3005	0.1005	0.2599	0.3508
1.0	0.1158	0.2438	0.2776	0.1328	0.2781	0.3103	0.1595	0.3306	0.3547
1.2	0.1702	0.3003	0.2876	0.1947	0.3409	0.3171	0.2328	0.4015	0.3537
1.4	0.2360	0.3587	0.2955	0.2693	0.4048	0.3208	0.3201	0.4717	0.3481
1.6	0.3137	0.4184	0.3010	0.3567	0.4690	0.3209	0.4213	0.5404	0.3379
1.8	0.4034	0.4789	0.3034	0.4569	0.5329	0.3170	0.5361	0.6066	0.3231
2.0	0.5053	0.5395	0.3024	0.5697	0.5955	0.3089	0.6638	0.6694	0.3038
2.2	0.6192	0.5996	0.2972	0.6949	0.6561	0.2960	0.8036	0.7278	0.2802
2.4	0.7450	0.6581	0.2872	0.8320	0.7136	0.2780	0.9546	0.7812	0.2525
2.6	0.8823	0.7141	0.2720	0.9801	0.7670	0.2551	1.1156	0.8286	0.2214
2.8	1.0304	0.7665	0.2513	1.1384	0.8153	0.2275	1.2856	0.8696	0.1881
3.0	1.1886	0.8143	0.2256	1.3058	0.8578	0.1965	1.4630	0.9038	0.1543
3.2	1.3557	0.8565	0.1959	1.4811	0.8938	0.1636	1.6466	0.9314	0.1217
3.4	1.5307	0.8925	0.1638	1.6629	0.9232	0.1310	1.8351	0.9527	0.0921
3.6	1.7123	0.9220	0.1316	1.8500	0.9463	0.1006	2.0273	0.9685	0.0669
3.8	1.8991	0.9453	0.1015	2.0411	0.9637	0.0741	2.2222	0.9798	0.0466
4.0	2.0900	0.9628	0.0750	2.2351	0.9763	0.0523	2.4190	0.9875	0.0312
4.2	2.2839	0.9756	0.0532	2.4313	0.9850	0.0355	2.6171	0.9925	0.0201
4.4	2.4800	0.9844	0.0363	2.6389	0.9908	0.0232	2.8159	0.9957	0.0125
4.6	2.6775	0.9904	0.0239	2.8275	0.9945	0.0147	3.0153	0.9977	0.0075
5.0	3.0751	0.9966	0.0093	3.2261	0.9982	0.0053	3.4148	0.9995	0.0024
6.0	4.0740	0.9999	0.0005	4.2256	1.0000	0.0003	4.4148	1.0002	0.0001
7.0	5.0740	1.0000	0.0000	5.2256	1.0000	0.0000	5.4150	1.0002	0.0000

Table 7a.- Energy and Species Continuity Solutions: g_I, g_I', Z_A, Z_A'

$g_{Iw} = 0.4$, $Z_{Aw} = 0.05$, $J = 0.2$

	D = 0.0				D = 0.6			
	g_I	g_I'	Z_A	Z_A'	g_I	g_I'	Z_A	Z_A'
0.0	0.4000	0.1115	0.0500	0.1522	0.4000	0.1209	0.0500	0.1655
0.2	0.4230	0.1183	0.0815	0.1634	0.4251	0.1297	0.0844	0.1787
0.4	0.4474	0.1256	0.1154	0.1757	0.4519	0.1390	0.1216	0.1933
0.6	0.4733	0.1334	0.1519	0.1891	0.4807	0.1487	0.1618	0.2092
0.8	0.5007	0.1415	0.1911	0.2036	0.5114	0.1586	0.2053	0.2263
1.0	0.5299	0.1500	0.2334	0.2191	0.5441	0.1683	0.2524	0.2445
1.2	0.5607	0.1584	0.2788	0.2354	0.5787	0.1775	0.3032	0.2632
1.4	0.5932	0.1665	0.3276	0.2520	0.6150	0.1855	0.3577	0.2818
1.6	0.6273	0.1739	0.3796	0.2684	0.6528	0.1918	0.4158	0.2990
1.8	0.6627	0.1798	0.4348	0.2835	0.6916	0.1954	0.4771	0.3133
2.0	0.6991	0.1837	0.4928	0.2959	0.7307	0.1955	0.5408	0.3226
2.2	0.7360	0.1846	0.5529	0.3040	0.7695	0.1914	0.6056	0.3247
2.4	0.7727	0.1818	0.6140	0.3059	0.8070	0.1826	0.6700	0.3176
2.6	0.8084	0.1747	0.6748	0.2999	0.8422	0.1691	0.7320	0.2999
2.8	0.8422	0.1632	0.7334	0.2848	0.8743	0.1515	0.7893	0.2719
3.0	0.8734	0.1476	0.7881	0.2605	0.9026	0.1309	0.8402	0.2356
3.2	0.9011	0.1289	0.8371	0.2284	0.9266	0.1090	0.8832	0.1943
3.4	0.9248	0.1084	0.8791	0.1914	0.9463	0.0874	0.9179	0.1525
3.6	0.9444	0.0879	0.9135	0.1529	0.9617	0.0676	0.9444	0.1138
3.8	0.9600	0.0687	0.9404	0.1165	0.9735	0.0504	0.9638	0.0809
4.0	0.9720	0.0518	0.9604	0.0846	0.9821	0.0364	0.9773	0.0550
4.2	0.9809	0.0378	0.9747	0.0588	0.9882	0.0254	0.9862	0.0358
4.4	0.9873	0.0267	0.9843	0.0391	0.9925	0.0173	0.9919	0.0223
4.6	0.9918	0.0183	0.9907	0.0249	0.9953	0.0114	0.9954	0.0134
5.0	0.9968	0.0079	0.9970	0.0090	0.9983	0.0045	0.9987	0.0043
6.0	0.9998	0.0006	0.9999	0.0004	0.9999	0.0003	1.0000	0.0001
7.0	1.0000	0.0000	1.0000	0.0000	1.0000	0.0000	1.0000	0.0000

Table 7b. Energy and Species Continuity Solutions: g_I, g_I', Z_A, Z_A'

$g_{Iw} = 0.4$, $Z_{Aw} = 0.05$, $J = 0.2$

	D = 1.2				D = 1.8			
	g_I	g_I'	Z_A	Z_A'	g_I	g_I'	Z_A	Z_A'
0.0	0.4000	0.1254	0.0500	0.1719	0.4000	0.1283	0.0500	0.1760
0.2	0.4261	0.1356	0.0858	0.1861	0.4268	0.1395	0.0867	0.1909
0.4	0.4542	0.1460	0.1245	0.2018	0.4558	0.1509	0.1265	0.2074
0.6	0.4845	0.1567	0.1666	0.2189	0.4871	0.1620	0.1697	0.2252
0.8	0.5169	0.1672	0.2122	0.2373	0.5206	0.1728	0.2167	0.2444
1.0	0.5513	0.1772	0.2616	0.2567	0.5562	0.1828	0.2675	0.2645
1.2	0.5877	0.1862	0.3149	0.2764	0.5936	0.1914	0.3225	0.2849
1.4	0.6257	0.1936	0.3721	0.2956	0.6326	0.1982	0.3814	0.3043
1.6	0.6650	0.1987	0.4330	0.3128	0.6728	0.2024	0.4440	0.3213
1.8	0.7050	0.2006	0.4970	0.3260	0.7134	0.2032	0.5096	0.3336
2.0	0.7450	0.1986	0.5630	0.3330	0.7538	0.1998	0.5770	0.3388
2.2	0.7841	0.1920	0.6296	0.3313	0.7930	0.1916	0.6445	0.3343
2.4	0.8214	0.1805	0.6948	0.3190	0.8301	0.1785	0.7100	0.3186
2.6	0.8560	0.1644	0.7564	0.2955	0.8641	0.1610	0.7712	0.2913
2.8	0.8870	0.1447	0.8123	0.2618	0.8943	0.1402	0.8258	0.2542
3.0	0.9137	0.1227	0.8606	0.2209	0.9200	0.1175	0.8724	0.2110
3.2	0.9360	0.1002	0.9005	0.1772	0.9413	0.0948	0.9101	0.1663
3.4	0.9539	0.0788	0.9316	0.1350	0.9581	0.0737	0.9391	0.1245
3.6	0.9677	0.0597	0.9548	0.0979	0.9709	0.0552	0.9603	0.0887
3.8	0.9780	0.0437	0.9712	0.0676	0.9804	0.0399	0.9751	0.0603
4.0	0.9854	0.0310	0.9823	0.0447	0.9871	0.0279	0.9849	0.0392
4.2	0.9905	0.0212	0.9895	0.0283	0.9918	0.0189	0.9912	0.0244
4.4	0.9940	0.0141	0.9940	0.0172	0.9949	0.0125	0.9950	0.0146
4.6	0.9963	0.0092	0.9967	0.0101	0.9969	0.0080	0.9973	0.0084
5.0	0.9987	0.0035	0.9991	0.0031	0.9989	0.0030	0.9993	0.0025
6.0	0.9999	0.0002	1.0000	0.0001	1.0000	0.0002	1.0000	0.0001
7.0	1.0000	0.0000	1.0000	0.0000	1.0000	0.0000	1.0000	0.0000

Table 7c. Energy and Species Continuity Solutions: g_I, g_I', Z_A, Z_A'

$g_{Iw} = 0.4$, $Z_{Aw} = 0.05$, $J = 0.2$

	D = 2.3				D = 2.9			
	g_I	g_I'	Z_A	Z_A'	g_I	g_I'	Z_A	Z_A'
0.0	0.4000	0.1302	0.0500	0.1786	0.4000	0.1319	0.0500	0.1810
0.2	0.4272	0.1422	0.0872	0.1939	0.4277	0.1447	0.0878	0.1968
0.4	0.4569	0.1540	0.1277	0.2108	0.4579	0.1571	0.1288	0.2141
0.6	0.4888	0.1655	0.1717	0.2292	0.4905	0.1688	0.1735	0.2329
0.8	0.5230	0.1763	0.2194	0.2488	0.5253	0.1796	0.2221	0.2530
1.0	0.5593	0.1861	0.2712	0.2694	0.5622	0.1892	0.2747	0.2739
1.2	0.5974	0.1945	0.3272	0.2900	0.6009	0.1972	0.3316	0.2949
1.4	0.6369	0.2008	0.3872	0.3096	0.6409	0.2030	0.3926	0.3146
1.6	0.6775	0.2044	0.4508	0.3264	0.6819	0.2061	0.4573	0.3311
1.8	0.7185	0.2045	0.5174	0.3380	0.7231	0.2055	0.5247	0.3421
2.0	0.7590	0.2002	0.5856	0.3420	0.7638	0.2005	0.5935	0.3448
2.2	0.7982	0.1912	0.6535	0.3358	0.8030	0.1907	0.6619	0.3368
2.4	0.8352	0.1772	0.7191	0.3178	0.8398	0.1759	0.7274	0.3168
2.6	0.8688	0.1589	0.7799	0.2883	0.8731	0.1569	0.7878	0.2851
2.8	0.8985	0.1375	0.8337	0.2493	0.9023	0.1349	0.8409	0.2444
3.0	0.9237	0.1144	0.8792	0.2048	0.9270	0.1116	0.8853	0.1989
3.2	0.9443	0.0917	0.9156	0.1597	0.9470	0.0888	0.9205	0.1537
3.4	0.9605	0.0707	0.9433	0.1183	0.9626	0.0680	0.9470	0.1127
3.6	0.9728	0.0526	0.9634	0.0834	0.9744	0.0502	0.9660	0.0787
3.8	0.9818	0.0378	0.9772	0.0561	0.9829	0.0358	0.9790	0.0525
4.0	0.9881	0.0262	0.9863	0.0361	0.9889	0.0247	0.9875	0.0335
4.2	0.9925	0.0177	0.9921	0.0223	0.9930	0.0165	0.9928	0.0205
4.4	0.9953	0.0115	0.9956	0.0132	0.9957	0.0107	0.9960	0.0121
4.6	0.9972	0.0073	0.9976	0.0076	0.9974	0.0068	0.9978	0.0069
5.0	0.9991	0.0027	0.9994	0.0022	0.9992	0.0025	0.9994	0.0020
6.0	1.0000	0.0001	1.0000	0.0001	1.0000	0.0001	1.0000	0.0000
7.0	1.0001	0.0000	1.0000	0.0000	1.0000	0.0000	1.0000	0.0000

Table 7d. Energy and Species Continuity Solutions: g_I, g_I', Z_A, Z_A'

$g_{Iw} = 0.4$, $Z_{Aw} = 0.05$, $J = 0.0$

	D = 0.6				D = 0.9			
	g_I	g_I'	Z_A	Z_A'	g_I	g_I'	Z_A	Z_A'
0.0	0.4000	0.1203	0.0500	0.1599	0.4000	0.1227	0.0500	0.1632
0.2	0.4248	0.1273	0.0832	0.1724	0.4253	0.1300	0.0839	0.1762
0.4	0.4509	0.1348	0.1190	0.1862	0.4520	0.1378	0.1206	0.1906
0.6	0.4787	0.1427	0.1578	0.2013	0.4804	0.1460	0.1602	0.2064
0.8	0.5080	0.1509	0.1997	0.2178	0.5105	0.1545	0.2032	0.2236
1.0	0.5390	0.1592	0.2450	0.2354	0.5422	0.1631	0.2497	0.2419
1.2	0.5717	0.1672	0.2939	0.2538	0.5757	0.1713	0.3000	0.2609
1.4	0.6059	0.1747	0.3465	0.2723	0.6107	0.1788	0.3541	0.2799
1.6	0.6415	0.1810	0.4027	0.2899	0.6471	0.1850	0.4119	0.2977
1.8	0.6782	0.1854	0.4623	0.3053	0.6846	0.1890	0.4730	0.3128
2.0	0.7155	0.1873	0.5273	0.3165	0.7225	0.1902	0.5367	0.3230
2.2	0.7529	0.1858	0.5885	0.3213	0.7604	0.1877	0.6017	0.3260
2.4	0.7896	0.1803	0.6525	0.3177	0.7973	0.1809	0.6664	0.3197
2.6	0.8247	0.1705	0.7149	0.3038	0.8324	0.1696	0.7289	0.3027
2.8	0.8575	0.1564	0.7733	0.2795	0.8649	0.1541	0.7868	0.2750
3.0	0.8870	0.1389	0.8260	0.2459	0.8939	0.1354	0.8383	0.2386
3.2	0.9129	0.1191	0.8713	0.2062	0.9189	0.1147	0.8819	0.1970
3.4	0.9346	0.0984	0.9084	0.1645	0.9397	0.0937	0.9170	0.1545
3.6	0.9523	0.0785	0.9372	0.1248	0.9565	0.0738	0.9439	0.1153
3.8	0.9661	0.0603	0.9586	0.0901	0.9694	0.0560	0.9635	0.0819
4.0	0.9766	0.0448	0.9737	0.0620	0.9791	0.0412	0.9771	0.0555
4.2	0.9843	0.0322	0.9839	0.0409	0.9861	0.0293	0.9862	0.0360
4.4	0.9897	0.0225	0.9905	0.0258	0.9910	0.0202	0.9919	0.0224
4.6	0.9934	0.0152	0.9946	0.0157	0.9943	0.0135	0.9954	0.0134
5.0	0.9975	0.0064	0.9984	0.0052	0.9979	0.0055	0.9987	0.0043
6.0	0.9999	0.0004	1.0000	0.0002	0.9999	0.0004	1.0000	0.0001
7.0	1.0000	0.0000	1.0000	0.0000	1.0000	0.0000	1.0000	0.0000

Table 7e. Energy and Species Continuity Solutions: g_I, g_I', Z_A, Z_A'

$g_{Iw} = 0.4$, $Z_{Aw} = 0.05$, $J = 0.6$

	D = 0.6				D = 0.9			
	g_I	g_I'	Z_A	Z_A'	g_I	g_I'	Z_A	Z_A'
0.0	0.4000	0.1232	0.0500	0.1798	0.4000	0.1260	0.0500	0.1842
0.2	0.4260	0.1373	0.0875	0.1950	0.4268	0.1422	0.0884	0.2002
0.4	0.4550	0.1518	0.1281	0.2115	0.4569	0.1583	0.1302	0.2174
0.6	0.4868	0.1663	0.1722	0.2293	0.4901	0.1738	0.1755	0.2358
0.8	0.5214	0.1802	0.2199	0.2480	0.5263	0.1881	0.2245	0.2551
1.0	0.5588	0.1930	0.2714	0.2674	0.5652	0.2005	0.2776	0.2750
1.2	0.5985	0.2038	0.3268	0.2866	0.6064	0.2103	0.3345	0.2945
1.4	0.6401	0.2117	0.3860	0.3046	0.6491	0.2167	0.3953	0.3125
1.6	0.6829	0.2158	0.4485	0.3198	0.6927	0.2187	0.4593	0.3273
1.8	0.7261	0.2151	0.5136	0.3304	0.7363	0.2158	0.5258	0.3368
2.0	0.7686	0.2088	0.5802	0.3340	0.7787	0.2073	0.5935	0.3385
2.2	0.8092	0.1968	0.6466	0.3286	0.8188	0.1932	0.6606	0.3305
2.4	0.8469	0.1792	0.7109	0.3126	0.8556	0.1741	0.7249	0.3113
2.6	0.8806	0.1574	0.7709	0.2859	0.8882	0.1513	0.7844	0.2814
2.8	0.9097	0.1328	0.8246	0.2503	0.9160	0.1264	0.8369	0.2429
3.0	0.9337	0.1076	0.8706	0.2088	0.9388	0.1015	0.8812	0.1996
3.2	0.9528	0.0837	0.9081	0.1659	0.9567	0.0783	0.9167	0.1559
3.4	0.9674	0.0626	0.9371	0.1254	0.9703	0.0581	0.9438	0.1159
3.6	0.9781	0.0451	0.9586	0.0903	0.9802	0.0415	0.9635	0.0821
3.8	0.9857	0.0314	0.9737	0.0621	0.9871	0.0287	0.9771	0.0555
4.0	0.9909	0.0211	0.9839	0.0409	0.9919	0.0192	0.9862	0.0360
4.2	0.9944	0.0138	0.9905	0.0258	0.9950	0.0125	0.9919	0.0224
4.4	0.9966	0.0088	0.9946	0.0157	0.9970	0.0079	0.9955	0.0134
4.6	0.9980	0.0054	0.9970	0.0092	0.9982	0.0048	0.9975	0.0077
5.0	0.9993	0.0019	0.9992	0.0028	0.9994	0.0017	0.9993	0.0023
6.0	1.0000	0.0001	1.0000	0.0001	1.0000	0.0001	1.0000	0.0001
7.0	1.0000	0.0000	1.0000	0.0000	1.0000	0.0000	1.0000	0.0000

Table 7f. Energy and Species Continuity Solutions: g_I, g_I', Z_A, Z_A'

$g_{Iw} = 0.4$, $\quad Z_{Aw} = 0.05$

	D = 1.2		J = 0.0		D = 1.2		J = 0.6	
	g_I	g_I'	Z_A	Z_A'	g_I	g_I'	Z_A	Z_A'
0.0	0.4000	0.1246	0.0500	0.1657	0.4000	0.1281	0.0500	0.1876
0.2	0.4257	0.1321	0.0845	0.1791	0.4274	0.1462	0.0892	0.2041
0.4	0.4529	0.1402	0.1217	0.1940	0.4585	0.1637	0.1317	0.2218
0.6	0.4818	0.1486	0.1621	0.2103	0.4928	0.1799	0.1780	0.2407
0.8	0.5124	0.1574	0.2060	0.2281	0.5303	0.1941	0.2281	0.2604
1.0	0.5447	0.1661	0.2535	0.2469	0.5703	0.2060	0.2822	0.2806
1.2	0.5788	0.1745	0.3048	0.2665	0.6124	0.2147	0.3403	0.3003
1.4	0.6145	0.1820	0.3600	0.2858	0.6559	0.2196	0.4022	0.3182
1.6	0.6515	0.1880	0.4190	0.3037	0.7000	0.2200	0.4673	0.3326
1.8	0.6895	0.1917	0.4813	0.3184	0.7436	0.2155	0.5348	0.3412
2.0	0.7280	0.1922	0.5460	0.3277	0.7858	0.2055	0.6033	0.3415
2.2	0.7661	0.1889	0.6118	0.3292	0.8255	0.1902	0.6708	0.3315
2.4	0.8032	0.1811	0.6770	0.3208	0.8616	0.1703	0.7351	0.3099
2.6	0.8383	0.1687	0.7394	0.3012	0.8934	0.1470	0.7940	0.2776
2.8	0.8704	0.1521	0.7968	0.2710	0.9203	0.1220	0.8456	0.2371
3.0	0.8989	0.1325	0.8472	0.2325	0.9422	0.0974	0.8886	0.1926
3.2	0.9233	0.1113	0.8895	0.1897	0.9593	0.0746	0.9227	0.1487
3.4	0.9434	0.0900	0.9231	0.1470	0.9723	0.0551	0.9483	0.1092
3.6	0.9594	0.0702	0.9485	0.1083	0.9816	0.0391	0.9668	0.0764
3.8	0.9717	0.0529	0.9669	0.0760	0.9882	0.0269	0.9794	0.0511
4.0	0.9808	0.0385	0.9794	0.0509	0.9926	0.0179	0.9877	0.0327
4.2	0.9873	0.0271	0.9877	0.0327	0.9955	0.0115	0.9929	0.0201
4.4	0.9918	0.0185	0.9929	0.0201	0.9973	0.0072	0.9960	0.0119
4.6	0.9949	0.0123	0.9960	0.0119	0.9985	0.0044	0.9978	0.0068
5.0	0.9981	0.0050	0.9989	0.0037	0.9996	0.0015	0.9994	0.0020
6.0	0.9999	0.0003	1.0000	0.0001	1.0000	0.0001	1.0000	0.0000
7.0	1.0000	0.0000	1.0000	0.0000	1.0001	0.0000	1.0000	0.0000

Table 7g. Energy and Species Continuity Solutions: g_I, g_I', Z_A, Z_A'

$g_{Iw} = 0.4$, $\quad Z_{Aw} = 0.05$

	D = 0.6			J = 1.3	D = 0.9			J = 1.2
	g_I	g_I'	Z_A	Z_A'	g_I	g_I'	Z_A	Z_A'
0.0	0.4000	0.1347	0.0500	0.2268	0.4000	0.1352	0.0500	0.2235
0.2	0.4310	0.1752	0.0976	0.2494	0.4313	0.1767	0.0969	0.2454
0.4	0.4698	0.2116	0.1498	0.2722	0.4703	0.2123	0.1482	0.2675
0.6	0.5152	0.2413	0.2065	0.2947	0.5157	0.2398	0.2039	0.2892
0.8	0.5657	0.2623	0.2676	0.3160	0.5656	0.2580	0.2638	0.3101
1.0	0.6195	0.2733	0.3327	0.3351	0.6182	0.2664	0.3278	0.3291
1.2	0.6743	0.2739	0.4014	0.3503	0.6715	0.2655	0.3952	0.3450
1.4	0.7283	0.2645	0.4725	0.3599	0.7238	0.2561	0.4654	0.3559
1.6	0.7795	0.2462	0.5448	0.3618	0.7735	0.2393	0.5372	0.3599
1.8	0.8263	0.2207	0.6166	0.3542	0.8191	0.2164	0.6088	0.3548
2.0	0.8675	0.1902	0.6858	0.3360	0.8597	0.1890	0.6784	0.3389
2.2	0.9023	0.1574	0.7503	0.3070	0.8945	0.1590	0.7436	0.3119
2.4	0.9305	0.1247	0.8080	0.2691	0.9233	0.1286	0.8025	0.2751
2.6	0.9523	0.0946	0.8575	0.2255	0.9461	0.0998	0.8532	0.2316
2.8	0.9686	0.0685	0.8981	0.1801	0.9634	0.0742	0.8949	0.1856
3.0	0.9801	0.0475	0.9297	0.1372	0.9760	0.0528	0.9276	0.1416
3.2	0.9879	0.0315	0.9533	0.0997	0.9849	0.0361	0.9519	0.1029
3.4	0.9930	0.0200	0.9701	0.0692	0.9908	0.0237	0.9693	0.0714
3.6	0.9961	0.0121	0.9815	0.0461	0.9946	0.0149	0.9810	0.0475
3.8	0.9980	0.0071	0.9889	0.0294	0.9969	0.0091	0.9887	0.0302
4.0	0.9991	0.0040	0.9936	0.0181	0.9983	0.0053	0.9935	0.0185
4.2	0.9997	0.0021	0.9964	0.0107	0.9992	0.0030	0.9964	0.0109
4.4	1.0000	0.0011	0.9981	0.0061	0.9996	0.0016	0.9980	0.0062
4.6	1.0001	0.0005	0.9990	0.0034	0.9999	0.0009	0.9990	0.0034
5.0	1.0003	0.0001	0.9997	0.0009	1.0000	0.0002	0.9997	0.0009
6.0	1.0003	0.0000	1.0000	0.0000	1.0001	0.0000	1.0000	0.0000
7.0	1.0003	0.0000	1.0000	0.0000	1.0001	0.0000	1.0000	0.0000

Table 7h. Energy and Species Continuity Solutions: g_I, g_I', Z_A, Z_A'

$g_{Iw} = 0.4$, $\quad Z_{Aw} = 0.05$

	D = 1.2			J = 0.9	D = 2.7			J = 0.2
	g_I	g_I'	Z_A	Z_A'	g_I	g_I'	Z_A	Z_A'
0.0	0.4000	0.1316	0.0500	0.2042	0.4000	0.1314	0.0500	0.1802
0.2	0.4292	0.1603	0.0927	0.2231	0.4275	0.1439	0.0876	0.1959
0.4	0.4639	0.1861	0.1393	0.2428	0.4575	0.1561	0.1285	0.2131
0.6	0.5034	0.2076	0.1899	0.2632	0.4899	0.1678	0.1729	0.2317
0.8	0.5466	0.2241	0.2446	0.2837	0.5246	0.1786	0.2212	0.2517
1.0	0.5927	0.2350	0.3033	0.3039	0.5613	0.1882	0.2737	0.2725
1.2	0.6403	0.2401	0.3660	0.3225	0.5998	0.1963	0.3303	0.2934
1.4	0.6883	0.2392	0.4321	0.3380	0.6397	0.2023	0.3909	0.3131
1.6	0.7355	0.2322	0.5009	0.3483	0.6805	0.2056	0.4553	0.3297
1.8	0.7808	0.2193	0.5710	0.3511	0.7217	0.2052	0.5224	0.3408
2.0	0.8229	0.2010	0.6406	0.3439	0.7623	0.2004	0.5911	0.3439
2.2	0.8609	0.1781	0.7078	0.3255	0.8015	0.1908	0.6593	0.3365
2.4	0.8939	0.1521	0.7701	0.2957	0.8383	0.1763	0.7249	0.3171
2.6	0.9217	0.1249	0.8254	0.2566	0.8717	0.1575	0.7854	0.2861
2.8	0.9440	0.0985	0.8724	0.2120	0.9011	0.1357	0.8387	0.2459
3.0	0.9612	0.0745	0.9102	0.1665	0.9259	0.1124	0.8834	0.2008
3.2	0.9740	0.0541	0.9392	0.1244	0.9461	0.0897	0.9190	0.1555
3.4	0.9831	0.0378	0.9604	0.0885	0.9619	0.0688	0.9459	0.1144
3.6	0.9894	0.0254	0.9751	0.0601	0.9738	0.0509	0.9652	0.0801
3.8	0.9935	0.0165	0.9849	0.0391	0.9825	0.0364	0.9785	0.0536
4.0	0.9962	0.0104	0.9912	0.0244	0.9886	0.0252	0.9871	0.0343
4.2	0.9978	0.0063	0.9950	0.0147	0.9928	0.0169	0.9926	0.0210
4.4	0.9988	0.0037	0.9973	0.0085	0.9955	0.0110	0.9959	0.0124
4.6	0.9993	0.0021	0.9985	0.0047	0.9973	0.0069	0.9978	0.0071
5.0	0.9999	0.0006	0.9996	0.0013	0.9991	0.0025	0.9994	0.0021
6.0	1.0000	0.0000	1.0000	0.0000	0.9999	0.0001	1.0000	0.0001
7.0	1.0000	0.0000	1.0000	0.0000	0.9999	0.0000	1.0000	0.0000

Table 7i. Energy and Species Continuity Solutions: g_I, g_I', Z_A, Z_A'

$g_{Iw} = 0.4$, $\quad Z_{Aw} = 0.05$

	D = 2.7			J = 0.4	D = 2.7			J = 0.6
	g_I	g_I'	Z_A	Z_A'	g_I	g_I'	Z_A	Z_A'
0.0	0.4000	0.1327	0.0500	0.1882	0.4000	0.1343	0.0500	0.1976
0.2	0.4284	0.1509	0.0893	0.2049	0.4295	0.1604	0.0913	0.2156
0.4	0.4603	0.1674	0.1320	0.2229	0.4638	0.1819	0.1363	0.2346
0.6	0.4952	0.1815	0.1786	0.2423	0.5020	0.1986	0.1852	0.2545
0.8	0.5327	0.1934	0.2290	0.2627	0.5430	0.2107	0.2382	0.2752
1.0	0.5724	0.2027	0.2837	0.2837	0.5860	0.2187	0.2953	0.2961
1.2	0.6136	0.2095	0.3425	0.3044	0.6302	0.2229	0.3566	0.3163
1.4	0.6559	0.2133	0.4053	0.3232	0.6749	0.2232	0.4216	0.3340
1.6	0.6987	0.2136	0.4715	0.3383	0.7192	0.2196	0.4898	0.3470
1.8	0.7411	0.2097	0.5402	0.3471	0.7625	0.2117	0.5600	0.3528
2.0	0.7823	0.2012	0.6098	0.3469	0.8036	0.1990	0.6303	0.3485
2.2	0.8213	0.1879	0.6782	0.3354	0.8417	0.1817	0.6986	0.3323
2.4	0.8571	0.1698	0.7431	0.3116	0.8760	0.1604	0.7624	0.3039
2.6	0.8890	0.1482	0.8021	0.2766	0.9057	0.1363	0.8194	0.2650
2.8	0.9162	0.1244	0.8532	0.2337	0.9305	0.1113	0.8680	0.2197
3.0	0.9387	0.1004	0.8953	0.1873	0.9503	0.0873	0.9072	0.1728
3.2	0.9565	0.0779	0.9283	0.1426	0.9656	0.0657	0.9373	0.1290
3.4	0.9700	0.0581	0.9527	0.1031	0.9768	0.0475	0.9592	0.0916
3.6	0.9800	0.0418	0.9700	0.0710	0.9848	0.0331	0.9745	0.0621
3.8	0.9870	0.0290	0.9817	0.0468	0.9903	0.0223	0.9846	0.0402
4.0	0.9918	0.0195	0.9892	0.0295	0.9939	0.0145	0.9910	0.0250
4.2	0.9949	0.0127	0.9938	0.0179	0.9963	0.0091	0.9949	0.0149
4.4	0.9970	0.0080	0.9966	0.0104	0.9977	0.0056	0.9972	0.0086
4.6	0.9983	0.0049	0.9982	0.0059	0.9986	0.0033	0.9985	0.0048
5.0	0.9995	0.0017	0.9995	0.0017	0.9994	0.0011	0.9996	0.0013
6.0	1.0000	0.0001	1.0000	0.0000	0.9997	0.0000	1.0000	0.0000
7.0	1.0001	0.0000	1.0000	0.0000	0.9997	0.0000	1.0000	0.0000

Table 7j. Energy and Species Continuity Solutions: g_I, g_I', Z_A, Z_A'

$g_{Iw} = 0.04$, $D = 0.6$, $J = 1.0$

	$Z_{Aw} = 0.05$				$Z_{Aw} = 0.15$			
	g_I	g_I'	Z_A	Z_A'	g_I	g_I'	Z_A	Z_A'
0.0	0.4000	0.1278	0.0500	0.2011	0.4000	0.1381	0.1500	0.2021
0.2	0.4280	0.1521	0.0920	0.2195	0.4304	0.1654	0.1922	0.2197
0.4	0.4608	0.1757	0.1379	0.2390	0.4661	0.1911	0.2379	0.2378
0.6	0.4982	0.1975	0.1877	0.2592	0.5066	0.2137	0.2873	0.2560
0.8	0.5396	0.2164	0.2416	0.2798	0.5513	0.2321	0.3403	0.2738
1.0	0.5844	0.2311	0.2996	0.2999	0.5990	0.2448	0.3967	0.2901
1.2	0.6317	0.2405	0.3614	0.3184	0.6487	0.2508	0.4561	0.3037
1.4	0.6802	0.2434	0.4267	0.3338	0.6989	0.2494	0.5179	0.3132
1.6	0.7286	0.2393	0.4946	0.3441	0.7480	0.2404	0.5810	0.3166
1.8	0.7755	0.2280	0.5639	0.3471	0.7945	0.2241	0.6441	0.3124
2.0	0.8193	0.2097	0.6328	0.3408	0.8372	0.2015	0.7054	0.2992
2.2	0.8590	0.1858	0.6995	0.3237	0.8748	0.1744	0.7631	0.2768
2.4	0.8934	0.1580	0.7616	0.2959	0.9068	0.1450	0.8155	0.2461
2.6	0.9221	0.1288	0.8172	0.2591	0.9328	0.1156	0.8612	0.2095
2.8	0.9450	0.1005	0.8649	0.2164	0.9531	0.0883	0.8992	0.1703
3.0	0.9624	0.0750	0.9037	0.1723	0.9684	0.0648	0.9294	0.1322
3.2	0.9752	0.0536	0.9339	0.1306	0.9793	0.0456	0.9523	0.0979
3.4	0.9842	0.0368	0.9563	0.0944	0.9869	0.0309	0.9689	0.0693
3.6	0.9902	0.0243	0.9721	0.0652	0.9920	0.0202	0.9804	0.0470
3.8	0.9941	0.0154	0.9829	0.0431	0.9952	0.0127	0.9881	0.0306
4.0	0.9966	0.0095	0.9898	0.0274	0.9972	0.0078	0.9930	0.0192
4.2	0.9981	0.0056	0.9941	0.0167	0.9984	0.0046	0.9960	0.0115
4.4	0.9989	0.0032	0.9967	0.0098	0.9991	0.0027	0.9978	0.0067
4.6	0.9994	0.0018	0.9983	0.0056	0.9995	0.0015	0.9988	0.0038
5.0	0.9999	0.0005	0.9995	0.0016	0.9999	0.0004	0.9997	0.0011
6.0	1.0000	0.0000	1.0000	0.0000	1.0000	0.0000	1.0000	0.0000
7.0	1.0000	0.0000	1.0000	0.0000	1.0000	0.0000	1.0000	0.0000

Table 7K. Energy and Species Continuity Solutions: g_I, g_I', Z_A, Z_A'

$g_{Iw} = 0.1$, $Z_{Aw} = 0.0$, $D = 1.2$

	J = 0.2				J = 0.6			
	g_I	g_I'	Z_A	Z_A'	g_I	g_I'	Z_A	Z_A'
0.0	0.1000	0.1127	0.0000	0.1050	0.1000	0.1182	0.0000	0.1145
0.2	0.1238	0.1253	0.0223	0.1177	0.1252	0.1338	0.0243	0.1290
0.4	0.1502	0.1385	0.0472	0.1313	0.1536	0.1502	0.0517	0.1445
0.6	0.1792	0.1523	0.0749	0.1460	0.1853	0.1675	0.0822	0.1611
0.8	0.2111	0.1668	0.1056	0.1619	0.2206	0.1855	0.1162	0.1788
1.0	0.2460	0.1819	0.1397	0.1792	0.2596	0.2039	0.1538	0.1979
1.2	0.2938	0.1975	0.1774	0.1978	0.3022	0.2226	0.1955	0.2183
1.4	0.3250	0.2134	0.2189	0.2178	0.3486	0.2409	0.2412	0.2398
1.6	0.3693	0.2290	0.2646	0.2389	0.3985	0.2581	0.2914	0.2620
1.8	0.4166	0.2439	0.3146	0.2607	0.4517	0.2732	0.3460	0.2840
2.0	0.4667	0.2572	0.3689	0.2821	0.5076	0.2850	0.4050	0.3047
2.2	0.5193	0.2678	0.4273	0.3026	0.5653	0.2919	0.4677	0.3222
2.4	0.5736	0.2745	0.4894	0.3184	0.6239	0.2926	0.5334	0.3340
2.6	0.6287	0.2758	0.5543	0.3288	0.6819	0.2858	0.6008	0.3377
2.8	0.6835	0.2706	0.6204	0.3307	0.7377	0.2707	0.6678	0.3307
3.0	0.7365	0.2580	0.6858	0.3219	0.7896	0.2476	0.7322	0.3116
3.2	0.7862	0.2382	0.7483	0.3010	0.8362	0.2178	0.7916	0.2807
3.4	0.8313	0.2120	0.8055	0.2689	0.8765	0.1839	0.8439	0.2407
3.6	0.8708	0.1816	0.8553	0.2285	0.9097	0.1488	0.8876	0.1958
3.8	0.9039	0.1494	0.8966	0.1841	0.9361	0.1154	0.9222	0.1511
4.0	0.9306	0.1182	0.9290	0.1406	0.9562	0.0859	0.9483	0.1106
4.2	0.9513	0.0899	0.9532	0.1020	0.9708	0.0615	0.9669	0.0770
4.4	0.9668	0.0659	0.9703	0.0704	0.9811	0.0425	0.9796	0.0512
4.6	0.9780	0.0467	0.9819	0.0464	0.9881	0.0283	0.9879	0.0326
5.0	0.9911	0.0213	0.9939	0.0177	0.9957	0.0115	0.9962	0.0117
6.0	0.9994	0.0018	0.9998	0.0008	0.9998	0.0007	0.9999	0.0005
7.0	1.0000	0.0001	1.0000	0.0000	1.0000	0.0000	1.0000	0.0000

Table 7L. Energy and Species Continuity Solutions: g_I, g_I', Z_A, Z_A'

$g_{Iw} = 0.1$, $Z_{Aw} = 0.0$, $D = 1.2$

	J = 1.0			
	g_I	g_I'	Z_A	Z_A'
0.0	0.1000	0.1270	0.0000	0.1285
0.2	0.1275	0.1482	0.0274	0.1461
0.4	0.1594	0.1705	0.0585	0.1645
0.6	0.1957	0.1934	0.0933	0.1838
0.8	0.2368	0.2167	0.1321	0.2041
1.0	0.2824	0.2396	0.1750	0.2255
1.2	0.3325	0.2614	0.2223	0.2478
1.4	0.3868	0.2810	0.2742	0.2705
1.6	0.4447	0.2972	0.3305	0.2929
1.8	0.5054	0.3087	0.3912	0.3138
2.0	0.5677	0.3139	0.4558	0.3312
2.2	0.6304	0.3114	0.5233	0.3429
2.4	0.6917	0.3001	0.5924	0.3461
2.6	0.7499	0.2799	0.6610	0.3384
2.8	0.8031	0.2514	0.7269	0.3184
3.0	0.8500	0.2167	0.7876	0.2866
3.2	0.8896	0.1787	0.8409	0.2455
3.4	0.9215	0.1409	0.8855	0.1995
3.6	0.9462	0.1062	0.9208	0.1538
3.8	0.9643	0.0766	0.9473	0.1126
4.0	0.9772	0.0531	0.9663	0.0784
4.2	0.9860	0.0353	0.9792	0.0522
4.4	0.9917	0.0227	0.9876	0.0332
4.6	0.9953	0.0141	0.9929	0.0203
5.0	0.9988	0.0049	0.9979	0.0068
6.0	1.0004	0.0002	0.9999	0.0002
7.0	1.0005	0.0000	1.0000	0.0000

Table 8. Momentum, Energy and Species Continuity Solutions

$f, f', f'', \quad g_I, g_I', Z_A, Z_A'$

$g_{Iw} = 0.4, \quad D = 0.0, \quad J = 0.0, \quad Z_{Aw} = 0.05$

	f	f'	f''	g_I	g_I'	Z_A	Z_A'
0.0	0.0000	0.0000	0.2181	0.4000	0.1117	0.0500	0.1483
0.2	0.0044	0.0448	0.2298	0.4229	0.1177	0.0807	0.1590
0.4	0.0181	0.0920	0.2423	0.4471	0.1241	0.1137	0.1707
0.6	0.0414	0.1417	0.2554	0.4726	0.1309	0.1491	0.1836
0.8	0.0750	0.1942	0.2688	0.4995	0.1379	0.1872	0.1976
1.0	0.1192	0.2492	0.2821	0.5278	0.1452	0.2282	0.2126
1.2	0.1748	0.3070	0.2949	0.5575	0.1525	0.2723	0.2286
1.4	0.2422	0.3671	0.3063	0.5888	0.1595	0.3197	0.2450
1.6	0.3218	0.4293	0.3155	0.6213	0.1660	0.3703	0.2614
1.8	0.4140	0.4931	0.3212	0.6551	0.1713	0.4241	0.2769
2.0	0.5191	0.5575	0.3221	0.6897	0.1751	0.4809	0.2902
2.2	0.6370	0.6215	0.3169	0.7250	0.1766	0.5400	0.2998
2.4	0.7676	0.6838	0.3045	0.7602	0.1751	0.6004	0.3038
2.6	0.9103	0.7428	0.2843	0.7948	0.1702	0.6610	0.3003
2.8	1.0644	0.7970	0.2566	0.8280	0.1615	0.7200	0.2880
3.0	1.2287	0.8450	0.2228	0.8591	0.1491	0.7756	0.2664
3.2	1.4019	0.8858	0.1853	0.8874	0.1334	0.8260	0.2365
3.4	1.5825	0.9191	0.1472	0.9123	0.1155	0.8698	0.2006
3.6	1.7690	0.9449	0.1113	0.9335	0.0965	0.9061	0.1622
3.8	1.9600	0.9639	0.0802	0.9510	0.0779	0.9347	0.1250
4.0	2.1542	0.9773	0.0550	0.9648	0.0607	0.9563	0.0918
4.2	2.3506	0.9863	0.0359	0.9754	0.0457	0.9718	0.0643
4.4	2.5485	0.9921	0.0224	0.9833	0.0333	0.9825	0.0431
4.6	2.7473	0.9956	0.0133	0.9889	0.0235	0.9895	0.0277
5.0	3.1463	0.9988	0.0042	0.9955	0.0107	0.9966	0.0102
6.0	4.1460	1.0000	0.0001	0.9997	0.0009	0.9999	0.0004
7.0	5.1460	1.0000	0.0000	1.0000	0.0000	1.0000	0.0000

LITERATURE CITED

1. G. Giannini, "Electrical Propulsion in Space," *Scientific American, 204,* 57-65, (March 1961).

2. G. P. Sutton, *Rocket Propulsion Elements,* John Wiley and Sons, Inc., New York, *31,* (1963).

3. W. F. Cope and D. R. Hartree, "The Laminar Boundary Layer in Compressible Flow," *Phil Transactions of the Royal Society of London, 241A,* 1-69, (1948).

4. D. M. Morris and J. W. Smith, "The Compressible Laminar Boundary Layer with Arbitrary Pressure and Surface Temperature Gradients," *Journal of the Aeronautical Sciences, 20,* 805-818, (1953).

5. I. E. Bechwith, "Heat Transfer and Skin Friction by an Integral Method in the Compressible Laminar Boundary Layer with a Streamwise Pressure Gradient," *NACA TN No. 3005,* National Advisory Committee for Aeronautics, Lewis Research Center, Ohio, (September, 1953).

6. P. A. Libby and M. Morduchow, "Method for Calculation of Compressible Laminar Boundary Layer with Axial Pressure Gradient and Heat Transfer," *NACA TN No. 3157,* National Advisory Committee for Aeronautics, Polytechnical Institute of Brooklyn, N. Y., (January, 1954).

7. K. T. Yang, "An Improved Integral Procedure for Compressible Laminar Boundary Layer Analysis," *Journal of Applied Mechanics, 28,* 9-20, (1961).

8. C. B. Cohen and E. Reshotko, "Similar Solutions for the Compressible Laminar Boundary Layer with Heat Transfer and Pressure Gradient," *NACA TN No. 3325,* National Advisory Committee for Aeronautics, Lewis Flight Propulsion, Ohio, (February, 1955).

9. C. B. Cohen and E. Reshotko, "The Compressible Boundary Layer with Heat Transfer and Arbitrary Pressure Gradient," *NACA TN No. 3326,* National Advisory Committee for Aeronautics, Lewis Flight Propulsion, Ohio, (April, 1955).

10. J. C. Williams III, "A Study of Compressible and Incompressible Viscous Flow in Slender Channels," School of Engineering, *TN USCEC Rept. 83-213,* University of Southern California, (June, 1962).

11. J. R. Baron, "The Binary-Mixture Boundary Layer Associated with Mass Transfer Cooling at High Speeds," Naval Supersonic Laboratory, *TR 160,* Massachusetts Institute of Technology, (May, 1956).

12. J. A. Fay and F. R. Riddell, "Theory of Stagnation Point Heat Transfer in Dissociated Air," *Journal of the Aeronautical Sciences, 25,* 73-86, (1958).

13. L. Lees, "Convective Heat Transfer with Mass Addition and Chemical Reactions," *Combustion and Propulsion 3rd Agard Colloquim,* Pergamon Press, New York, 451-497, (1958).

14. J. A. Fay, "Hypersonic Heat Transfer in the Air Laminar Boundary Layer," *Report AMP 71,* Avco-Everett Research Laboratory, Massachusetts, (March, 1962).

15. I. E. Bechwith and M. B. Cohen, "Application of Similar Solutions to Calculation of Laminar Heat Transfer on Bodies with Yaw and Large Pressure Gradient in High-Speed Flow," *NASA TN No. D-625,* National Aeronautics and Space Administration, Langley Research Center, Virginia, (January, 1961).

16. G. R. Inger, "Nonequilibrium Dissociated Boundary Layers with a Reacting Inviscid Flow," *AIAA Journal, 1,* 2057-2062, (1963).

17. F. G. Blottner, "Nonequilibrium Laminar Boundary Layer Flow of Ionized Air," *AIAA Journal, 2,* 1921-1927, (1964).

18. A. J. Pallone, J. A. Moore and J. I. Erdos, "Nonequilibrium, Nonsimilar Solutions of the Laminar Boundary Layer Equations," *AIAA Journal, 2,* 1706-1714, (1964).

19. A. M. O. Smith and N. A. Jaffe, "General Method for Solving the Nonequilibrium Boundary Layer Equations of a Dissociating Gas," *AIAA 2nd Aerospace Sciences Meeting,* 65-129, American Institute of Aeronautics and Astronautics, New York, New York, (January, 1965).

20. D. R. Bartz, "An Approximate Solution of Compressible Turbulent Boundary Layer Development and Convective Heat Transfer in Convergent-Divergent Nozzles," *Transactions of ASME, 77,* 1235-1245, (1955).

21. E. Mayer, "Analysis of Convective Heat Transfer in Rocket Nozzles," *American Rocket Society Journal, 31,* 911-917, (1961).

22. J. D. Clem, Jr., W. H. Groetzinger, III, J. E. Johnson, and C. H. Parr, "Experimental Determination of Heat Transfer Film Coefficients in Uncooled Rocket Nozzles," *Quarterly Progress Report on Weapons Research (U) P-75-5,* Redstone Arsenal Research Division, Rohm and Haas Company, 1, (1961).

23. P. F. Massier, H. L. Gier, A. B. Witte, and E. Y. Harper, "Convective Heat Transfer in Nozzles," *Research Summary 36-11,* Jet Propulsion Laboratory, 80-89, (August, 1961).

24. A. B. Witte and E. Y. Harper, "Heat Transfer in Rocket Motors,"

Research Summary 36-12, Jet Propulsion Laboratory, 132-133, (December, 1961).

25. R. K. Rose, "Experimental Determination of the Heat Flux Distribution in a Rocket Nozzle" Master's Thesis, School of Mechanical Engineering, Purdue University, (1958).

26. P. F. Massier, L. H. Black, A. B. Witte, and M. B. Noel, "Heat Transfer from Ionized Gases," *Research Summary No. 37-23*, Jet Propulsion Laboratory, 109-118, (October, 1963).

27. P. F. Massier, "Heat Transfer to Convergent Divergent Nozzles from Ionized Argon," *Research Summary No. 37-24*, Jet Propulsion Laboratory, 105-108, (December, 1963).

28. G. B. Heller and B. P. Jones, "Survey of Arc Propulsion," *Space Nuclear Conference*, American Rocket Society, Gatlinburg, Tennessee, (May, 1961).

29. R. J. Page, "Current Status and Prospects of Electrothermal Propulsion," *17th Annual Meeting and Space Flight Exposition 2644-62*, American Rocket Society, Los Angeles, California, (November, 1962).

30. J. R. Jack, "Theoretical Performance of Propellants Suitable for Electrothermal Jet Engines," *NASA TN D-682*, National Aeronautics and Space Administration, Lewis Research Center, Ohio, (March, 1961).

31. S. Bennett, W. Huss, R. R. John, and A. Tuchman, "Experimental Propulsion Performance of a Low Power Pulsed Resistojet," *AIAA 2nd Aerospace Sciences Meeting, 65-97*, American Institute of Aeronautics and Astronautics, New York, New York, (January, 1965).

32. H. Schlichting, Personal Communication, (May, 1962).

33. A. H. Shapiro, *Thermodynamics and Dynamics of Compressible Fluid Flow, 1*, The Ronald Press Company, New York, (1953).

34. K. N. C. Bray, "Atomic Recombination in a Hypersonic Wind Tunnel Nozzle," *Journal of Fluid Mechanics, 6*, 1, (1959).

35. E. A. Lezberg and R. B. Lancashire, "Recombination of Hydrogen-Air Combustion Products in an Exhaust Nozzle," *NASA TN D-1052*, National Aeronautics and Space Administration, Lewis Research Center, Ohio, (August, 1961).

36. W. H. Dorrance, *Viscous Hypersonic Flow*, McGraw-Hill Book Company, Inc., New York, (1962).

37. C. H. King, "Compilation of Thermodynamic Properties, Transport Properties, and Theoretical Rocket Performance of Gaseous Hydrogen,"

NASA TN D-275, National Aeronautics and Space Administration, Lewis Research Center, Ohio, (April, 1960).

38. D. B. Spalding, *Convective Mass Transfer*, McGraw Hill Book Company, Inc., New York, 138, (1963).

39. J. O. Hirschfelder, C. F. Curtis, and R. B. Bird, *Molecular Theory of Gases and Liquids*, John Wiley and Sons, Inc., New York, (1954).

40. C. J. Chen, "Experimental Investigation of Atomic Recombination in a Supersonic Nozzle," *Journal of Fluid Mechanics, 17*, 450-458, (1963).

41. E. C. Kunz, "Development of an Experimental Method for the Determination of Local Heat Flux in Small Diameter Cooled Nozzles," *Master's Thesis*, School of Mechanical Engineering, Georgia Institute of Technology, (1965).

42. P. G. Hill, C. R. Peterson, *Mechanics and Thermodynamics of Propulsion*, Addison-Wesley Publishing Company, Inc., New York, (1965).

43. J. Todd, "Survey of Numerical Analysis," McGraw Hill Book Company, Inc., New York, (1962).

44. Bird, R. B., Stewart, W. E., and Lightfoot, E. N., *Transport Phenomena*, John Wiley and Sons, Inc., New York, (1960).

OTHER REFERENCES

Baxter, D. C. and Flugge-Lotz, I., "The Solution of Compressible Boundary Layer Problems by a Finite Difference Method, Part 2," Stanford University Division of Engineering Mechanics, *Technical Report No. 110*, (1957).

Bray, K. N. C., "Electron-Ion Recombination in Argon Flowing Through a Supersonic Nozzle," University of Southhampton, *A.A.S.U. Report 213*, (1962).

Bird, R. B., Stewart, W. E., and Lightfoot, E. N., *Transport Phenomena*, John Wiley and Sons, Inc., New York, (1960).

Chapman, S., and Cowling, T. G., *Mathematical Theory of Non-Uniform Gases*, Cambridge University Press, New York, (1952).

Erickson, W. D. and Creekmore, H. S., "A Study of Equilibrium Real Gas Effects in Hypersonic Air Nozzles, Including Charts of Thermodynamic Properties for Equilibrium Air," *NASA TN D231*, April, 1960.

Flugge-Lotz, I. and Baxter, D. C., "The Solution of Compressible Boundary Layer Problems by a Finite Difference Method Part I," Stanford University Division of Engineering Mechanics, *Technical Report No. 103*, (1956).

Flugge-Lotz, I. and Howe, J. T., "The Solution of Compressible Boundary Layer Problems by a Finite Difference Method Part 3," Stanford University Division of Engineering Mechanics, *Technical Report No. 111*, (1957).

Gudenley, K. G. and Armitage, J. V., "A General Method for the Determination of Best Supersonic Rocket Nozzles," Boeing Scientific Research Laboratory Symposium, Seattle, Washington, December 3-4, 1962.

Johnson, C. B., Boney, L. R., Ellison, J. C., and Erickson, W. D., "Real Gas Effects on Hypersonic Nozzle Contours with a Method of Calculation," *NASA TN D-1622*, (1955).

McCracken, D. D., *A Guide to Algol Programming*, John Wiley & Sons, Inc., New York, (1962).

Meksyn, D., *New Methods in Laminar Boundary Layer Theory*, Pergamon Press, New York, (1960).

Stollery, J. L. and Park, C., "Computer Solutions to the Problem of Vibrational Relaxation in Hypersonic Nozzle Flows," *Journal of Fluid Mechanics, 19*, 113-123, (1964).

Techo, R., *A Problem Language Primer*, Rich Electronic Computer Center, Georgia Institute of Technology, Atlanta, Georgia (1962).

VITA

William S. Shepard was born in Colquitt, Georgia on September 28, 1932. He received a Bachelor of Mechanical Engineering degree from the Georgia Institute of Technology in December, 1953. After graduation, he was employed by Ford Motor Company as a Research Engineer. His employment there was interrupted for 21 months during which time he was stationed in Germany with the U. S. Army, VII Corps Ordnance Section. He was discharged as First Lieutenant in March, 1956.

While employed with Rohm and Haas Company, Huntsville, Alabama, Mr. Shepard decided to return to Georgia Tech and received the degree of Master of Science, June, 1959. September, 1958 he was appointed Instructor of Mechanical Engineering and was promoted to Assistant Professor in that department in 1960.

Mr. Shepard was married in 1957 to the former Betty Jane Kelsey and they have one child.